VANDERBILT UNIVERSITY
CENTER FOR THE SPACE PROCESSING OF ENGINEERING MATERIALS

ANNUAL REPORT
OCTOBER 1, 1985 - OCTOBER 31, 1986

VANDERBILT UNIVERSITY
CENTER FOR THE SPACE PROCESSING OF ENGINEERING MATERIALS

ANNUAL REPORT
OCTOBER 1, 1985 - OCTOBER 31, 1986

CENTER FOR THE SPACE PROCESSING

OF ENGINEERING MATERIALS

Vanderbilt University

Annual Report

This first annual report of the Center for the Space Processing of Engineering Materials relates the work for the period October 1, 1985 through October 31, 1986. The unusual time period, 13 months rather than 12 months, reflects adjustments on the part of both Vanderbilt University and NASA with respect to funding arrangements.

After an initial period of administrative organizational activity in the Center, considerable work on project planning was done. Following this, research began and is well underway with results already being obtained. The number of materials research projects is now thirteen. There are ten companies active in the materials research. These are:

Aluminum Company of America
Armco, Inc.
Cabot Corporation
Engelhard Corporation
General Electric Company
General Motors Corporation, Delco-Remy Division
GTE Corporation
Lockheed Missiles and Space Company, Inc.
Special Metals Company
Teledyne Wah Chang Albany

Each of the projects is reported herein by company association and follow according to alphabetical order of the company names. An additional two companies, Boeing Aerospace Company and Teledyne Brown Engineering, are involved in long range planning for the Center, marketing of the Center, and Center hardware projects.

CENTER FOR THE SPACE PROCESSING OF ENGINEERING MATERIALS

UNOFFICIAL EXPENDITURES DURING FIRST YEAR OF OPERATION

	NASA	V.U. IN-KIND
Salaries, Wages & Fringe Benefits	408,215	70.202
Materials, Supplies and Utilities	23,808	20,112
Telephone, Long Distance	2,958	
Travel	33,903	2,681
Other Major Costs Incl. Equipment	106,163	47,500
Sub-contracts	143,019	
Overhead	252,935	49,802
TOTALS	971,001	190,297

CORPORATE CONTRIBUTIONS TO THE CENTER

Corporate contributions to the Center are reported in the following three categories:

I. **DIRECT CONTRIBUTIONS**: defined as direct cash payments, cost of materials or equipment donated, and other contributions equivalent to cash.

II. **DIRECT IN-KIND**: defined as costs related to activities that a company would not have undertaken if it were not a member of the Center. This includes R & D, travel to the Center or to NASA facilities, etc., and other related activities.

III. **IN-KIND COLLABORATION**: defined as work in a company that would have been done even without Center involvement, but is related to or supportive of Center projects.

All Figures Are Unofficial Estimates.

	I	II	III	Total
Alcoa		37,000 (798PH)	90,000 (1597PH)	127,000
Armco		18,682 (220PH)	85,000	103,682
Boeing		111,628		111,628
Cabot		10,000	70,000	80,000
Engelhard	5,810	80,000		85,810
General Electric		10,225 (200PH)		10,225
General Motors	2,650	48,350 (450PH)	270,000	321,000
GTE	--	--	--	*
Lockheed		124,464 (1595PH)	8,553 (128PH)	133,017
Special Metals		45,109 (216PH)		45,109
TBE		54,056 (1512PH)		54,056
TWCA	200	39,196 (465PH)		39,396
TOTAL	8,660	578,710	523,553	1,110,923

PH = Person Hours

* = Figures Not Available

PROJECT TITLE: The Effect of Microgravity on the Microstructure of Directionally Solidified Aluminum Alloys.

COMPANY INVOLVED: Alcoa

PROJECT LEADER: Robert L. Lott, Jr.

PROJECT DESCRIPTION:

The objective of this project is to study the effect of microgravity on the microstructure of directionally solidified aluminum-iron-silicon alloys. Directional solidification of several different alloys will be conducted under earth gravity conditions with various combinations of temperature gradient and furnace traverse rate to yield the sample cooling rate over the range (0.01 to 50°C/s) of expected interest. The resulting microstructure from these experiments will be determined and examined using appropriate instruments (microscope, scanning electron microscope, Guinier x-ray analysis, etc.) to measure the cell spacing, interparticle spacing, composition of the resulting alloys of the cell and the precipitate phases in the intercellular regions. Similar experiments are planned to be conducted under microgravity conditions aboard the space shuttle so that a comparison of the resulting microstructure can be made with the 1g experiments.

Land-Based Experiments

Land-based directional solidification experiments have been conducted using a Mellen gradient furnace at the Alcoa Technical Center, Pittsburgh. A schematic diagram of the thermal gradient furnace is shown in Figure 1. These land-based experiments are being conducted to investigate the effect of solidification parameters on the composition and formation of intermetallic phases in the Al-0.5Fe (% weight) alloy, with further experiments to include additions of silicon and/or magnesium. These experiments will permit comparisons of microstructures between the land-based 1g experiments and those obtained from space gravity experiments. These comparative experiments are essential for understanding the nucleation and growth behavior during formation of the intermetallic phases. A better understanding of the mechanisms governing the intermetallic phases formation is expected to lead to better control in the production of these solidified microstructures and therefore enhance ground-based processing. The ability to produce a specific microstructure will also permit material properties measurement and characterization.

The Mellen gradient furnace consists of three independently controlled resistance heating coils for bulk heating of the sample and, to enhance thermal gradient, a platinum-rhodium booster heating coil located near the bottom of the heating section of the furnace. To minimize vibration of the solidifying specimen, the crucible containing the sample is held stationary while the furnace is translated vertically. A water cooling section located at the bottom end of the furnace moves with the furnace to provide for a constant thermal gradient in the longitudinal direction of the sample under steady state conditions of solidification.

The crucible is a high density, high thermal conductivity graphite tube, which is typically 24 inches long with an inside diameter of 5/16 inch and an outside diameter of 7/16 inch. The alloy rod is placed inside the crucible under an argon atmosphere and is heated to bring the sample to a superheat melt temperature. The temperature is maintained for 30 minutes to insure a uniform liquid melt under steady state conditions. The furnace is then moved at a prescribed speed, with directional solidification commencing on the unmelted solid end of the sample located at the cooling end section. The directional solidification proceeds with the liquid melt on top and the solid forming at the bottom of the liquid melt. A period of approximately 15 minutes at a prescribed speed is considered necessary to reach a steady thermal state and thus to obtain a solidified microstructure representative of the prescribed solidification rate and thermal gradient for the alloy being solidified.

A liquid thermal gradient of 30 to 140°C/cm is created across the solid/liquid interface, depending upon the temperature of the liquid melt, the cooling temperatures and the solidification rate. The furnace had a maximum translation speed of 100 inches/hour when the first set of experiments was run. The furnace has recently been modified to have a maximum translation speed of 200 inches/hour. The solidification rate is assumed to be equal to the furnace translation speed. The product of the temperature gradient and solidification rate yields the cooling rate. Before modification of the furnace speed, the maximum cooling rate was approximately 10°C/second.

PRELIMINARY RESULTS:

A photograph of a sample (Al-0.5Fe) rod macroetched on the longitudinal cross section is shown in Figure 2. Solidification was observed to start on a polycrystalline unmelted substrate. A columnar structure developed. As solidification proceeded, the number of columnar grains decreased and in many cases became a single crystal or in some cases a bicrystal after only a few centimeters of solidification growth. The unidirectionally solidified casting was approximately 16 inches long. The sample shown in Figure 2 was solidified at the furnace translation speeds of 0.6, 2.0, 4.0, 8.0, and 16.0 inches per hour for different sections of the rod. A five minute dwell time between each furnace speed setting was used to permit homogenization of the solute in the melt.

Measurements of cell spacing and interparticle spacing as a function of the cooling rate is shown in Figure 3. The slopes of a straight line through each set of data were found to be approximately -0.5, which is in agreement with models of dendrite spacing based upon constitutional super-cooling as the driving force in the region between the primary dendrites. The slope of -0.5 for the interparticle spacing agrees with theoretical results for a two-dimensional development of lamellae morphology of a simple binary eutectic which yields α and β phases assumed to be formed at the same rate with a planar solid/liquid interface. Both phases in the theoretical model are assumed to be non-faceting and the melt is assumed to be at the eutectic composition far from the solid/liquid interface, with the constitutional supercooling assumed to be a minimum. At the present time, there is no clear justification for applying these theoretical models to the results obtained.

The results of the experiments to date have yielded identification of three intermetallic phases: equilibrium phase Al_3Fe, metastable phase Al_xFe, and metastable phase Al_6Fe. The range of cooling rates for the formation of each phase was found to be 0.7°C/s and below for Al_3Fe phase, 0.7°C/s to 3°C/s for Al_xFe phase, and 3°C/s to 5°C/s for Al_6Fe phase. These ranges are indicated on Figure 3.

The morphologies of these three intermetallic phases on a transverse cross-section are shown in Figures 4a to 4h, arranged (a to h) by increasing cooling rates. At very low cooling rates, below approximately 0.004°C/s, the structure consists of flaky precipitates scattered randomly throughout the entire cross section as shown in Figure 4a. It is believed that at these low cooling rates, a plane front solidification occurred. The cross section in Figure 4b shows a structure which is interpreted to be the beginning of a breakdown of "regular" cells, with the cell boundaries becoming more linked together in one direction while broken in the other direction. Figures 4c through 4e show the typical cell structure. Figure 4f shows a cellular-dendritic structure. The boundary (intercellular) phase appearing in Figures 4a through 4f was identified as the equilibrium intermetallic Al_3Fe by Guinier x-ray analyses. The Al_3Fe phase is imbedded in the -Al phase matrix. A typical Al_xFe phase in the intercellular region appears in lamellar eutectic as shown in Figure 4g. As the cooling rate increases beyond 3°C/s, the dominant intermetallic was observed to be the metastable phase Al_6Fe which appears as broken dots at the cell boundaries as shown in Figure 4h. Table 1 presents a summary of the data for the microstructures of Figures 4a to 4h.

The limits of the thermal gradient furnace did not permit cooling rates beyond 5°C/s to be obtained. Modifications to increase the furnace translation speed to 200 inches per hour will enable higher cooling rates to be achieved in future experiments. The Al_mFe ($9<m<11$) metastable intermetallic phase is expected to occur at cooling rates in excess of 5°C/s.

SPECIFICATIONS FOR HARDWARE REQUIRED FOR SPACE EXPERIMENTS:

Consideration of the land-based experiments which are to be compared with similar experiments under microgravity conditions of space leads to the specification of the directional solidification furnace shown in Table 2.

It is expected that 20 different cooling rates and 2 thermal gradients will be achieved for each alloy composition to be studied in order to obtain the desired range of cooling rates to achieve the formation of various intermetallic phases of interest. It is desirable to have a sample length of 30 to 35 cm with the ability to change the furnace speed several times during

the processing of each sample to obtain several sections with different solidification parameters. Thus, the total number of sample rods is estimated at eight as listed in Table 2. At the higher cooling rates (and higher furnace speeds) the length of sample required for the solidification process to reach steady state conditions increases; thus reducing the number of experiments per sample.

The ability to program the furnace speeds and dwell times for a given sample is needed to maximize the number of experiments per sample. Instrumentation to measure and record the furnace speed, the temperatures, and the gravitational acceleration as a function of the solid/liquid interface is needed to characterize the solidification parameters for each sample section.

Variable Gravity Experiments

It has been proposed (flight time and space have been requested) that some exploratory experiments be conducted using the existing NASA directional solidification furnace which is flown on the KC-135 flights. The alumina crucible used in previous flight experiments was reported to be 0.5 cm inside diameter with a length of 40 cm. The maximum furnace temperature of 1500°C is well above the requirements needed for the aluminum alloy systems of interest to this project. The maximum furnace speed has been reported as 63.3 mm/min. It is not clear from the reported data on the furnace what the thermal gradient would be for a melt temperature of 1000°C and thus additional temperature sensors may have to be incorporated to obtain the temperature gradient. Previously reported experience with the KC-135 flying parabolic maneuvers indicates time periods of 20 to 30 seconds of low g (0.1g to 0.001g) followed by approximately 90 seconds of high g (up to 1.75g) accelerations imposed upon the sample. These time periods at the specific g levels are not long enough to establish steady state conditions; thus, the results are not expected to be directly comparable with land-based results. However, it is believed that the KC-135 experiments will give some preliminary indications of the potential of low g effects and will provide valuable experience and information to guide the design of space environment experiments.

Modeling of Directional Solidification

A literature review of mathematical models and solution methods for various aspects of the directional solidification

process has been conducted. The particular experimental configuration using a thermal gradient directional furnace as described earlier is of course an attempt to attain a simplified one-dimensional process for which reasonable control of the solidification rate, thermal gradient and bulk melt alloy composition can be exercised.

The models of physical processes which can be important to the resulting microstructure formed from directional solidification include the thermal diffusion equation, the solute diffusion equation, the mass transport equation, the phase diagram, and the surface tension effect at the cell/intercellular boundaries.

Numerous studies dealing with modeling the physical phenomenon with specified boundary conditions have been reported where only the dominant effect for a particular set of parameters has effectively been considered.

Stability models for predicting the transition from planar to cellular growth of the solid based on the solute diffusion domination have been related to the ratio of the liquid thermal gradient to the solidification rate (G_L/R). These stability models incorporate the concept of constitutional supercooling and agree reasonably well with experimental observations for a range of (G_L/R). For conditions of a one-dimensional liquid/solid interface with isotropic surface tension and no convection, another model has been developed to predict instability of the interface.

Basically one-dimensional models have been proposed considering the solute diffusion as the controlling mechanism to predict and explain solute redistribution which leads to intercellular eutectic microsegregation for dilute binary alloy systems. Most of these models neglect tip curvature (surface tension), solid state diffusion, convection in the liquid and details of the three dimensional aspects of the solute diffusion.

The cellular and dendritic growth involve a region of the solidification front between the completely solid surface and the completely liquid surface which has been referred to as the mushy zone. Attempts to incorporate the influence of the mushy zone to investigate the influence of liquid convection induced by density variations (due to temperature and solute concentration variations as a function of position) in addition to the solute transport by diffusion have generally conceived of the mushy zone as a permeable solid through which the liquid melt must flow to

satisfy the transport equations. The methods of handling the solution to these sets of differential equations describing the formulated problem have included approximation techniques to linearize or simplify the expressions, finite difference representation of the differential equations which are then solved using numerical methods implemented by a computer, finite element model of the differential equations, boundary element model of the differential equation and a few restricted analytical solutions. These solutions are touted for their ability to predict macrosegregation and generally are for multi-dimensional solidification processes.

Fairly complete thermal modeling of the Bridgman type thermal gradient directional furnace has been reported for steady state conditions. Work has been reported for steady state modeling of directional solidification which considers thermal transport and solute diffusion transport, using finite difference solution methods.

The aluminum alloy systems being investigated are expected to form eutectic phases in the intercellular regions. The particular intermetallic phase in the eutectic (in the case of Al-0.5Fe: stable Al_3Fe or metastable phases Al_xFe, Al_6Fe, and Al_mFe) has been reported to be a function of the solidification parameters G and R under steady state growth conditions. For the alloy system being investigated with the directional solidification furnace, a number of observations can be made. The solute concentration is greater at the liquid/solid interface than it is in the bulk melt. Shrinkage during solidification will cause fluid flow toward the interface. The cell tips likely experience constitutional supercooling. The density of the liquid is greatest at the interface due to the temperature increasing and the solute concentration decreasing as the distance from the interface toward the melt increases. The radial variation in the temperature will not be zero unless the adiabatic section of the rod surface at the interface is perfectly adiabatic. The latent heat of fusion is conducted through the solid and convected from the outside walls of the crucible.

The above qualitative description is amenable to macro scale mathematical modeling, but does not attempt to consider the complex transport processes that occur at the cell and intercellular level. One approach to the mathematical modeling is to consider the macro scale model with transient and steady state conditions as expected from the experimental configuration,

then use these results as starting points for a theoretical model of a single cell and intercellular region. Another approach is to model the cell and dendrite structure as a permeable solid with liquid flow (effectively an averaging effect model for the mushy zone) which is then part of the macro scale model. A difficulty which exists in any of these mathematical models is obtaining reliable transport property data, particularly for any of the metastable phases of interest in this project.

The macro scale mathematical model of the directional solidification process is currently being developed, using a computer implemented finite-difference method of representing the differential equations. A literature review summary is being prepared.

PLANS FOR FUTURE WORK:

Further experiments on the Al-0.5Fe alloy will be completed to obtain results at the higher furnace speeds now possible with the recent modification of the Mellen thermal gradient furnace. It is expected that experiments to achieve directional solidification results for an Al-Fe-Si alloy will also be conducted in the future.

Plans have been made to conduct experiments on the Al-0.5Fe alloy using the thermal gradient furnace aboard the NASA KC-135 undergoing parabolic flight paths to give periods of low gravity.

Completion of the macro-scale math model of the experiments is expected in the next several months. Results from this investigation will be evaluated to determine the appropriate direction of effort in further mathematical modeling of the directional solidification experiments.

A comparison of results from the ground-based experiments, the KC-135 experiments and the mathematical model will be made to determine refinements or changes needed in the investigation.

ADDITIONAL PROJECT PERSONNEL:

Q.T. Fang, Alcoa
D. A. Granger, Alcoa
G. D. Scott, Alcoa

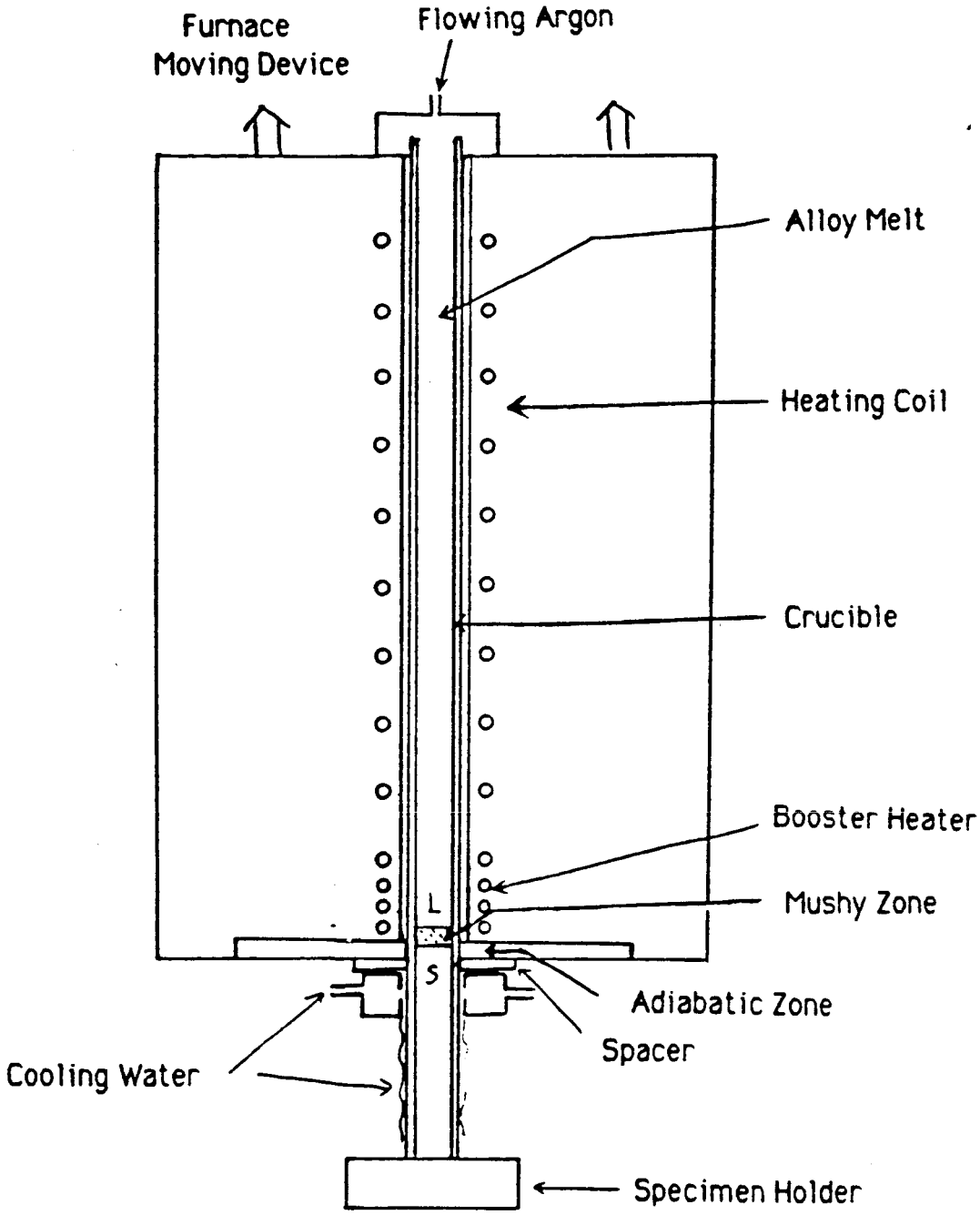

Fig. 1 Schematic of the thermal gradient furnace.

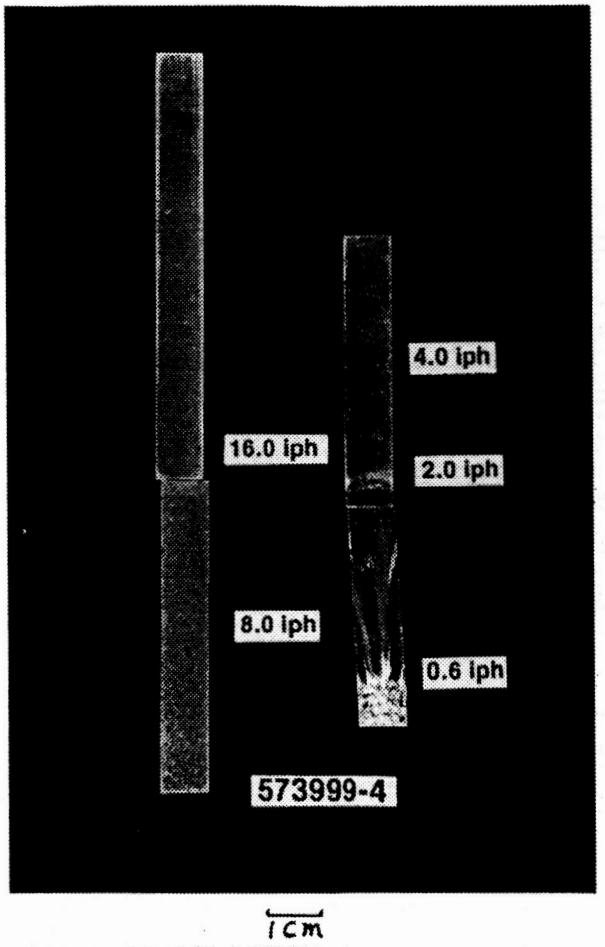

FIGURE 2. Longitudinal cross-section of a sample rod.

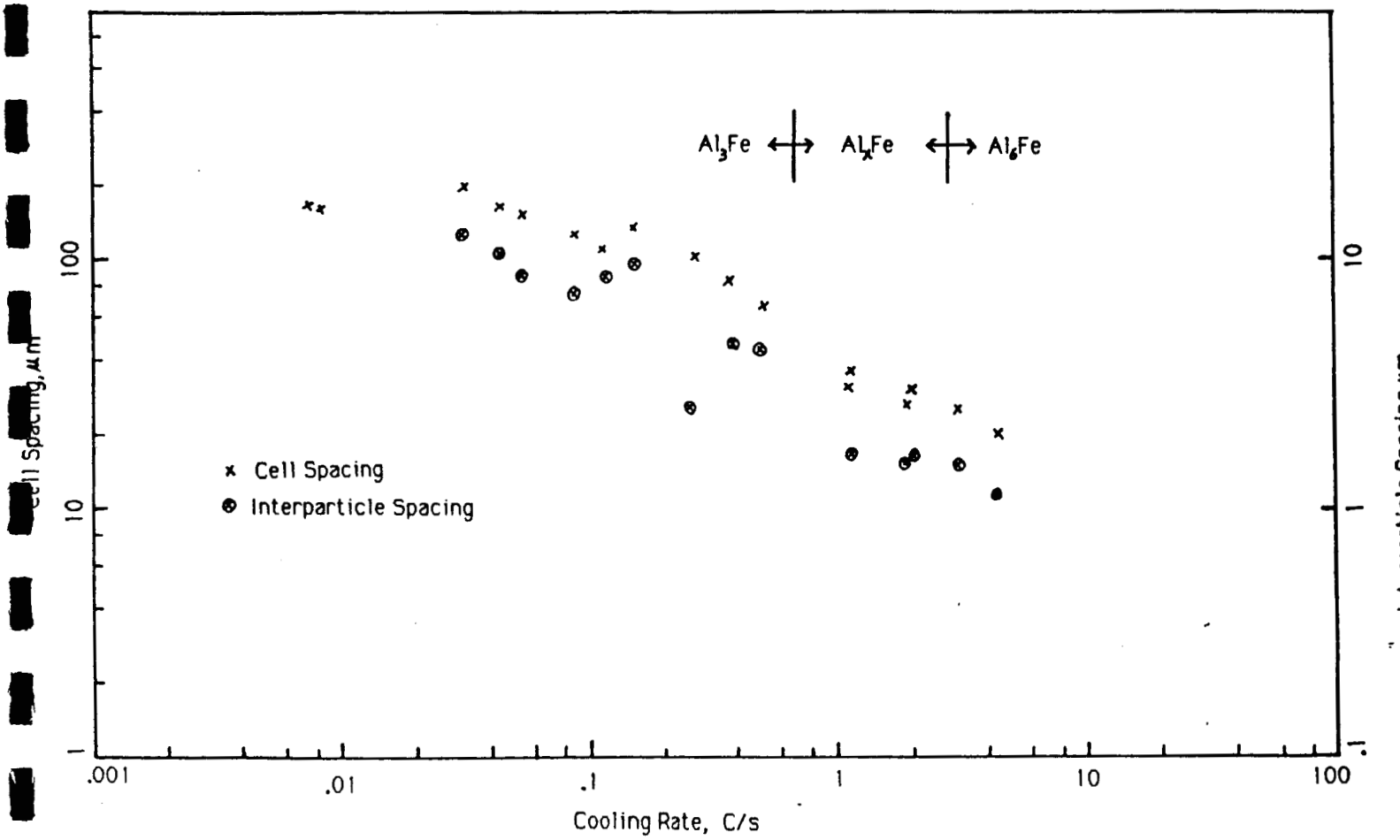

Fig 3. Cell spacing and interparticle spacing as a function of cooling rate.

TABLE 1. Conditions of Formation for Al-0.5% Fe Alloy

Directionally Solidified Microstructures

Photo #	Sample #	Growth Rate, in/hr	Thermal Gradient, °C/sec	Cooling Rate, °C/sec	Interdendritic (intercellular) phase and morphology
a	5A	0.12	28	0.0024	Al_3Fe, planar
b	5B	0.6	18	0.0076	Transition from Al_3Fe planar to cellular
c	4B	0.8	15	0.0085	Al_3Fe, cellular
d	3B	2	20	0.028	Al_3Fe, cellular-dendritic
e	2B	8	20	0.11	Al_3Fe, cellular
f	4H	16	25	0.28	Al_3Fe, cellular-dendritic
g	8F	24	69.4	1.18	Al_xFe, lamellar eutectic
h	7A	45	97	3.1	Al_6Fe, rod eutectic

T:C:12

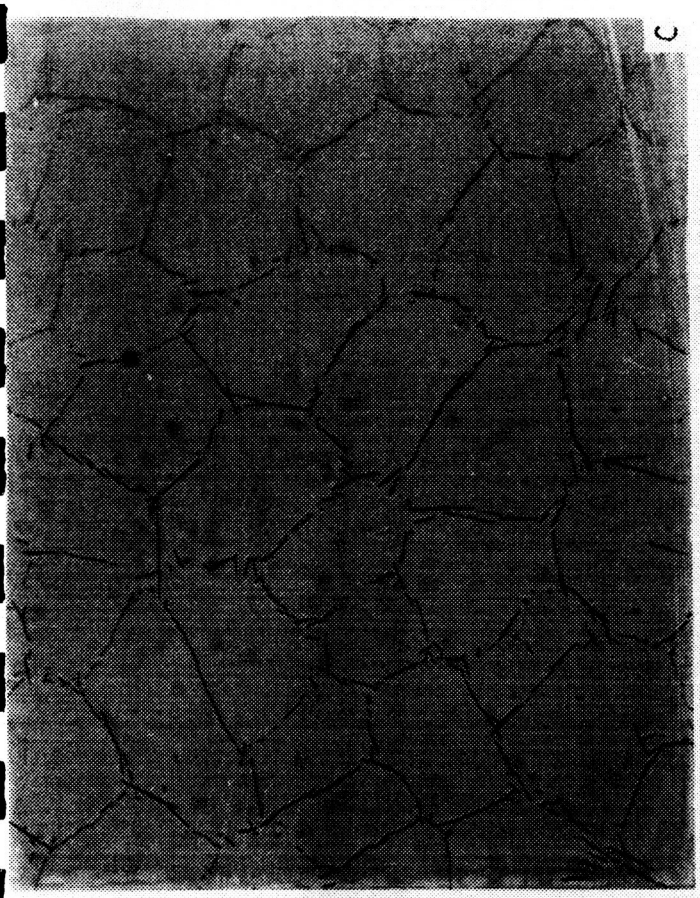

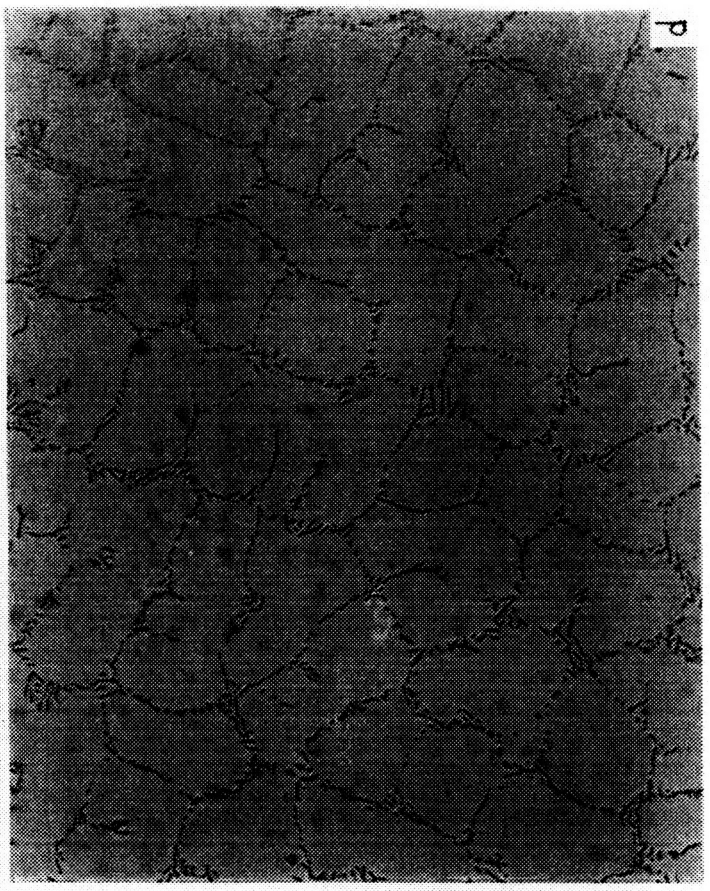

ORIGINAL PAGE IS
OF POOR QUALITY

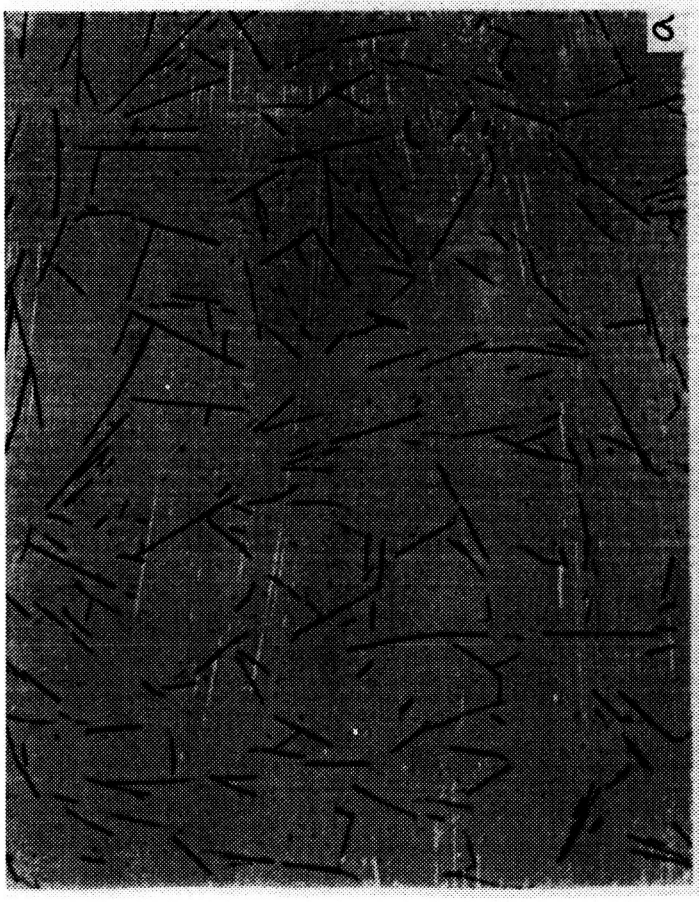

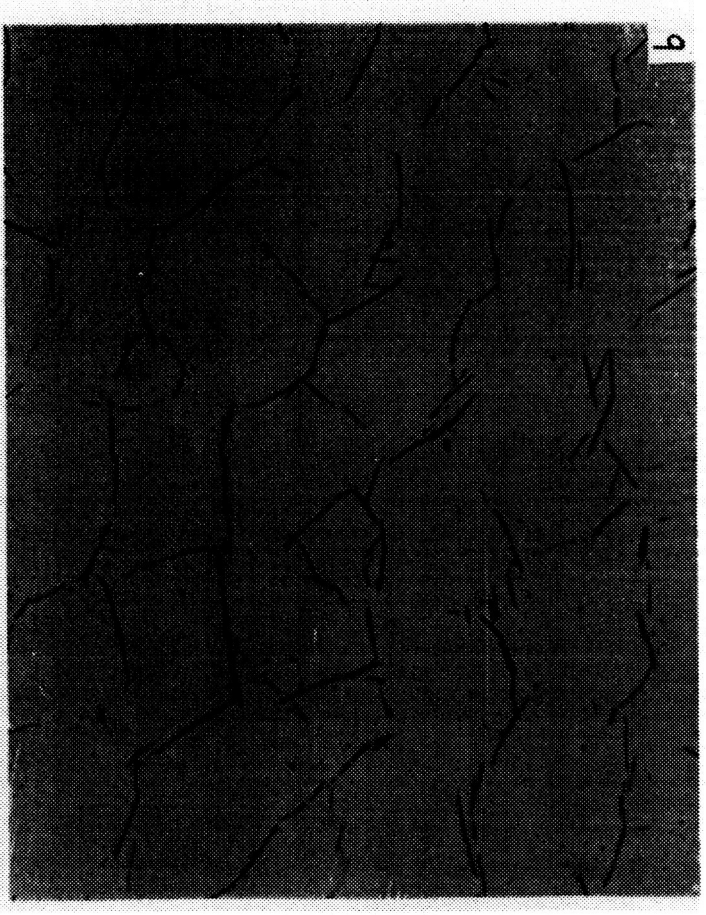

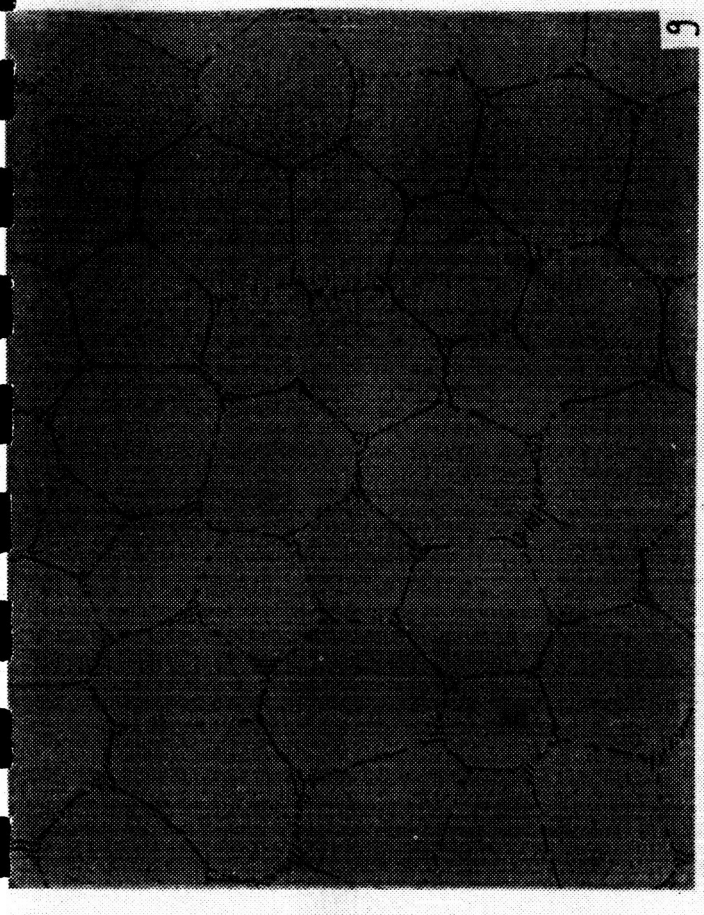

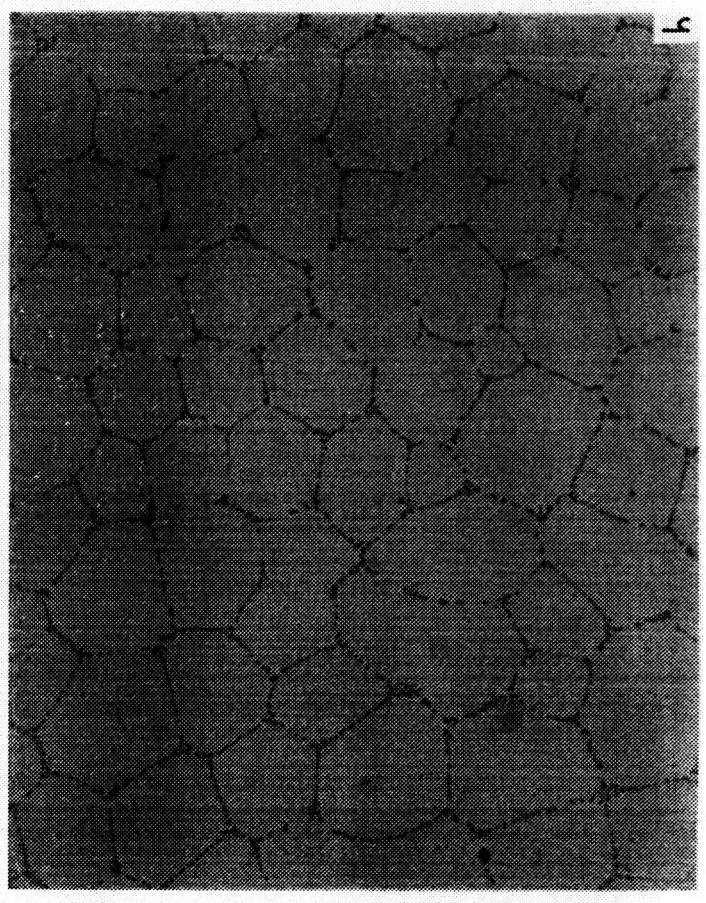

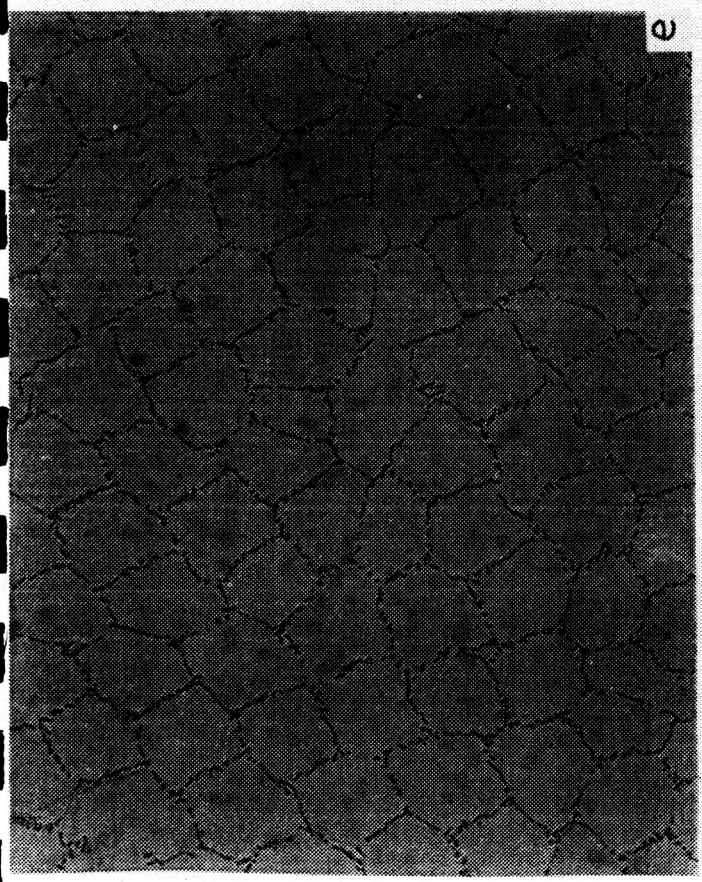

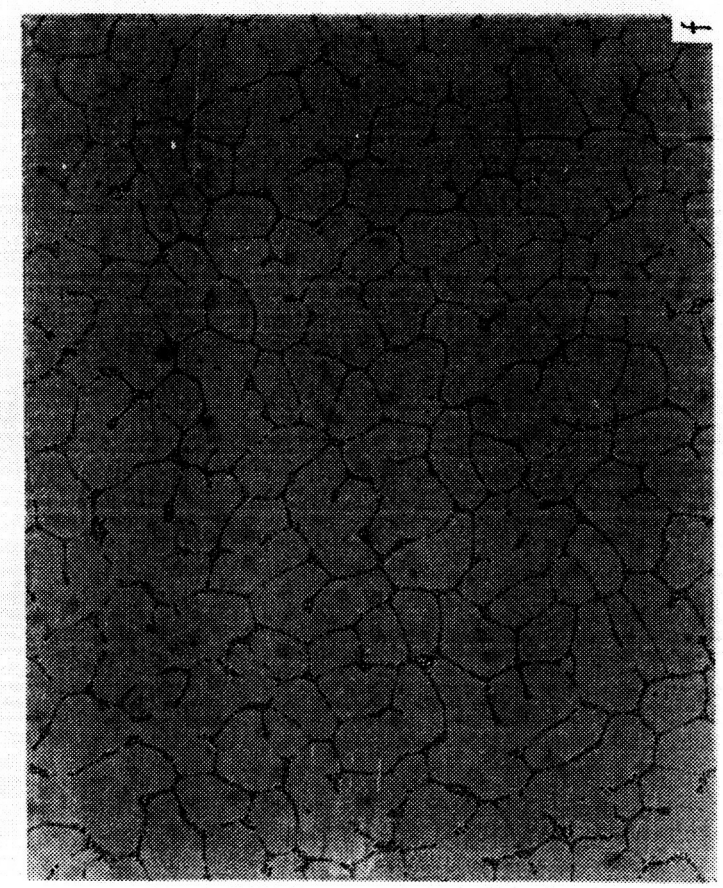

TABLE 2. Furnace Performance Requirements

For Space Experiments

Parameter	Requirement
Number of Space Samples	8
Gravitational Level	10^{-4} g
Sample Size (diameter & length)	5-6mm and 30-35cm
Sample Material	Al alloys
Maximum Sample Temperature	1000°C
Temperature Gradient	50 to 150°C/cm
Cold End Temperature	10 to 40°C
Quench Capability	10 to 15°C/s
Translation Rate	4 to 40 mm/min
Crucible Atmosphere	argon
Crucible Material	graphite
Sample Instrumentation	6 temperature sensors

PROJECT TITLE: Deep Undercooling of Ni and Fe Aluminides

COMPANY INVOLVED: Armco, Inc.

PROJECT LEADERS: William F. Flanagan, Vanderbilt University
Rollin Hook, Armco, Inc.

PROJECT DESCRIPTION:

Solidification of metal alloys far below their equilibrium freezing point results in a refinement of the microstructure and a more chemically homogeneous alloy. Such "deep undercooling" is expected to improve the properties of alloys of aluminides. Such an example is an alloy containing zirconium, where embrittlement occurs due to incipient melting of a zirconium-rich phase. Initial work on this project is concentrated on Ni-based aluminides. The intrinsic low-temperature brittleness of these alloys is ameliorated by boron additions to sub-stochiometric Ni_3Al alloys. The effect of boron on the refined microstructures is therefore of particular importance.

PROGRESS:

Several of the goals set out at the initiation of the project have been achieved this past year. One of our first tasks was to develop a test for obtaining values of the mechanical properties of the aluminides; in particular, a quantitative measure of ductility. The need for a nonstandardized test arose due to the small size of samples resulting from low-g experimentation in drop tubes. Given the facilities readily available, it was envisioned that bend test complemented with finite element modeling (FEM) should yield the desired information with good reproducibility and fast implementation. The data obtained from a bend tests are in the from of a force vs. deflection (F vs.δ) curve (cf. Figures 1 and 2). These data alone give very little quantitative information about the plastic properties of the material. However, these properties may be obtained indirectly by comparing experiments with finite element results. Given that one of the input parameters in FEM is the flow stress as a function of strain (σ vs. ε in tension) for the material under study, we expect that this parameter can be treated as a variable in order to obtain different theoretical F vs. δ curves, which can then be matched with the experimental one. The validity of this technique can be verified by doing bend tests on materials of known flow properties, thus the FEM results should match the experimental ones if in fact the technique is sound. At present this assessment is under way.

Obtaining good samples has unfortunately been a problem this year due to inadequate time available on the drop tube, which is mostly beyond our control. This situation is improving, and rapid progress is expected.

Theoretical analyses of the aluminides solidifying in the drop tube have shown that it is possible to deeply undercool samples of adequate sizes (i.e., $\approx$ 5mm dia.) of these alloys. Notwithstanding limited access to the drop tube, a few samples have been obtained. The first one, obtained earlier this summer, was an aluminide of composition 72.77wt%Ni, 16.6wt%Fe, 10.2wt%Al, 0.6wt%Zr, and 0.015wt%B. Although the extent of undercooling (if it occurred at all) could not be determined, microstructural examination revealed distinct differences between the as-received ingot material and this sample (see Figures 3 and 4). As shown in Figure 3, the as-received alloy consists of large plates of ß in a matrix of γ (which has decomposed on cooling into $\gamma + \gamma'$). Notably, a reaction occurred between the ß and γ which resulted in γ' forming peritectically at the interface between the two phases. In some instances, the peritectic γ' is contiguous with the γ' which later forms in the γ phase on cooling. The phases are confirmed by EDX measurements of their compositions. Figure 4, a micrograph of the sample processed in the drop tube, shows that the peritectic reaction has been suppressed, the ß-phase distribution completely modified, and the $\gamma \rightarrow \gamma + \gamma'$ reaction not noticeable. The significance of these first results is the confirmation of the expectation that drop tube solidification yields different phase distribution and morphologies in nickel aluminides. Recently we have obtained more samples, but analysis of them is not yet complete. We still have no undercooling information for this last set of samples, but we expect that we will get information from their microstructures.

We expect the equipment problem to be circumvented soon, and to start testing dropped samples in three months' time. For next year, we intend to generate a considerable amount of data as outlined here, and also plan to perform experiments other than drop tube, such as splat quenching.

ADDITIONAL PROJECT PERSONNEL:

Gabriel Carro, Vanderbilt University
Donald W. Johnson, Armco, Inc.

ORIGINAL PAGE IS
OF POOR QUALITY

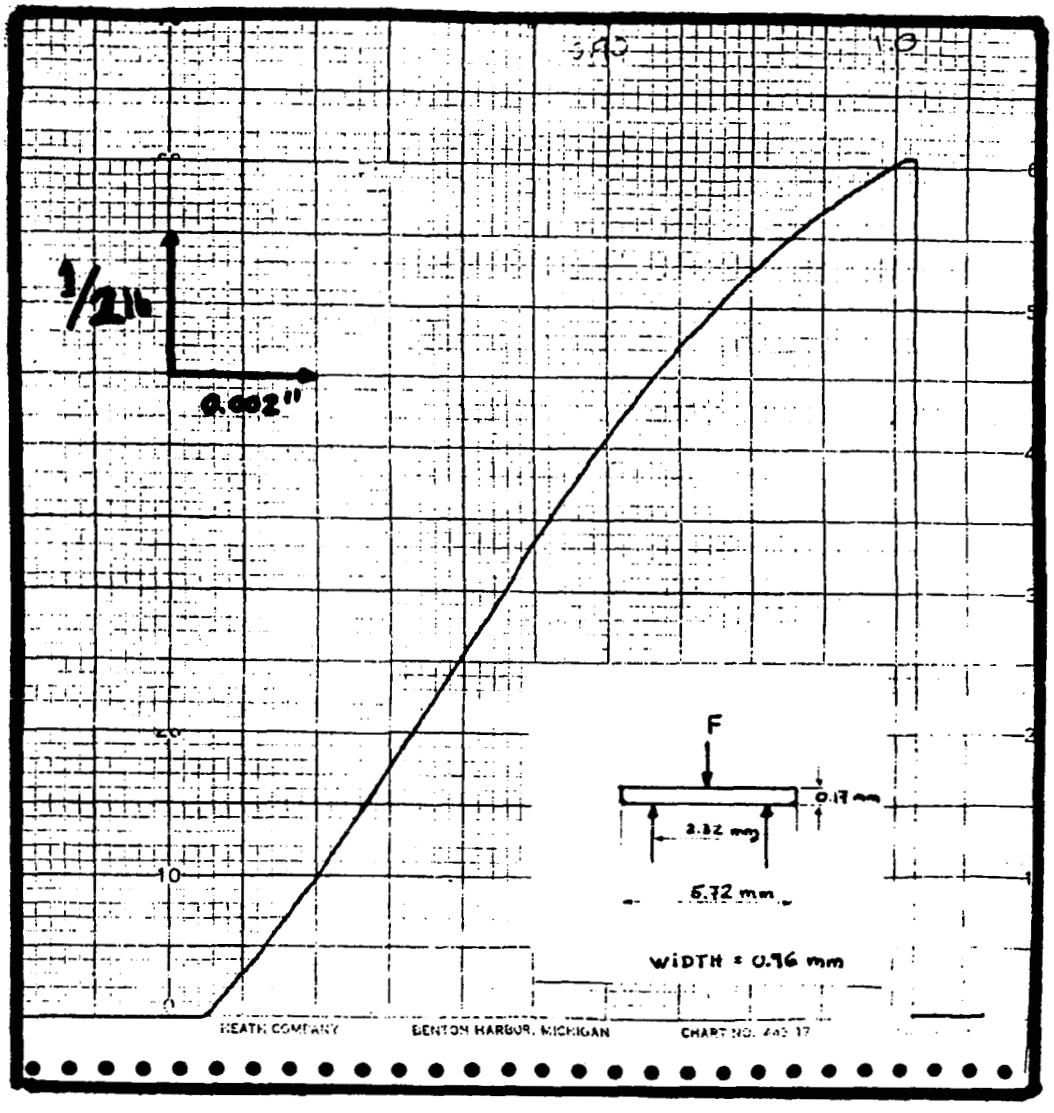

Fig. 1 F vs δ curve obtained with a sample of 440C stainless steel. Dimensions are shown.

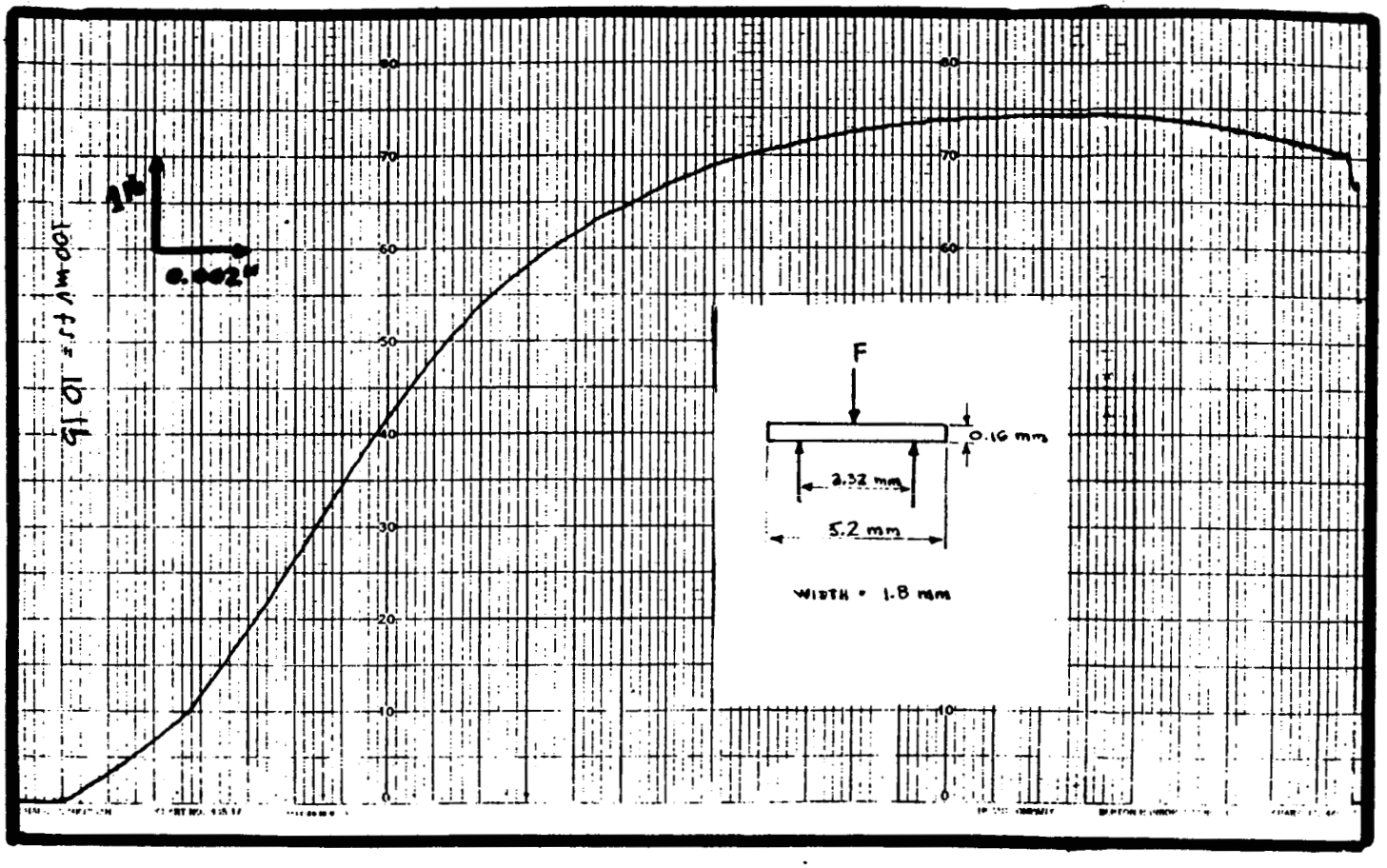

Fig. 2 F vs δ curve obtained with a sample of 4140 steel. Dimensions are shown.

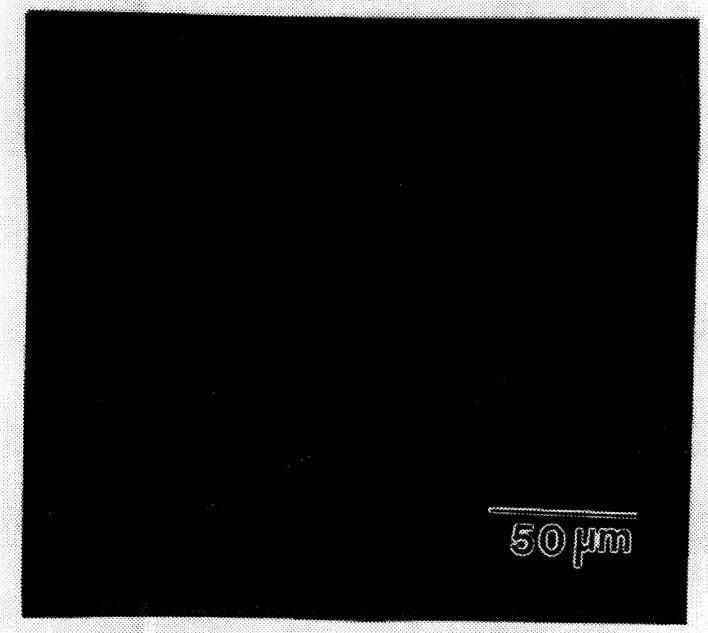

Figure 3a. Optical micrograph of as-received Ni-Aluminide alloy, V2096. (400X)

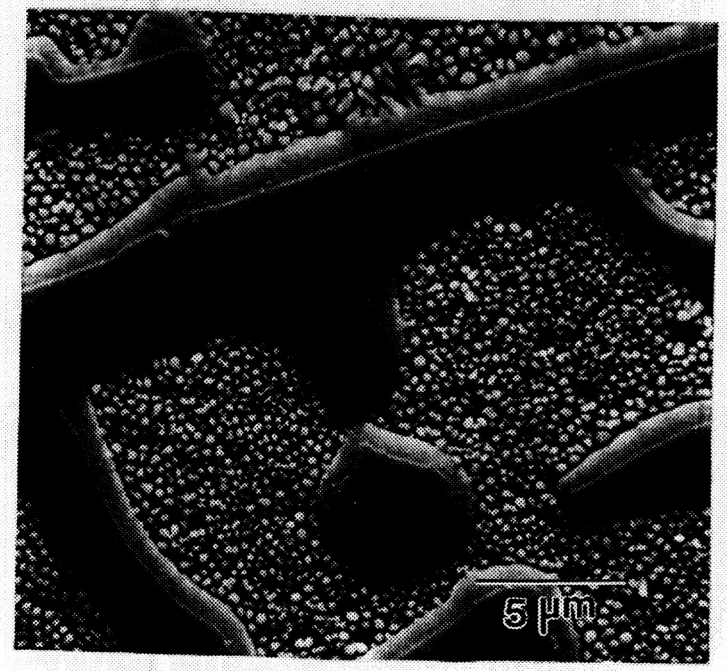

Figure 3b. SEM micrograph of as-received Ni-aluminide alloy, V2096. (4000X)

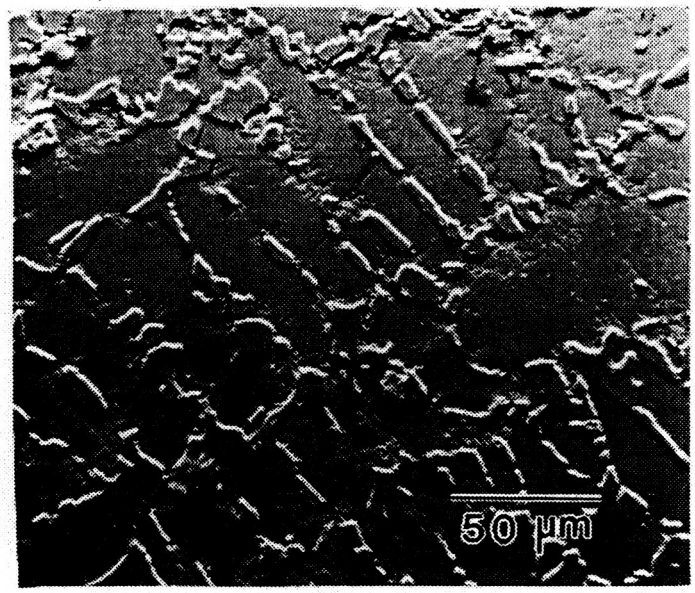

Figure 4a. Ni-alumnide alloy, V2096, levitated and solidified in the drop tube. (400X)

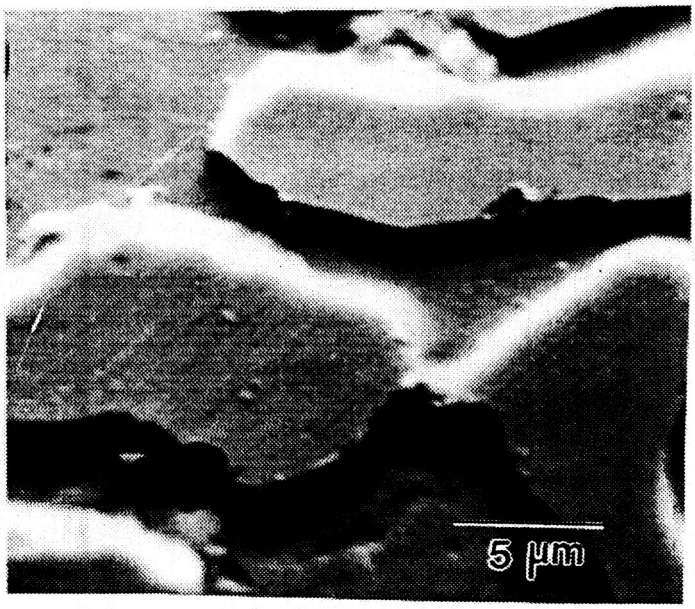

Figure 4b. Ni-alumnide alloy, V2096, levitated and solidified in the drop tube. (4000X)

PROJECT TITLE: Purification of Niobium by Containerless Processing

COMPANY INVOLVED: Cabot Corporation

PROJECT LEADER: G. J. Abbaschian, University of Florida

PROJECT DESCRIPTION:

This project was initiated in June, 1986 with the cooperation of Cabot Corporation, University of Florida, and Vanderbilt University. During this period, initial planning and a literature summary of the project have been completed. The project goals and schedule are described below.

MAIN OBJECTIVES

The primary objectives of this research program, based on theoretical, technological, and experimental considerations, may be summarized as follows:

A. Create a thermodynamic data base for the process of desorption of interstitial impurities. The data base is expected to yield information about the most efficient path for purification as well as the hierarchy of interstitial desorption, i.e., in the presence of two or more impurities, the sequence of the desorption of interstitials.

B. Determine the mechanism of desorption of the impurities in order to determine the rate-controlling step in each case.

C. Determine the kinetics of desorption.

D. Identify the most efficient measurements for monitoring the purification process.

E. Gain a capability to predict the extent of purification under a given set of conditions.

EXPERIMENTAL PLAN

All experiments at the University of Florida will be performed by using an electromagnetic (EM) levitation apparatus. Since the melting of Nb samples will be carried out in a containerless manner, the possibility of impurity pick-up during processing is greatly reduced. In addition, the system offers

the advantages of using various gas atmospheres of vacuum, easy control and analysis of the gases, and the ability to control the sample temperature at will, followed by rapid quenching if desired. Also, samples can be cycled through desired temperature ranges for long periods of time, thus offering a way to monitor the purification process with relative ease. Concurrently, additional experiments will be performed in the NASA drop tube facility by Vanderbilt. These experiments will be followed by KC-135 and/or shuttle experiments.

The following binaries will be used initially to study the purification process:

Nb-H, Nb-C, Nb-N, and Nb-O.

Ternary and higher-order systems will be considered at a later date.

In addition to vacuum, the effect of gas atmosphere on the purification will be investigated by using the following gas mixtures:

* Neutral : Ar, (Ar+He)
* Oxidizing : ($Ar+O_2$)
* Reducing : ($He+H_2$)
* Mixed : H_2/H_2O, CO/CO_2

The following monitoring/controlling and characterization techniques will be used in the EM levitation experiments:

Temperature: Two color pyrometer for temperatures up to 1700 °C and a calibrated single color pyrometer for higher temperatures, both with automatic recording capability.

Gas Flow and Composition: Gas flow will be monitored and controlled with on-line flow meters. The gas composition will be monitored by using a gas chromatograph with an automatic time-based sampling system for both inlet and outlet gases (Teledyne Brown has indicated that it may be able to donate a gas chromatography unit for this purpose).

Impurity Measurement: Samples quenched from the holding temperature (or after a predetermined number of cycles) at various time intervals will be analyzed by electron microprobe for microstructure. Samples also will be sent to Cabot for their in-house analysis of C, N, O, and H contents.

Surface Tension: As discussed later, surface tension (of the gas/metal interface) is one of the variables which affects the purification kinetics. Also, a reliable measurement of surface tension may offer a simple method to monitor the purification process in-situ.

KINETIC MEASUREMENTS

In general, the exact functional dependence of purification kinetics on the rate limiting (controlling) step for a particular species of impurity will probably depend on several factors:

* Temperature
* Interfacial Tension
* Gas Composition and Pressure
* Gas Flow Rate
* Diffusivity in the Liquid
* Convective Currents in the Liquid
* Interaction Between Impurities (for ternary and higher order systems)

Therefore, in order to determine the purification kinetics, the functional dependence will be investigated by varying the temperature, interfacial tension, and/or gas composition. It should be noted that among other factors, the interfacial tension is a function of both the temperature and the composition.

In the presence of convective currents in the liquid, diffusivity in the liquid is not expected to be rate controlling for any of the species. The interactions between impurities are not a consideration for binary systems; however, they may have a significant effect in higher order systems.

INTERFACE TENSION MEASUREMENTS

The kinetics of gas/liquid interfacial reactions are altered by the magnitude of the interfacial tension. Conversely, the interfacial tension is affected by the presence of surface-active impurities. Since the interstitial impurities presently under consideration can be categorized as being surface-active, surface tension measurements can be correlated with the impurity content of the liquid metal. Thus, a continuous surface tension measurement of the levitated droplet may offer a simple method for monitoring the purification process in-situ.

The interfacial tension of a levitated liquid droplet can be measured "accurately"* by measuring its natural oscillation frequency in an electromagnetic field; the interfacial tension and principal frequency of oscillation are related through the Raleigh equation.

It is conceivable that the above mentioned technique can be used to qualitatively measure the surface tension as a function of temperature, gas composition, and impurity concentration and type. These measurements should create a comprehensive data base which can then be used to monitor the purification process. The results will be used to compliment the data gathered by the other methods for measuring impurity content of the metal, which are essentially non-continuous.

SCHEDULE

A meeting between the cooperating parties was held in Orlando on the 5th of October. The experimental plan and schedule were finalized during this meeting. Purification experiments to test the various systems will be started by the end of this year. Cabot will supply samples in rod shapes with 1/4 inch diameter. The samples will be cut at Vanderbilt and then sent to the University of Florida for levitation and purification experiments.

---

*At this time we are skeptical of the claimed accuracy of the measurements. This is because our experiments show that levitated samples show mixed rotational, oscillatory and translational vibrations, and it may be difficult to isolate one from the other.

ADDITIONAL PROJECT PERSONNEL:

R. J. Bayuzick, Vanderbilt University
P. K. Kumar, Cabot Corporation

PROJECT TITLE: Containerless Processing and Rapid Solidification of Platinum-Cobalt Magnet Alloys

COMPANY INVOLVED: Engelhard Corporation, Carteret, NJ

PROJECT LEADER: Tony Overfelt, Vanderbilt University

PROJECT DESCRIPTION:

Excellent permanent magnets can be made from the 50-50 atomic percent Pt-Co alloy. In addition to the large energy products available (9.5 MGOe), these magnets also exhibit ductility, toughness, and superb corrosion resistance. Some difficulty has been encountered in consistently producing Pt-Co alloy cast bars and this has resulted in a variation of the magnetic properties. This variability is thought to be due to macrosegregation effects when the casting solidifies. The Pt-Co phase diagram shows the liquidus and solidus lines to be separated by no more than about 20°C throughout the composition range. This usually is indicative of an alloy system that is not strongly segregating. However, it is well known that the coercivity of a permanent magnet is extremely structure sensitive. In this system, the coercivity mechanism is thought to be domain wall pinning due to the high crystal anisotropy of crystallites of ordered FCT material in a disordered FCC matrix. The suspected segregation would affect the size and/or distribution of the FCT crystallites. It is felt that containerless processing and rapid solidification driven by deep undercooling will eliminate the segregation. Alloys to be investigated include PtCo, PtCo-C, and PtCo-B.

PROGRESS:

An extensive review of the literature of PtCo permanent magnets has been completed. The theoretical mechanisms are understood and a need has been established for a re-examination of the magnetization reversal mechanism in light of contemporary reverse domain nucleation and growth theory.

Production samples of PtCo magnets were supplied to the Vanderbilt Center for analysis. One group of samples was of high remanence and had been noted by Engelhard as being of satisfactory quality. Another group of samples was of low remanence and had been rejected by Engelhard quality control. These materials were magnetically characterized at Vanderbilt and the results are shown in Table I. The conforming material is

slightly enriched in platinum and shows a high remanence ($4\pi Mr$) with a moderate H_{ci}. The composition of the nonconforming material is a little more enriched in cobalt, its remanence less than half that of the conforming material, and its H_{ci} is 32% larger. These results are in agreement with Engelhard's quality control results. However, the magnitude of the property differences does not appear to have been caused by the slight compositional difference. The microstructures of the high remanence and the low remanence samples are shown in Figures 1a and 1b, respectively. The ordering reaction (FCC → FCT) appears to have progressed further in the low remanence sample as evidenced by the mottled appearance of the large grain in Figure 1a. X-ray diffraction experiments on polished metallographic samples were unable to distinguish any significant differences in the production samples. Further x-ray diffraction work is in progress on powder samples. The most probable cause for this behavior is an unusual manufacturing variation.

Engelhard Corporation is preparing a series of PtCo and PdCo alloys with minor additions of Boron. These materials should arrive at Vanderbilt in the very near future, but to gain early insight into the behavior of the PtCo-B system, a couple of sample heats were prepared in the Vanderbilt levitation melter. The nominal compositions of these samples were $Pt_{50}Co_{50}$, $Pt_{47.5}Co_{47.5}B_5$, and $Pt_{45}Co_{45}B_{10}$ all in atomic percent. A couple of drops of each composition were made in the MSFC 100m drop tube. The tube was backfilled to 200 torr with He-6%H_2. No recalescence events were detected in the drop tube experiments on any drop due to detector signal amplification problems. Two splats were also produced from the 10 a/o B heat.

Hysteresis loops were obtained from each sample and the intrinsic coercivities are shown in Table II. As noted in the Project Description of this report, the coercivity mechanism in these materials is thought to be domain wall pinning due to the large crystal anisotropy of ordered FCT crystallites in a disordered FCC matrix. The ordering reaction occurs at 825° C for the equiatomic composition of PtCo. The levitated and slow cooled samples (undercooling not measured) with B exhibit H_{ci} from 2100 - 2830 Oe, whereas the PtCo sample's H_{ci} was measured as only 80 Oe. This large difference could be due to differences in cooling rate through the ordering region as well as differences in composition. The effect of cooling rate (and probably also large undercooling) is demonstrated by the low H_{ci} values of the drop tube samples and the splats. The low coercivities of these samples are probably due to the absence of

appreciable amounts of the ordered phase. Electron microscopy and x-ray diffraction experiments are planned to confirm this point.

During alloy preparation experiments, it was discovered that large masses of $Pt_{50}Co_{50}$ alloy could be significantly undercooled while in contact with a quartz crucible. In fact, a 10g sample of $Pt_{50}Co_{50}$ was repeatedly undercooled in excess of 17% of T_{melt}. The molten alloy apparently did not wet the quartz. The sample was sectioned and polished for metallographic examination. Figures 2a and 2b shows 61X and 250X micrographs of this sample after etching with 60% HCl and 40% HNO_3. In Figure 2a the surface that was in contact with the quartz is at the bottom and the contact angle is at the bottom left and appears to be about 125°. Large grains (~300μm) are present along the alloy/quartz interface. The grain size decreased rapidly to about 80μm in the interior of the sample (Figure 2b). Only a few grain boundaries in the interior of the sample were attacked by the etchant. There appears to be a considerable amount of second phase in Figure 2b. This second phase was attacked by the etchant and is the pitted regions in Figure 2b.

X-ray diffraction experiments were performed on polished metallographic samples of production PtCo material, material completely disordered at 1000°C, a sample completely ordered at 600°C, and a specimen from the 10g, 17% undercooled sample. These spectra are shown in Figure 3. The familiar FCC peaks are shown on the spectrum from the disordered sample. The spectra from the ordered sample exhibits well defined peaks from the FCT phase. The production sample's spectra shows a mixture of the two phases. The spectra from the 17% undercooled sample exhibits the FCC peaks almost exclusively. Two broad peaks at 54.5° and 81° and a small sharp peak at 90.5° indicate the presence of a small amount of the FCT phase.

Many rapidly solidified permanent magnet materials exhibit low intrinsic coercivities in the as-solidified condition. Subsequent annealing then often increases H_{ci} by orders of magnitude. It was anticipated that these alloys would exhibit similar behavior. A series of ordering experiments at 600-650°C were then performed on the splat quenched sample and a specimen from the 10g 17% undercooled sample. The intrinsic coercivities were measured as a function of time at temperature. The sample was cooled from the annealing temperature in a 5 kOe magnetic field to assure saturation. Figure 4 shows the results. H_{ci} increases by an order of magnitude for both the $Pt_{50}Co_{50}$ sample

and the $Pt_{45}Co_{45}B_{10}$ sample upon annealing for 15 minutes at 600-650°C. Both samples exhibit a peak in H_{ci} at 15 minutes and then H_{ci} declines thereafter. H_{ci} for the $Pt_{45}Co_{45}B_{10}$ sample doesn't increase as much as for the $Pt_{50}Co_{50}$ sample but shows less scatter in the data presumably due to a more homogeneous bulk structure.

PLANS FOR NEXT YEAR:

The PtCoB and PdCoB samples from Engelhard Corporation will be processed in the standard manufacturing sequence, in the MSFC drop tube, in the melt spinning system at LRC, and in the Vanderbilt levitation melter with and without the splat quencher. Characterization of the magnetic properties and microstructures will continue.

ADDITIONAL PROJECT PERSONNEL:

John Teubert, Vanderbilt University
Richard D. Lanam, Engelhard Corp.

TABLE I

PROPERTY COMPARISON: CONFORMING AND NONCONFORMING MATERIAL

PROPERTY	CONFORMING	NONCONFORMING
a/o Pt	50.81	51.25
a/o Co	49.19	48.75
$4\pi M_r$ (kG)*	5.2	2.5
H_{ci} (kOe)	6.2	8.2

*corrected for demagnetizing effects

TABLE II

INTRINSIC COERCIVITY (H_{ci}) OF AS-CAST SAMPLES

	H_{ci} (Oe)		
COMPOSITION	LEVITATED AND SLOW COOLED	DROP TUBE	SPLAT QUENCHED
PtCo	80	60	X
$Pt_{47.5}Co_{47.5}B_5$	2830	300	X
	2100	60	X
$Pt_{45}Co_{45}B_{10}$	2290	160	X
	2140	160	220

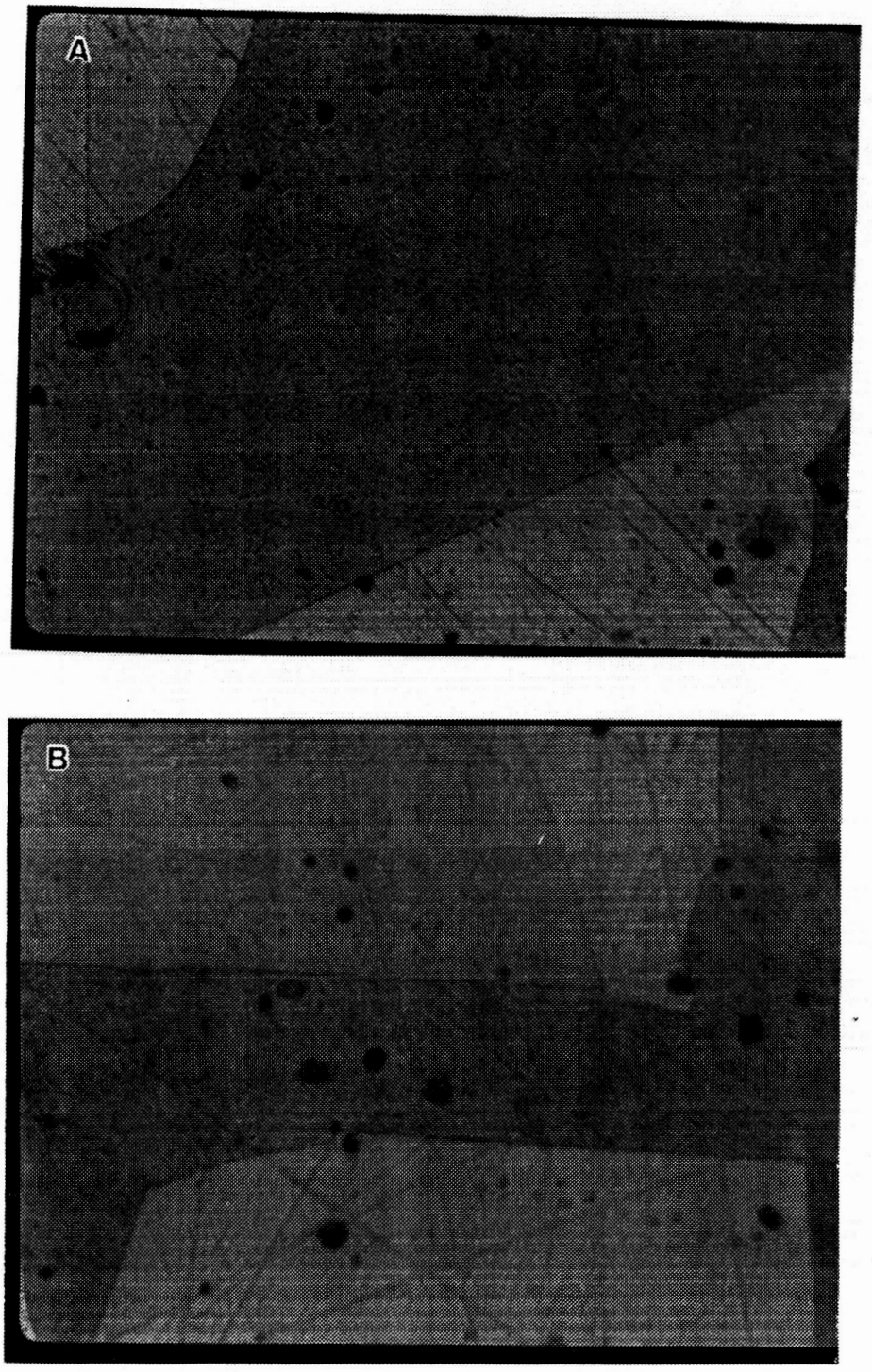

FIGURE 1. (a) High Remanence PtCo Production Sample.
(b) Low Remanence PtCo Production Sample.
Etched with 60% HCl and 40% HNO_3. 1000X

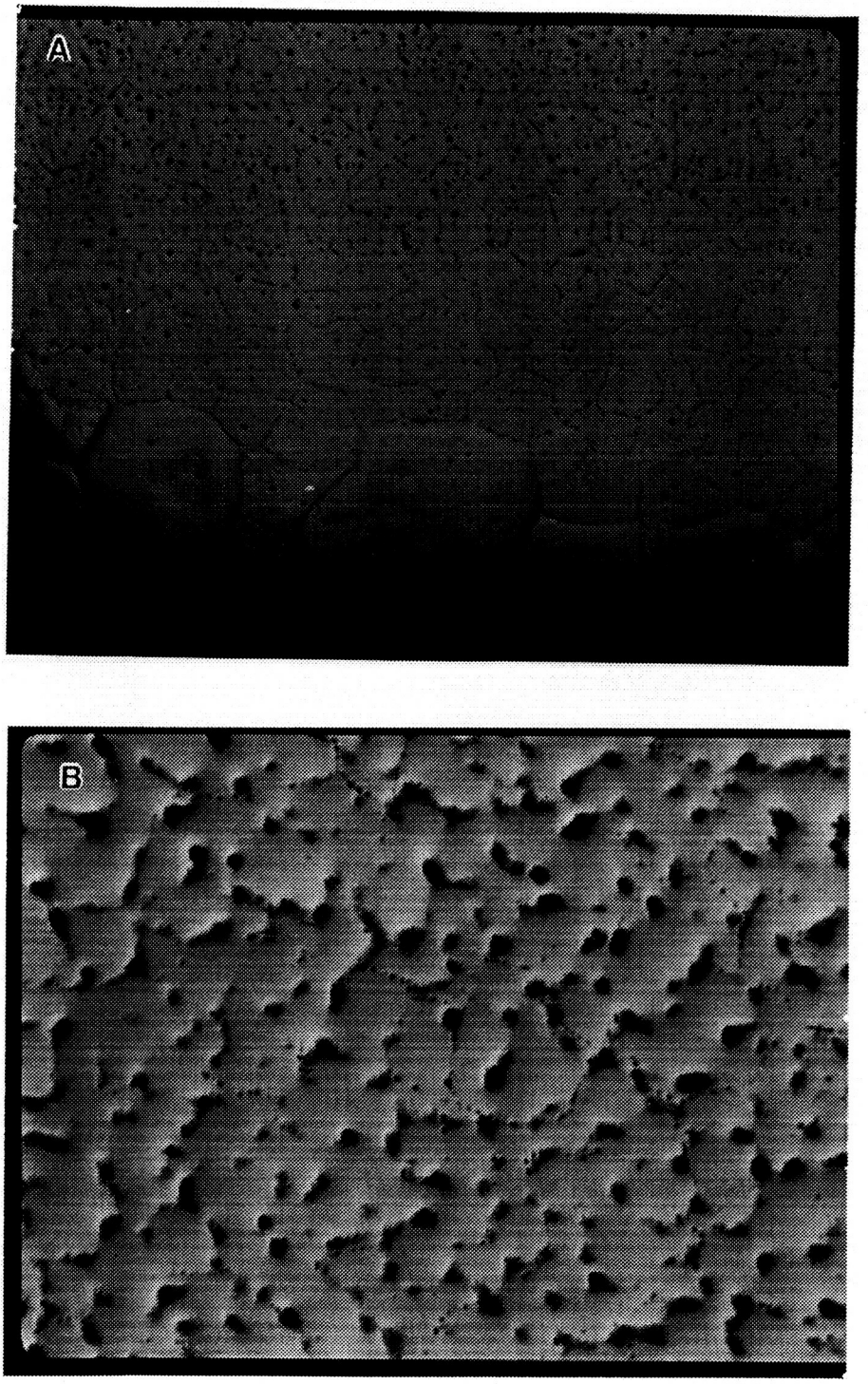

FIGURE 2. (a) Contact Angle Region of the 10g PtCo Sample Undercooled 17%. The surface in contact with the quartz is at the bottom. 61X

(b) The Interior of the 10g Sample. Etched with 60% HCl and 40% HNO_3. 250X

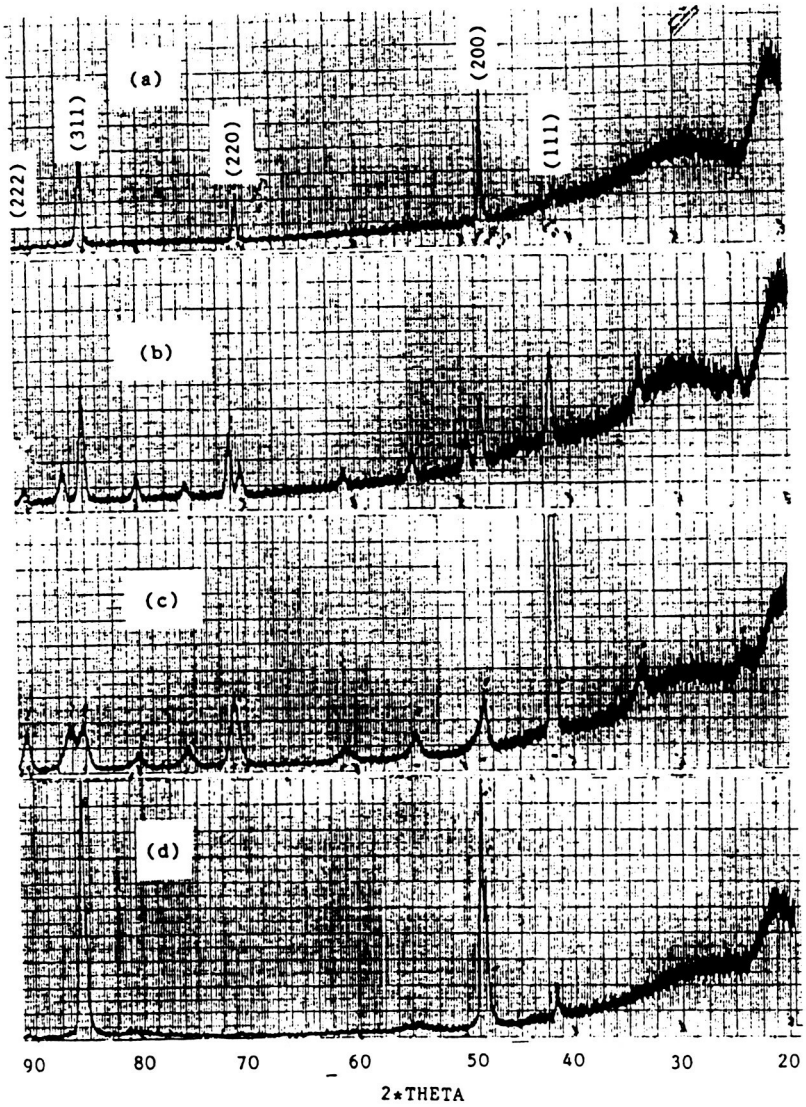

FIGURE 3. X-ray diffraction spectra from polished samples of:
(a) completely disordered,
(b) completely ordered,
(c) production sample, and
(d) 17% undercooled

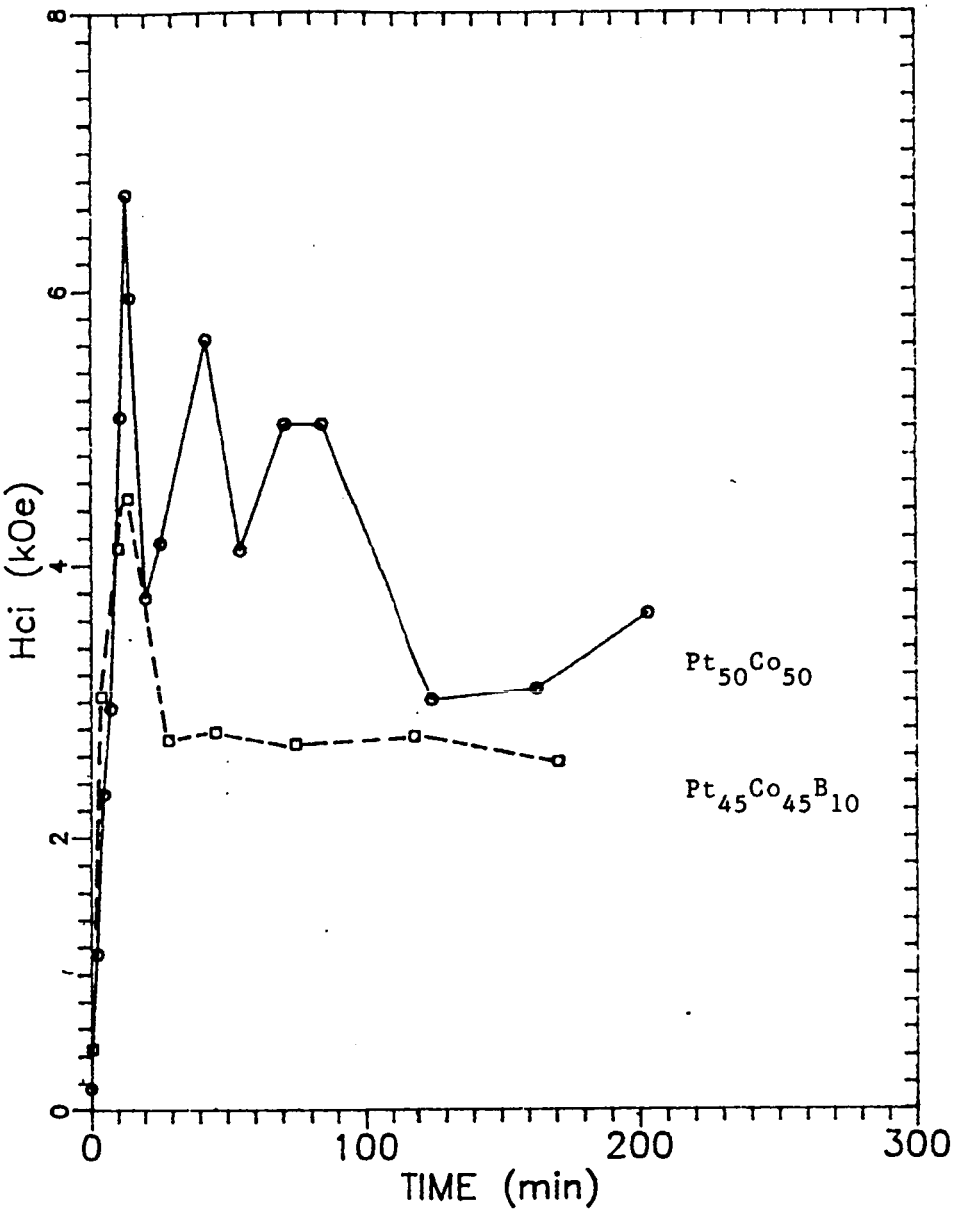

Figure 4. Variation of intrinsic coercivity with approximate time at 600-650°C for $Pt_{45}Co_{45}B_{10}$ splat and $Pt_{50}Co_{50}$ sample undercooled 17%.

PROJECT TITLE: Containerless Processing and Directional Solidification of Platinum Group Refractory Metal In-Situ Composite Materials

COMPANY INVOLVED: Engelhard Corp., Carteret, NJ

PROJECT LEADERS: A. M. Strauss & J. M. Williamson, Vanderbilt University

PROJECT DESCRIPTION:

The maximum operating temperature of many combustion processes is determined by the temperature that the materials are able to withstand. The platinum group metals have unique characteristics of relatively high melting points, good oxidation resistance, and good corrosion properties. However, the use of these metals is limited by the high initial cost of the metal. The refractory metals, on the other hand, are far less expensive, have even higher melting points, but suffer from poor oxidation resistance. It is postulated that forming in-situ composites from eutectic or off-eutectic binary alloy combinations of refractory and platinum-group metals could result in a new generation of high-temperature materials. A major problem in doing experiments with such alloys is the high temperatures required and consequent interactions with crucible materials. Containerless processing in space would overcome this problem. Added benefits of space would be vacuum processing (which is required for many of the refractory materials) and microgravity to produce a more perfect continuity and alignment of the fiber components.

The mechanical properties of in-situ composites are governed by the volume fraction of the reinforcing phase, the morphology of the eutectic structure (lamellar or fibrous), and the distance between the phases. Variations in volume fraction can be obtained by using off-eutectic alloys or by using ternary alloys. The morphology of the eutectic structure is usually fibrous at volume fractions of about 30% or less and lamellar at higher volume fractions. The distance between the phases can be minimized by maximizing the growth velocity during solidification.

Long term microstructural stability at elevated temperatures is required to maintain the mechanical properties. Degradation of the microstructure can result from oxidation, matrix-fiber interaction, and fiber coarsening. Each of these can lead to ineffective load transfer from the matrix to the fibers and subsequent loss of mechanical properties.

It is felt that initial drop tube solidification experiments with eutectic and off-eutectic alloys of platinum group and refractory metals will provide insight into the microstructures obtainable under low-g solidification with various solidification rates. High temperature stability experiments can also be done on these samples and thus the most promising alloy(s) determined for additional work with much larger directionally solidified specimens. The directional solidification studies would be performed in both conventional 1g furnaces as well as the directional solidification furnace in the KC-135 aircraft.

Testing of the composite materials would include determining mechanical properties at elevated temperatures, determining oxidation and environmental interactions at elevated temperatures, and determining the corrosion resistance. The resulting composite materials may represent a new generation of high-performance materials for critical applications.

PROGRESS TO DATE:

The Pt-Cr and Pd-Cr alloy systems have been identified as candidates for the initial study. Both of these alloys have been classified as normal eutectics, meaning they produce rod or lamellar microstructures which are more desirable from a mechanical strength perspective than the discontinuous or flake microstructures of the anomalous non-normal eutectics. Transformations below the eutectic are minimal in both alloys. A survey of the literature related to directional solidification, in-situ composites, and convection has been conducted.

We have found that a directional solidification furnace that meets the high temperature requirements of this project is not currently available (commercially or otherwise). Consequently, we are in the process of developing and building a high temperature (2000°C +) furnace. The automated directional solidification furnace at the Marshall Space Flight Center will suffice for Pd-Cr and Pt-Cr studies. The first Pt-Cr sample rod has just been received from the Engelhard Corporation and other samples are on order. Metallography techniques have been developed for the Pd-Cr alloy.

ADDITIONAL PROJECT PERSONNEL:

Mark Wells, Vanderbilt University
Richard D. Lanam, Engelhard Corp.

PROJECT TITLE: Containerless Purification of Iridium and Ruthenium

COMPANY INVOLVED: Engelhard Corporation, Carteret, NJ

PROJECT LEADERS: Alvin M. Strauss and John W. Williamson
Vanderbilt University

PROJECT DESCRIPTION AND OBJECTIVES:

Iridium and ruthenium possess corrosion and high temperature strength properties which make them attractive for industrial applications. Both materials exhibit brittle behavior and poor workability. While these characteristics may be inherent to the structure of the materials, it is possible that they are a result of interstitial impurities at the grain boundaries.

It is the purpose of this investigation to determine the role of impurities and their effect on the ductility of these materials. The purity of sample materials will be improved by processing in a variety of environments using containerless processing methods. Once samples have been produced, mechanical tests will be conducted to characterize the workability and ductility of these elements. These properties will then be correlated to the level of impurities which may still exist within the material.

PROGRESS:

Sample Preparation by Containerless Processing

A total of fourteen successful sample drops have been made at the Marshall Space Flight Center in the 105m long drop tube. Seven of these were iridium; the remainder were ruthenium. All of these were melted by electron beam melting. Pure elements normally show 18 to 20% undercooling and impure materials typically exhibit undercoolings less than that. In the case of Ir, the range of undercooling has been 8 to 16%, and the two most recent tests indicate about 15.5%. For Ru, the range of undercooling has been 4 to 15%. Average undercooling of the three most recent tests was 12%. Ir drops are recovered as distorted spheres; however, Ru drops produce partial, external shells, powdered material, or some splat formed material. It is believed that the electron beam processing technique has decreased the impurity level somewhat, but the undercooling percentages tend to indicate that considerable impurities remain.

The electromagnetic levitator at Vanderbilt University is operational and has been significantly improved by Center personnel. A two-color pyrometer and a gas gettering system have been added. The gas gettering system includes a solid state monitor for measurement of O_2 levels. Continuous monitoring of O_2 levels during the processing of samples should permit the measurement of the reduction in oxygen levels with time. It has recently been demonstrated that Ir spherical samples can be levitated and processed with this EM levitator.

Aerodynamic levitation studies are continuing. Approximately two hundred tests of solid, spherical shapes have been conducted, and drag coefficient data have been produced. Regions of instability and the types of instability have been identified. A few initial efforts to couple the aerodynamic levitator with the electrodynamic levitator have been made, but--at this point in time--these efforts have been unsuccessful. These efforts are continuing with the expectation that these coupled methods may provide rapid undercooling, permit immersion of the samples in high-purity inert gases, or allow the introduction of a reducing atmosphere to help eliminate oxygen.

Measurement of Impurities

Some of the drop tube samples have been shipped to England for analysis by means of a glow discharge mass spectrometer. The results of these analyses have not been received.

Mechanical Property Characterization

Two methods are being studied for use in mechanical characterization:

1. This method seems to be promising. A three-point bending test rig has been designed by Mr. Gabe Carro. The test rig has been constructed and tested at room temperature. Results of circular specimens match the available theory well. (Also, FEM results

appear to match the experimental results.) Additional information concerning this apparatus has been reported by Prof. Flanagan and Mr. Carro in the project entitled, "Deep Undercooling of Ni and Fe Aluminides." An ATS furnace, capable of raising the temperature of the sample to 1200°C, has been ordered and will be incorporated into this apparatus.

2. An alternative method has been conceived for use with samples formed at the Marshall Space Flight Center drop tube. This method measures the total amount of energy dissipated within the sphere at the time of impact. Although specimen porosity will affect these results, we intend to pursue this alternative because of its relative simplicity. The method may have some value as a quick measure for comparing materials with various levels of impurities.

WORK PLAN: NOVEMBER 1, 1986 - OCTOBER 31, 1987

1. Additional drops of Ir and Ru utilizing higher grades of material will be conducted. Energy dissipation resulting from the impact and deformation of these drops will be attempted.

2. Additional materials will be processed at Oak Ridge National Labs at higher vacuum levels than those achieved at MSFC or Vanderbilt.

3. Additional test work associated with the combined jet and electromagnetic levitator will be conducted to test viability.

4. The ATS furnace and the bending test rig should be complete and available. Some Ir samples already processed at MSFC will be tested shortly thereafter.

5. It is expected that the element analysis by Engelhard Corporation of samples produced at MSFC will soon be available. These should show whether any reduction in impurity level has occurred.

6. Preliminary testing of preparation methods of Ir and Ru samples is now underway utilizing the electromagnetic levitator at Vanderbilt University. If the important process parameters can be adequately identified, then the probability of success in processing samples should be greatly enhanced.

ADDITIONAL PROJECT PERSONNEL:

R. A. (Tony) Overfelt, Vanderbilt University
Richard D. Lanam, Engelhard Corporation

PROJECT TITLE: Containerless Processing of Titanium Alloys

COMPANY INVOLVED: General Electric Corporate Research & Development

PROJECT LEADER: Robert J. Bayuzick

PROJECT DESCRIPTION:

Rapid solidification is being shown to offer a significant opportunity for new titanium alloy compositions based upon alloying constituents which have been previously unattainable because of segregation during ingot or powder solidification. The use of rapid solidification has permitted the creation of metastable solid solutions of titanium and elements like the rare earths, which can react at low temperatures in the solid state rather than the normal liquid state to form oxide or sulfide dispersoids. It has been found that dispersoid formers with the highest thermodynamic stability in the titanium alloy matrix, and therefore the greatest resistance to coarsening at high temperatures, are also often the elements which segregate most strongly during solidification or come out of solution at the highest temperature. Substrate quenching of these alloys by melt extraction or melt spinning results in a characteristic low segregation columnar grain structure for the bottom portion of the ribbon with an equiaxed much more heavily segregated structure in the upper portion of the ribbon. The reason for the abrupt transition from the columnar (slightly segregated) structure to the equiaxed (highly segregated) structure is not understood. Furthermore, the variegation in microstructure along with the large degree of segregation results in a poor product. Likewise, powder atomization of these same alloys results in a heavily segregated microstructure and again a poor product. The use of these advanced alloy systems to create high temperature titanium alloys depends on avoiding heavily segregated regions in order to prevent deleterious effects on the alloy's properties, and to fully utilize dispersoid additions. Containerless processing could well be the appropriate processing method to avoid segregation in bulk materials and/or to understand microstructural development in strongly segregating alloy systems. The ability to control solidification structure and to avoid heavy segregation in these alloys would significantly extend their capability as well as provide the basis for the development of new alloys.

RESULTS TO DATE:

Drop tube experiments have begun and the initial results are outlined in Table #1. Results of the optical studies of some of the samples which undercooled and solidified under microgravity conditions are encouraging. Ti-0.25B in the as-cast condition (Fig. 1a) is characterized by nonuniform grain size and strong segregation of boron to the grain boundaries. The processed sample (Fig. 1b) shows uniform grain size throughout. Strong segregation is still evident, but there is some evidence of sub-micron dispersions within the grains. Ti-4.0Ce in the as-cast condition (Fig. 2a) is also characterized by non-uniform grain size. The drop tube sample (Fig. 2b) displays an extremely fine grain size with strong segregation.

Current levitation melting experiments have been directed toward finding a suitable technique for in situ undercooling. Atmospheres of inert gas (argon at up to 300 torr) have proven inadequate for removing sufficient heat from the samples.

FUTURE PLANS:

Drop tube experiments on Ti-Ce, Ti-B, and Ti-Er alloys will continue. SEM and TEM will be used to characterize dispersoid distributions achieved. Levitation melting experiments with and without rapid quenching will also begin in the Vanderbilt University vacuum levitation system. Results of these experiments will be compared with melt spinning experiments done by GE.

ADDITIONAL PROJECT PERSONNEL:

Russell Kegley, Vanderbilt University
R. Grant Rowe, General Electric Co.
Gail Whoriskey, Vanderbilt University

TABLE 1

SUMMARY OF DROP TUBE RESULTS

Sample No.	Material	Undercooling		Notes
NT - 1254	Ti - 4.0 Ce	--		
NT - 1256	Ti - 1.0 Ce	296 K	15.2%	1
NT - 1257	Ti - 0.25 B	--		
NT - 1258	Ti - 2.0 Er	--		
NT - 1259	Ti - 4.0 Ce	260 K	13.4%	1,2
NT - 1260	Ti - 2.0 Er	--		1,3
NT - 1261	Ti - 2.0 Er	237 K	12.2%	1
NT - 1262	Ti - 0.25 B	289 K	14.9%	1,2
NT - 1263	Ti - 1.0 Ce	328 K	16.9%	1,2
NT - 1264	Ti - 0.25 B	--		3

NOTES:

1) Liquid present at impact
2) Recalescence detected before impact
3) Instrumentation problems

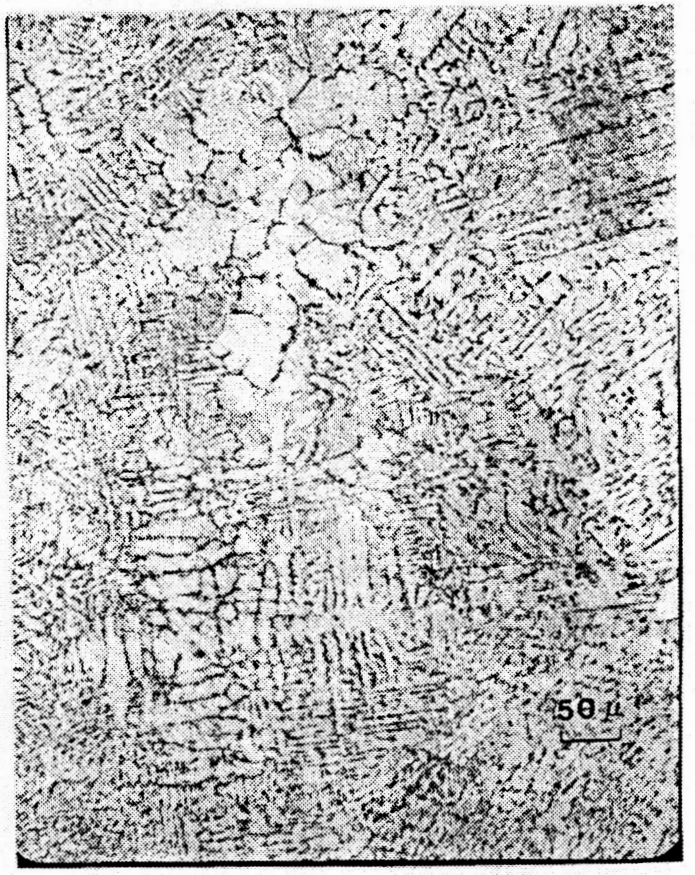

Fig. 1a
Ti-0.25B As-Cast

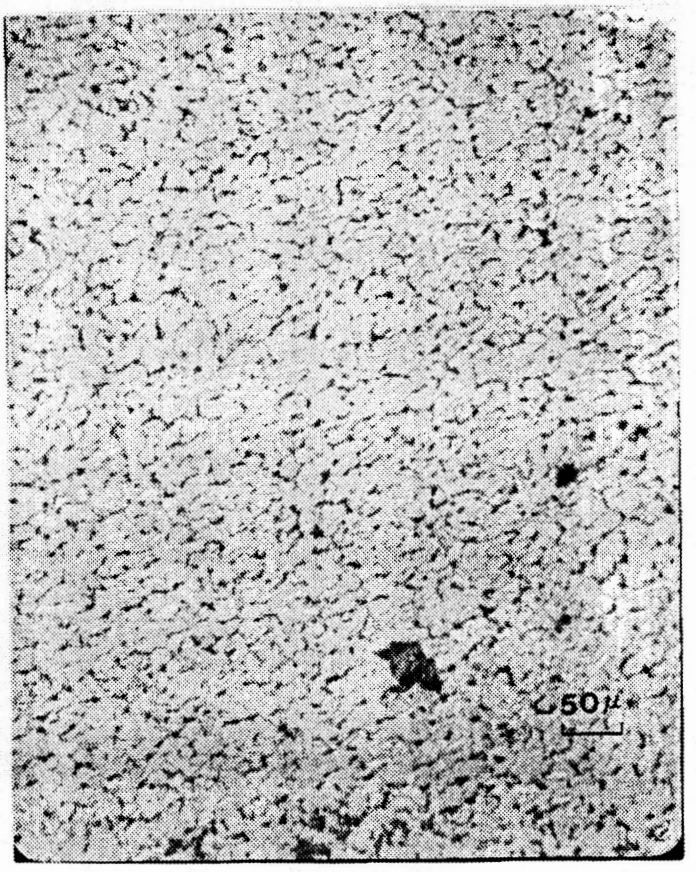

Fig. 1b NT-1262
Ti-0.25B Undercooled
289°K (14.9%)

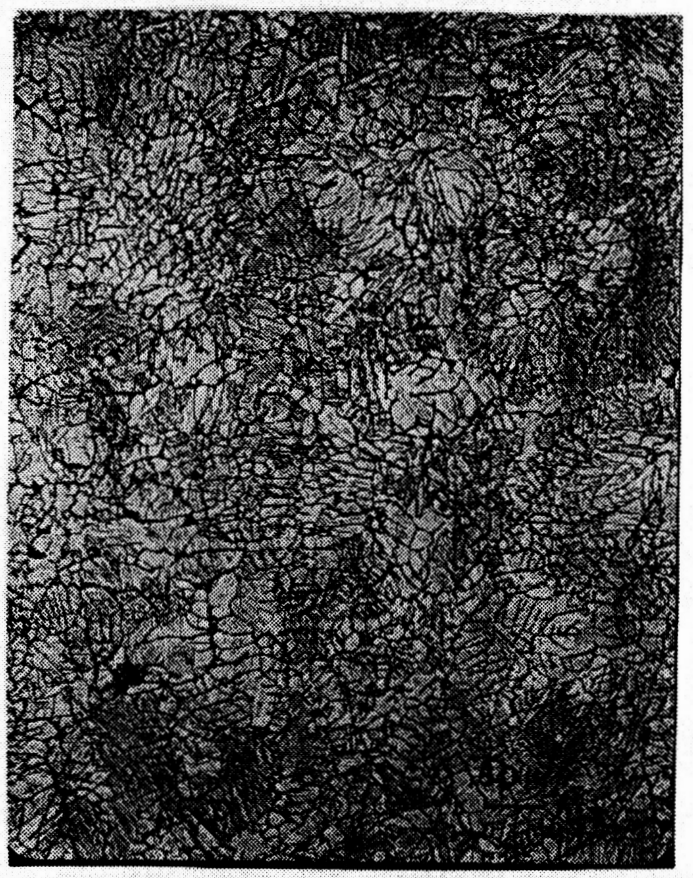

Fig. 2a
Ti-4.0Ce As-Cast

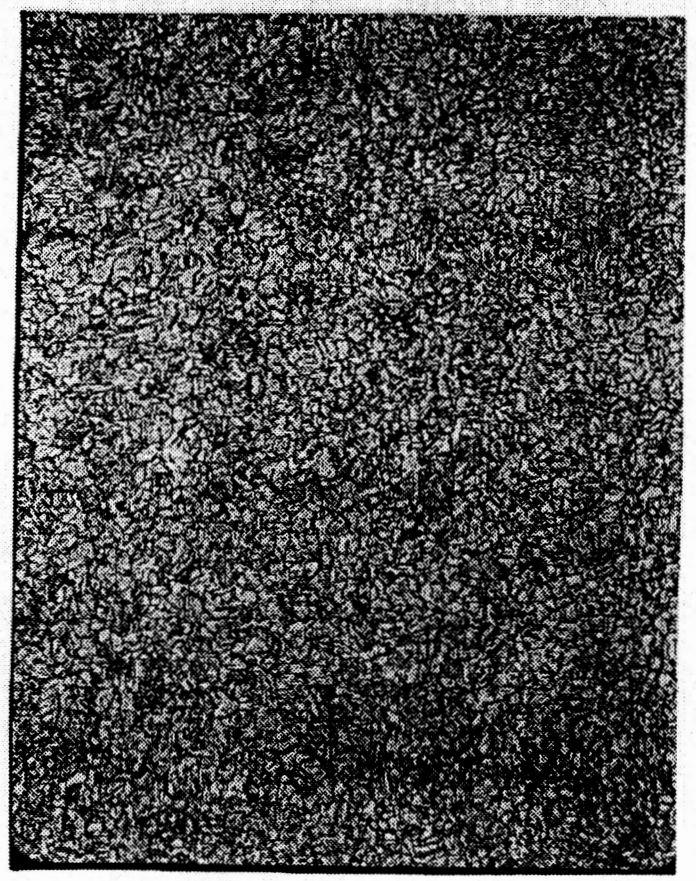

Fig. 2b NT-1259
Ti-4.0Ce Undercooled
260°K (13.4%)

PROJECT TITLE: Effect of Solidification Mode on Structure-Property Relationships of Lead-Base Immiscible Alloys [Pb-Cu, Pb-Al, Pb-Zn, Pb-Ni]

COMPANY INVOLVED: General Motors/Delco-Remy

PROJECT LEADER: B. D. Lichter

PROJECT DESCRIPTION:

The lead-base alloys of interest in the project show a liquid-liquid immiscibility gap at high temperatures. As a consequence, during solidification (casting), the liquids separate and tend to segregate due to the difference in the density of the two liquid phases. In the worst instance this may result in macro-inhomogeneity of the structure, and consequent deterioration of the properties (mechanical, electrical, etc.). It is observed that a high degree of undercooling promotes macro-homogeneity of the structure. This can be achieved through the process of rapid solidification.

Microgravity has been shown to promote a considerable degree of undercooling in melts with very high melting points. In some instances, this may eliminate segregation and therefore promote macrohomogeneity of the structure. Alternatively, a microgravity environment may, in general, promote a more uniform dispersion of a directionally solidified liquid-liquid immiscible system.

The studies conducted in this project will result in understanding of the electrochemical nature of certain alloy systems and will form a basis for identifying future grid alloys for further detailed investigation (i.e., fabrication, mass production, etc.). Hence, it was decided to start by studying the corrosion behavior of pure lead and the presently used Pb-Ca-Sn battery grid alloys ("standard" alloy) in order to develop a data-base which can be used to compare electrochemical properties of other lead-immiscible alloys (eg. Pb-Cu, Pb-Al, Pb-Zn, Pb-Ni) obtained under different modes of processing ,viz:

1. Rapid Solidification
2. Directional Solidification
   (a) Under a normal gravity environment
   (b) Under a microgravity environment

WORK PROGRESS:

In order to establish a data base on the corrosion behavior of pure lead and the Pb-Ca-Sn alloy, an extensive literature survey was done during the first quarter. During the same period, the following materials were procured from Delco-Remy:

(a) Pure Copper (99.99%)

(b) Pb-0.08wt%Ca-0.56wt%Sn-66ppmAl as cast and rolled sheet

The other materials which have been obtained are:

(1) Cu-37wt%Pb-3%Sn. A proprietary alloy, obtained through General Motors

(2) Rapidly solidified Pb-Cu alloys containing 10, 15, 20, 30% Cu - from General Motors

Metallographic Studies

We have carried out metallographic studies of the following materials:

(1) Pure lead

(2) Pb-Ca-Sn alloy

(3) Cu-Pb-alloy

The typical microstructures are as shown in Figure 1. The pure lead has equiaxed grains. The Pb-Ca-Sn alloy shows elongated grains due to the prior rolling treatment. The Cu-Pb-alloy shows a homogeneous distribution of lead and copper phases. The corrosion behavior of this alloy is expected to indicate the type of Pb-Cu alloys (in terms of composition and microstructure) that merit further investigation. Such Pb-Cu alloys can then be prepared by the different modes of solidification, as proposed.

Corrosion Studies

(A) Materials

Anodic and cathodic potentiodynamic polarization experiments were conducted to investigate the corrosion properties of the following:

(1) Pure lead (99.99%)

(2) Pb-0.08%Ca-0.56%Sn-66ppm Al

(3) Cu-37%Pb-3%Sn

(4) Pure copper (99.99%)

Varying concentrations of sulfuric acid solution electrolyte were used for these investigations:

	NORMALITY	SPECIFIC GRAVITY
1	10^{-3}	--
2	1	1.021
3	2.17	1.065
4	9.44	1.275

Employing the potentiodynamic method of investigation, rather than a galvanostatic technique, provides a quick screening of the alloys, which can be subjected to the entire gamut of potentials and acid concentrations, providing conditions not unlike deep-cycling battery applications. In addition, the corrosion rates at different potentials correspond to actual charge and discharge cycles.

(B) Experimental Conditions

All tests were conducted at room temperature. The experimental set-up consisted of a working electrode, two platinum counter electrodes, a reference electrode, a gas inlet and outlet, and a Luggin probe. Further experimental details are as follows:

(1) The potential values were measured against a saturated Hg/Hg_2SO_4 reference electrode. The standard potential of this reference electrode was found to be -650 mv on the standard hydrogen scale.

(2) The cell was purged with nitrogen prior and during the experiment.

(3) Acid solutions were prepared from concentrated sulfuric acid having an initial specific gravity of 1.84.

(4) A Princeton Applied Research Company (P.A.R.C.) potentiostat was utilized, which was interfaced with Apple IIE for computer controlled potentiodynamic experiments.

(5) The working electrode was allowed to reach the steady state corrosion potentials before scanning at a rate of 0.2 mv/sec.

(6) The results were compared on the basis of the following parameters as shown in Figure 2:

(a) Ecorr - Steady state corrosion potential

(b) Ip - Passive current density

(c) Ic - Critical anodic current density

(d) Epp - Primary passive potential

(C) Results

The behavior of the four different materials (i.e., Pb, Cu, standard alloy, Cu-Pb(-Sn) alloy) in the highest acid concentration (i.e., 9.44N acid solution) is summarized in Figures 3 and 4. Both pure lead and the standard lead alloy passivate in these solutions. Although a limiting current is attained for copper, "true" passivation does not occur.

For the copper-lead alloy, a "pseudo-passive" effect is observed. Nevertheless, for comparison purposes we present the apparent passive parameters (Epp and Ip) for these alloys.

In general, the following observations were made:

(1) Ecorr decreased (became more negative) with increasing acid concentration.

(2) Ic decreased with increasing acid concentrations indicating greater ease of passivation in higher acid concentration.

(3) Ip for pure lead and the standard lead alloy is of the same order, from 1 to 3 A/cm^2. For pure copper and the copper-lead alloy, a much higher limiting current was obtained which decreased with increasing acid concentrations.

(4) Epp was within 50 mv above Ecorr for pure lead and the standard lead alloy for all acid concentrations, indicating that it is independent of acid concentration. For copper and the copper-lead alloy, the difference between Ecorr and Epp decreased with increasing acid concentration.

(5) The value of Ic for Cu and Cu-Pb alloy is two orders of magnitude greater than for lead and the standard lead alloy, and Ip is four orders of magnitude higher. Hence, we refer to "pseudo-passivation" in this instance.

(6) Moreover, although Ecorr for the copper-lead alloy is between that for pure copper and pure lead, this alloy at higher potentials behaves like pure copper. See Figure 3.

(7) The cathodic scans for pure lead and the standard lead alloy show a non-Tafel behavior in the initial portion of the curve. This arises from the simultaneous occurrence of the oxidative conversion of lead to lead sulfate, coupled with hydrogen reduction. Thus, the net current shows the behavior observed.

(8) Copper shows Tafel-like behavior.

(9) The copper-lead alloy shows Tafel like behavior at potentials between Ecorr for the copper alloy and the Ecorr for the lead and lead alloy. However, a non-Tafel behavior was observed below the latter potential, which is explained in item (7) above. See Figure 4.

(D) Conclusions

From these results the following conclusions can be made:

(1) The standard lead alloy and lead passivate, presumably due to formation of a protective $PbSO_4$ film. This film seems to be more impervious at higher concentrations of acid.

(2) Copper shows a "pseudo passive" behavior in the media and, therefore, yields higher corrosion rates than lead.

(3) Although copper is more noble than lead, the copper-lead alloy behaves like pure copper. This indicates that the macroscopic homogeneity of copper and lead does not play a role in passivating this alloy.

(4) Hence, by decreasing the copper content from 60wt% to ~20-30wt%, it may be possible to form a protective film on lead which would protect the copper under homogeneous distribution of lead and copper, and the alloy would display lead-like behavior.

MECHANICAL PROPERTIES

As a part of the data base development, mechanical properties of Pb-0.08%Ca-0.56%Sn-66ppmAl were studied. Immediately after casting and rolling, the alloy samples were aged at the following temperatures:

1. Room temperature - 77 F (~20 C)
2. 125 F (51 C)
3. 175 F (80 C)

The ultimate tensile strength and the elongation of this alloy were measured at room temperature at one-day intervals for 30 days.

Three pulling rates were employed in the studies with a sample gage length of 2 inches, yielding the following strain rates:

1. 0.05 min^{-1}
2. 0.5 min^{-1}
3. 5 min^{-1}

Optical micrographs of this alloy were taken daily, to see the effect of aging temperature on the grain size and recrystallization behavior. The micrographs were taken from samples cut in three different directions of the rolled sheet as shown in Figure 5.

DROP TUBE AND RELATED STUDIES

Calculations were made for various lead-copper alloys with varying amounts of copper to determine the optimum mass of the sample which can be solidified using the drop tube at the

Marshall Space Flight Center. The alloys of interest contain copper in the range of 15 to 35% copper by weight. It was found that the mass of these alloys has to be limited to between 200 to 150 mg, the mass decreasing as the percentage of copper increases, for complete solidification to occur before hitting the bottom of the tube. The solidification has to be done in 700 torr pressure of He gas.

Experiments have been done on Pb-30% Cu alloy using the levitation melter at Vanderbilt University, and it was found that samples of this mass could be melted but not levitated. Thus, a modification in the coil geometry may be required so that the samples can be levitated. It may also require a different arrangement of melting, like the drip furnace, whereby the molten metal is held by surface tension in a tube with a small orifice. A droplet can be formed and released by increasing the gas pressure in the tube.

PLANS FOR THE FUTURE:

(1) Experiments described in this report will be reproduced for rapidly solidified Pb-Cu alloys. Because the samples are in the form of thin foils, we can anticipate the need for rapid potentiodynamic scanning.

(2) The standard Pb alloy will be studied as a function of heat-treatment and associated precipitation effects.

(3) Further investigation on the drop tube experiments for lead-copper alloy will be done.

(4) KC-135 experiments and ground based directional solidification experiments for lead-copper alloys are being planned.

ADDITIONAL PROJECT PERSONNEL:

Vani K. Dantam, General Motors, Delco-Remy Division
Sandeep Shah, Vanderbilt University

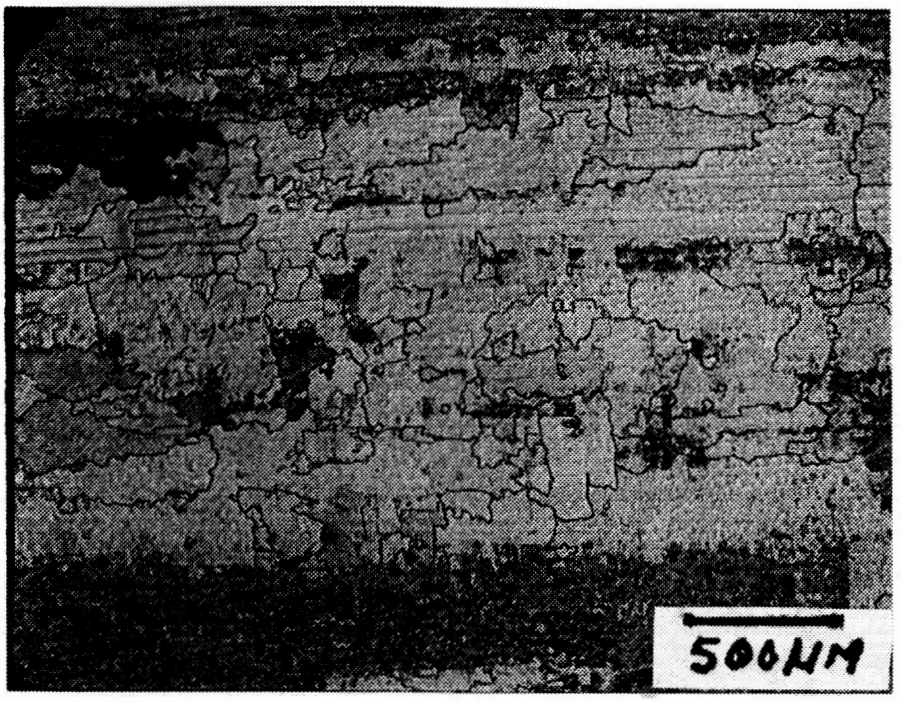

FIGURE 1A. Microstructure of Pb-Ca-Sn-Al alloy showing elongated grains.

**ORIGINAL PAGE IS
OF POOR QUALITY**

FIGURE 1B. Microstructure of Cu-Pb alloy showing dispersed lead in copper matrix with some segregation of lead.

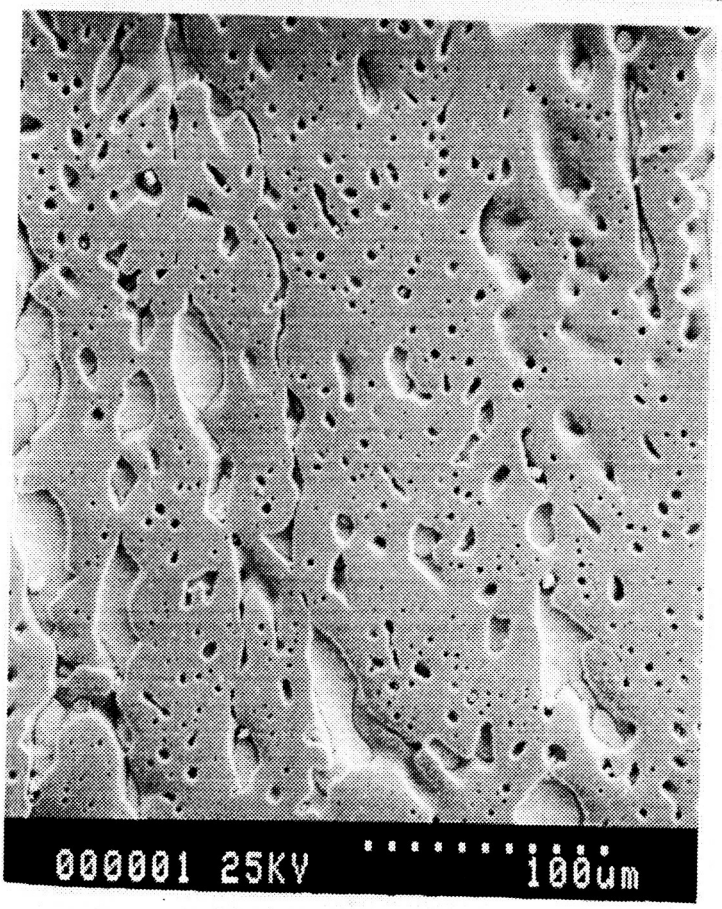

FIGURE 1C. Microstructure of Cu-Pb alloy at higher magnification.

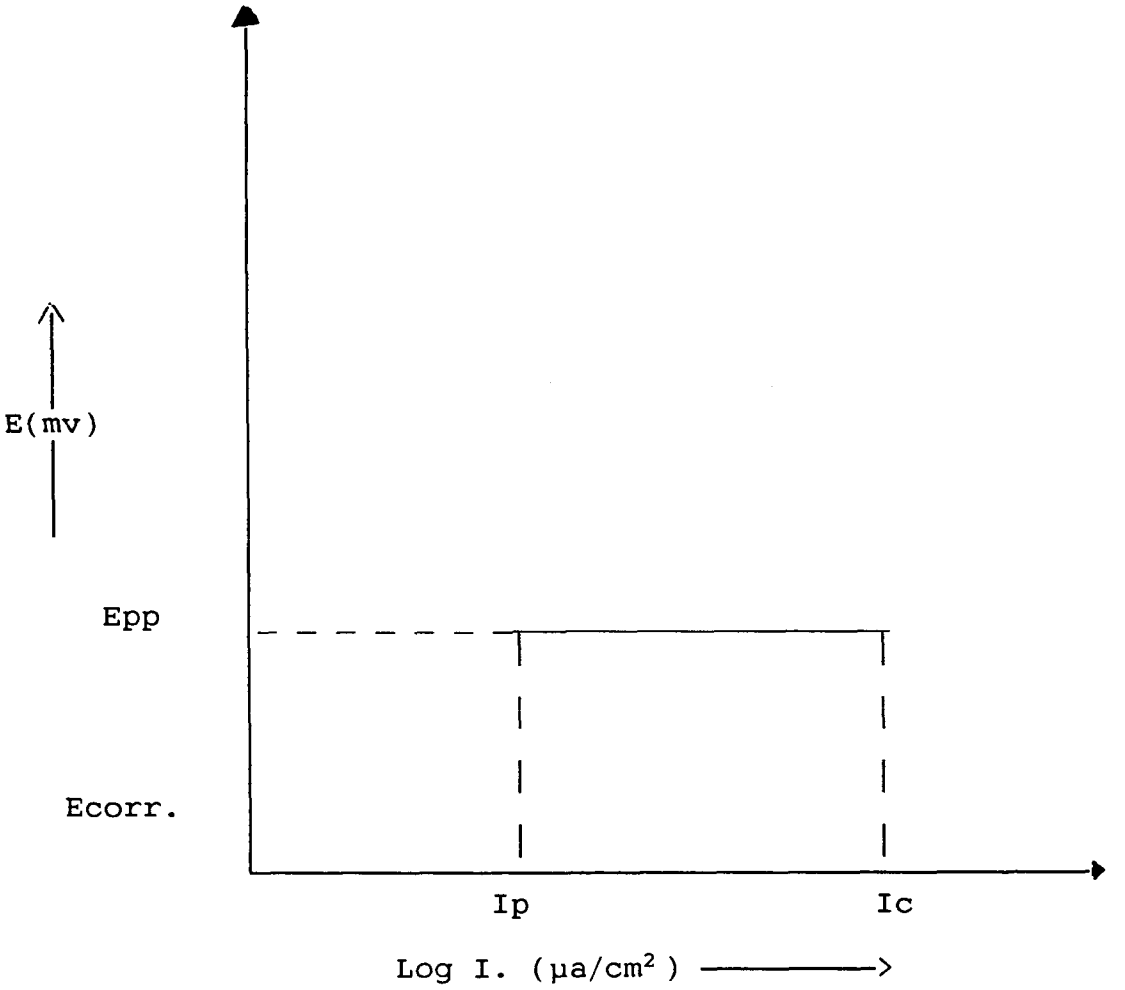

FIGURE 2. Schematic anodic polarization diagram.

FIGURE 3

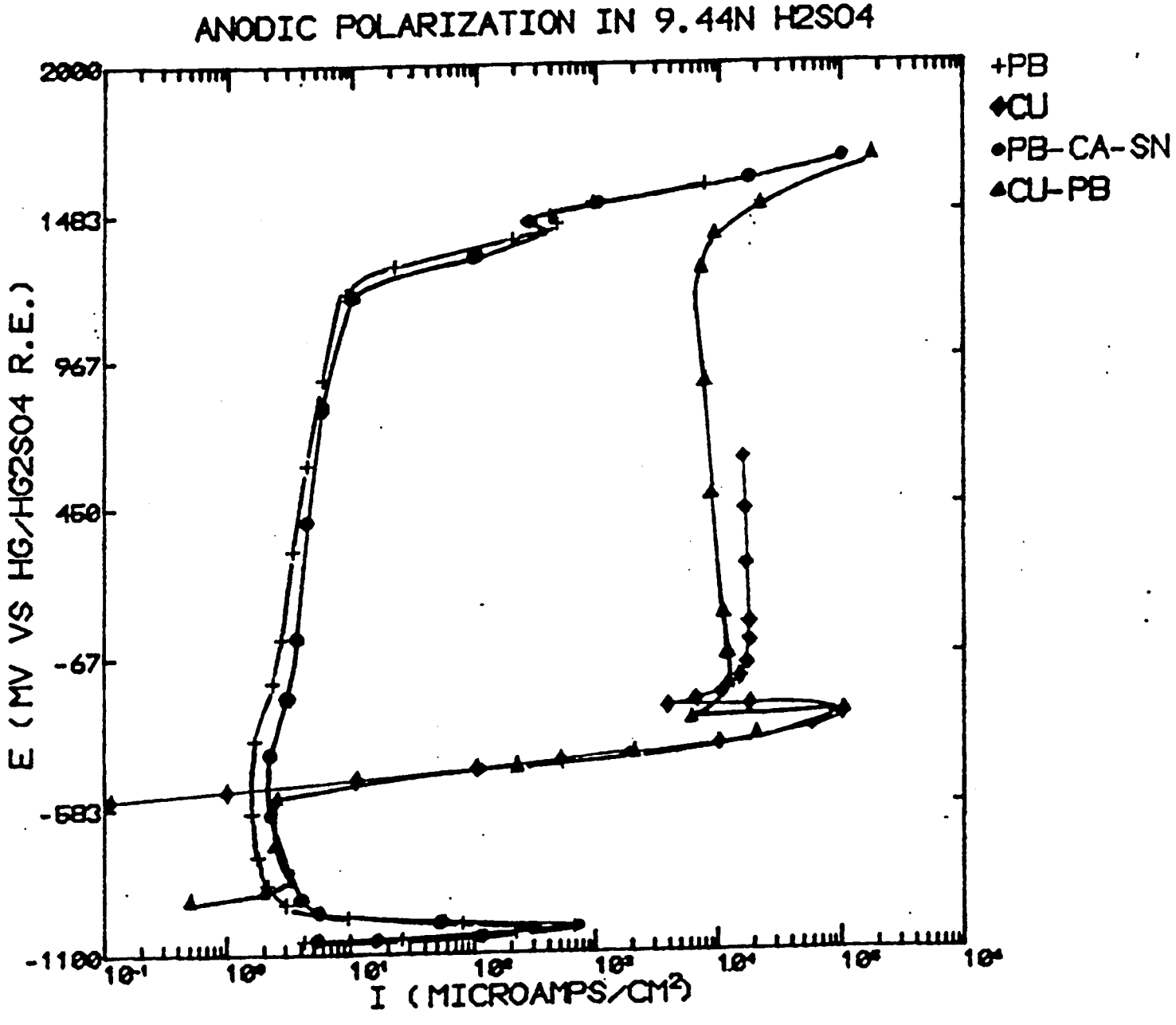
ANODIC POLARIZATION IN 9.44N H2SO4
+PB
CU
PB-CA-SN
CU-PB
2000
1483
967
450
-67
-583
-1100
E (MV VS HG/HG2SO4 R.E.)
I (MICROAMPS/CM2)

FIGURE 4

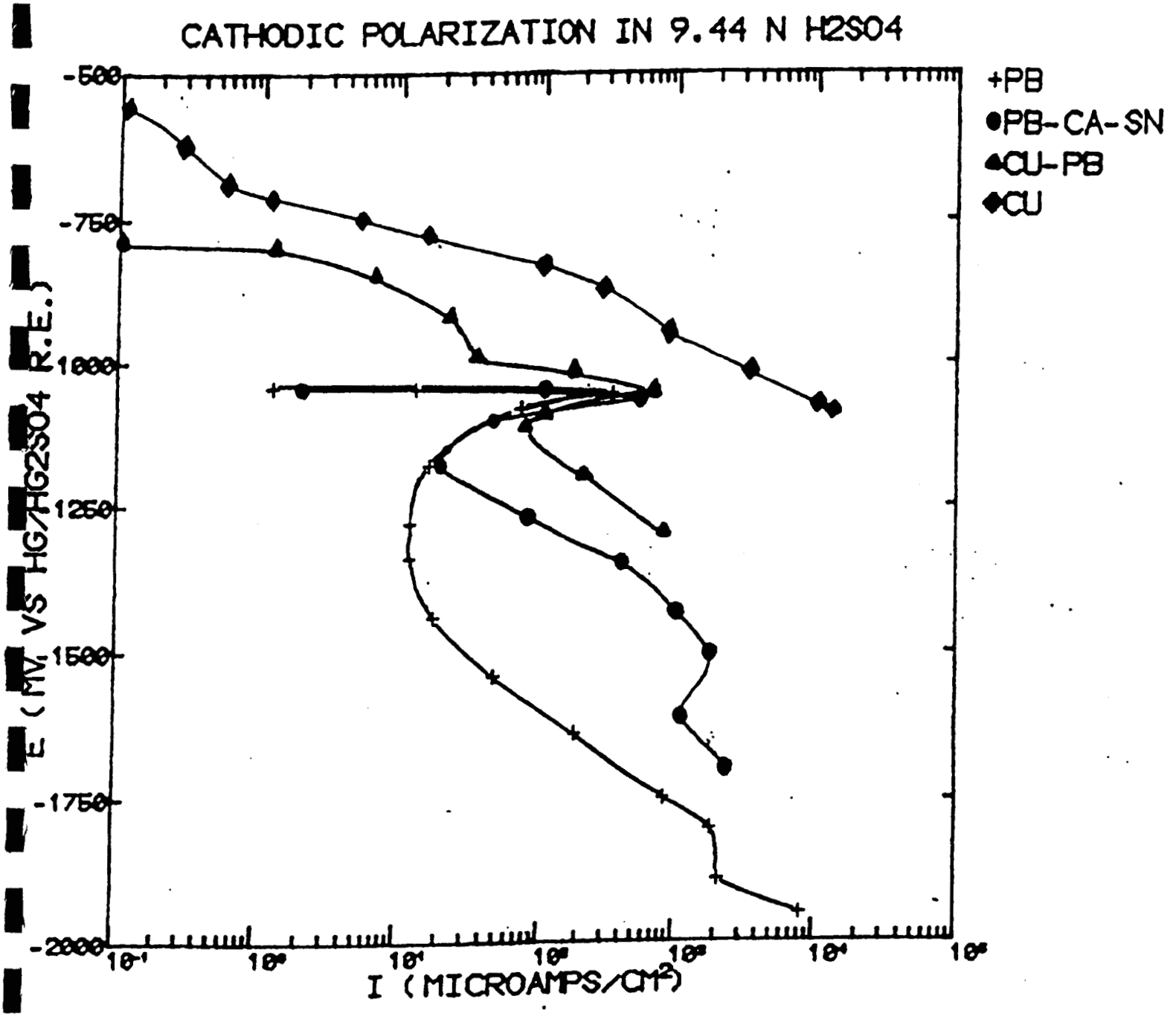
CATHODIC POLARIZATION IN 9.44 N H2SO4
+PB
●PB-CA-SN
▲CU-PB
◆CU
-500
-750
-1000
-1250
-1500
-1750
-2000
E (MV. VS HG/HG2SO4 R.E.)
10⁻¹
10⁰
10¹
10²
10³
10⁴
10⁵
I (MICROAMPS/CM²)

FIGURE 5

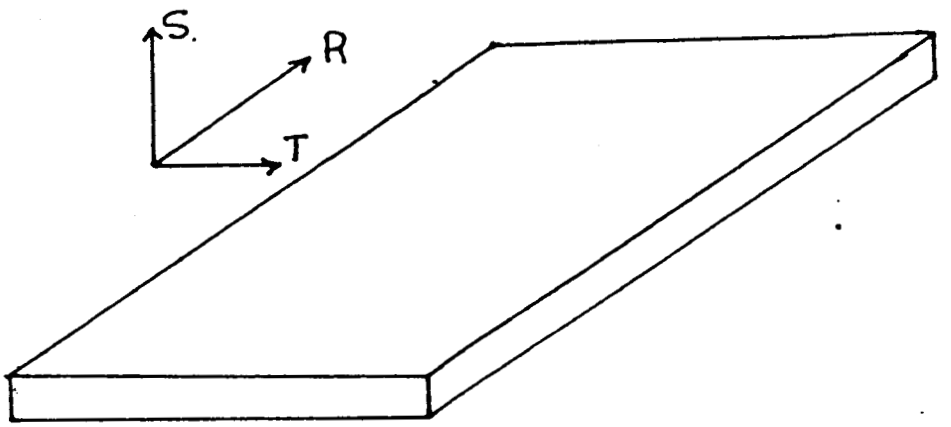

R: rolling direction

T: transverse direction

S: surface

PROJECT TITLE: Dispersion Strengthened Metal Alloys

COMPANY INVOLVED: GTE Corporation (Sylvania)

PROJECT LEADER: William F. Flanagan, Vanderbilt University

PROJECT DESCRIPTION:

This study, only recently initiated, concerns the solidification of alloys containing dispersed phases. The work relates to an interest at Sylvania GTE in details relating to the successful production of homogeneous dispersion-strengthened alloys. An important goal is to obtain fundamental information on the mechanism of nucleation on dispersed solid phases in a liquid. The industrial benefits of this research would be the enhancement of industrial efforts (a) to produce dispersion-strengthened alloy by casting processes, and (b) to develop better inoculants for the casting industry.

Containerless processing offers researchers a new tool for studying solidification. Specifically, containerless processing eliminates the heterogeneous nucleation by mold walls, and, as a consequence, either homogeneous nucleation or nucleation of dispersed phases becomes the dominant nucleation event. With this in mind, we are using containerless processing to study nucleation on dispersed phases, which touches on many different research areas. Specifically, we need to (1) know something about the physical processes occurring in a containerless melt, (2) know the surface interactions between the molten metal and the solid dispersions, and (3) have some insight in selecting materials which, in light of items (1) and (2), will allow for a productive research effort.

The first consideration is the physical processes occurring within a containerless melt. Briefly, the containerless processing techniques initially available to us allow high-frequency levitation melting of samples. These levitated samples can be cooled both during levitation (i.e., at 1 gravity) or during free fall (i.e., less than 1 gravity). Two drawbacks characteristic of this process are (a) the thin induction skin depths which necessitate thermal conduction for heating the bulk of large samples, and (b) the undefined electromagnetic stirring of molten samples. The aspect of stirring in the melt is of particular interest to this study.

Since the melt contains a dispersed phase which needs to be retained within the bulk of the sample and not collected on the surface of the sample, the degree of stirring in the sample (whether due to electromagnetic, Marongoni, or thermal forces) will affect both the forces exerted on dispersions and the availability of the sample's surface to the dispersions. For example, if dispersions tend to "stick" to the sample's surface, then a low degree of stirring will expose all the dispersions to the sample's surface. Thus, all the dispersions end up on the exterior of the sample. On the other hand, a high degree of stirring may pull dispersions into the sample resulting in a more homogeneous distribution. Although stirring will effect dispersion distribution, the actual interactions of solid, liquid, and gaseous interfaces will have an even greater effect. An additional concern relates to the dynamics of a moving solidification front on the particle dispersion, because of the interaction of the liquid/solid interface and the particles.

The second consideration is the interactions between the phases present (i.e., wettability). Wettability affects (1) the ability of a containerless melt to retain dispersed phases, and (2) the ability of dispersed phases to nucleate solid phases from a melt. The ability of a containerless melt to retain dispersed phases depends on "Sessile" wetting (i.e., a solid-liquid-vapor interaction characterized through Sessile-drop experiments). Such wetting is described by a dihedral angle, which, when equal to zero degrees, signifies complete wetting. In general, the dihedral angle is an equilibrium value which is dependent on (a) the time involved to reach local equilibrium as either a solid solution or an intermetallic phase forms on the interface, (b) the temperature, which affects both interface reaction rates and liquid surface tensions, and (c) the total and partial pressures present in the vapor phase which also affects surface tensions. In containerless processing, the melt will retain dispersions only when it wets them. Thus, the wettability and the various factors influencing wettability set limits to the possible materials which can be used in a containerless study of nucleation.

In addition to the relationship between wettability and the ability to retain dispersions in a containerless melt, wettability also influences the nucleation of a solid from a melt. In this situation, wettability involves consideration of two different solid-liquid interfaces and a solid-solid interface. For this situation, the dihedral angle can not be

directly measured. However, Sessile drop dihedral angles are available in the literature and they provide a measure for comparison between different melts and dispersions. In this situation it is desirable to discuss "Sessile" wettability in terms of a critical surface tension. Briefly, the critical surface tension for wetting is an empirically derived value of the maximum liquid-vapor surface tension required for wetting. Since the surface tension of molten metals changes with changes of temperature, the critical surface tension provides a means to compare the wettability of various systems with respect to temperature. By combining this information with the theoretical critical radius for nucleation of a solid in a melt, we hope to develop a model of nucleation on dispersed phases. Following this, we can then design containerless experiments which will test the theory.

The final consideration of this study is the selection of materials appropriate for use with currently available containerless processing facilities. From the previous brief discussion, one can see that there are many considerations involved in selecting sample materials. Initial attempts to study dispersives resulting from containerless processing used compacted aluminum-titanium diboride powders melted by magnetic levitation. Since Sylvania GTE has produced plasma-sprayed homogeneous dispersion-strengthened powders with these materials, we knew that titanium diboride particles had been retained in micron-size containerless melts. However, due to the excessive oxidation of aluminum and the high-frequency of the available levitation equipment, these initial attempts were not fruitful. The additional consideration of oxidation of powders used in samples was identified for future reference.

FUTURE WORK

With the factors influencing this study of nucleation in containerless melts identified, future work is directed toward (1) obtaining fundamental quantitative data, (2) defining experimental parameters, and (3) running experiments to determine the nature of nucleation on dispersed phases.

Obtaining fundamental quantitative data involves collecting values of wettability of ceramic particles by molten alloys. In particular, the effects of temperature and partial pressures on the wettability of ceramics by copper alloys are being evaluated. This information is being obtained from the literature and (if needed) by experimentation.

The role of the experimental parameters of temperature, environment, and sample composition will be determined from the previously mentioned fundamental quantitative data.

Nucleation experiments will be run and the data obtained from these experiments analyzed in relation to nucleation theories.

It is expected that initial deep cooling experiments on samples of titanium diboride in copper (alloy) will quickly allow us to ascertain whether wetting occurs in this system and whether undercooling is possible, which would say something about particle nucleation. The cooling rate may be varied by using gradient furnaces for the low rates and drop tube experiments with varying atmospheres or with splat-cooling for the high rates. These tests will shed light on the role of liquid/solid interface velocity on the dispersoid distribution.

ADDITIONAL PROJECT PERSONNEL:

Delbert Charles Allen, Vanderbilt University
Walter Johnson, GTE Corporation
Muktesh Paliwal, GTE, Sylvania

PROJECT TITLE: Metallic Bonding

COMPANY INVOLVED: Lockheed Missiles & Space Co., Inc.

PROJECT LEADER: Gail Whoriskey

PROJECT DESCRIPTION:

As interest in space development grows, it is clear there is a need to build structures to support efforts like space stations and space processing of materials. These structures will need to be assembled in space, and the methods for doing this are receiving considerable attention. Space shuttle astronauts have already experimented with various methods for joining and fastening structural supports in space.

A wide variety of welding processes are in common use for joining metals on earth. One technique that holds particular promise for space structures is metallic bonding. The term metallic bonding is defined herein as a solid state joining process in which two clean metal surfaces are brought together to within the bond spacing of the parent materials, allowing interatomic forces to join the surfaces together, without the application of heat or high contact pressure. The resulting bond then has the strength potential equal to that of the parent material. Earth based metallic bonding experiments involving Al to Al, Cu to Cu, and Al to Cu in vacuum have achieved bond strengths sufficiently high that the bond could not be pulled apart in a peel test (i.e., the base metal failed adjacent to the weld when loaded in tension). Metallic bonding is well suited for space applications since the vacuum of space provides natural protection against the re-formation of oxides on the clean metal surfaces prior to welding. And since there is no heating of the parts joining, the process requires much less energy than other welding techniques.

The important engineering parameters governing metallic bonding include surface cleanliness, contact pressure (resulting in surface deformation), surface smoothness, and the bond attraction of the mating metals. These parameters are interrelated; for example, cleaner, smoother surfaces require less pressure or deformation to achieve a strong bond.

The goal of this project is to determine the scientific boundaries for achieving satisfactory metallic bonds at low pressure. This will be done by focusing on three key technical questions:

1. How fast does an oxide film re-form after a metal surface is cleaned of all surface oxide films?

2. What normal pressure and shear displacement is required to achieve a metallic bond between metal surfaces containing thin oxide films (<5 to 10 atom layers)?

3. Can these data be used to successfully develop a space processing system which is technically viable and cost effective?

OVERALL PROJECT PLAN:

Vacuum facilities (absolute pressures $\leq 10^{-7}$ mmHg) on earth will be used to explore metallic bonding prior to conducting any experiments in space.

Lockheed Corporation will use analytical and experimental techniques to characterize the oxide reformation kinetics for a variety of metals and alloys. Auger analysis with sputter cleaning will be used to measure the oxide film thickness versus time for absolute pressures of 1×10^{-5} to 1×10^{-11} torr. Materials to be evaluated include pure aluminum and aluminum alloys 6061-T6, 7075-T6, 2024-T3, and T8. The most promising materials will be chosen for extended analysis.

Vanderbilt University will design and assemble an experimental apparatus for conducting metallic bonding experiments at vacuum levels ranging from 10^{-5} to 10^{-9} torr. This will include capabilities for mechanically preparing the welding surface under vacuum (via shaving, etc.) and measuring forces required for good bonds at a variety of low pressure (vacuum) levels. Special attention will be given to achieving smooth surfaces on the parts to be welded. Experiments will also be conducted at lower pressure levels ($<10^{-9}$ torr absolute) using vacuum systems available through NASA or Center member companies.

Results of the earth-based low pressure experiments will be used to design an experiment to fly into space.

PROGRESS TO DATE:

The design and construction of a vacuum system at Vanderbilt University has been initiated for the purpose of conducting bonding experiments. A chamber has been found and modified, a turbopump ordered and received, and the vacuum system is now operational. The system is being tuned to provide absolute pressure levels of 10^{-5} to 10^{-9} torr.

Evaluation of methods for mechanically cleaning specimen surfaces has begun. Results from experiments characterizing the surface roughness of aluminum after an assortment of cutting tools and abrasives are summarized in Tables I and II and Figures 1 through 8. SEM analysis of prepared surfaces is also being used to provide information on surface characteristics. Preliminary results for abrasively prepared surfaces are shown in Figures 9 through 12. Abrasive methods are shown to leave free particles on the specimen surface that are expected to interfere with bonding. Further experiments will concentrate on characterizing the surface smoothness of aluminum after shaving with a variety of razor blade materials.

IMMEDIATE PLANS:

Future project tasks include work on the vacuum system, design and test of surface cleaning techniques, and the design and test of the bonding apparatus. A project schedule is included in Figure 13.

ADDITIONAL PROJECT PERSONNEL:

Robert J. Bayuzick, Vanderbilt University
Richard E. Lewis, Lockheed Missiles & Space Co., Inc.
Jeffrey Moore, Vanderbilt University

TABLE I

PROFILOMETER RESULTS

Surface Finish	Avg. Peak Height (μ)	Max. Peak (μ)	Min. Peak (μ)
1/16" Radius Tip Carbon Tool Steel Blade	3	4	.25
Single Point Carbon Tool Steel Blade	7	7.5	1
Stainless Steel Razor Blade	2	2.5	.25
Polished Al	.05	.5	.01

TABLE II

PROFILOMETER RESULTS

Surface Prep.	Avg. Peak Height (μ)	Max. Peak (μ)	Min. Peak (μ)
240 Grit	2	5	.5
320 Grit	1.5	3	.25
400 Grit	.5	1	.25
600 Grit	.25	1	.10

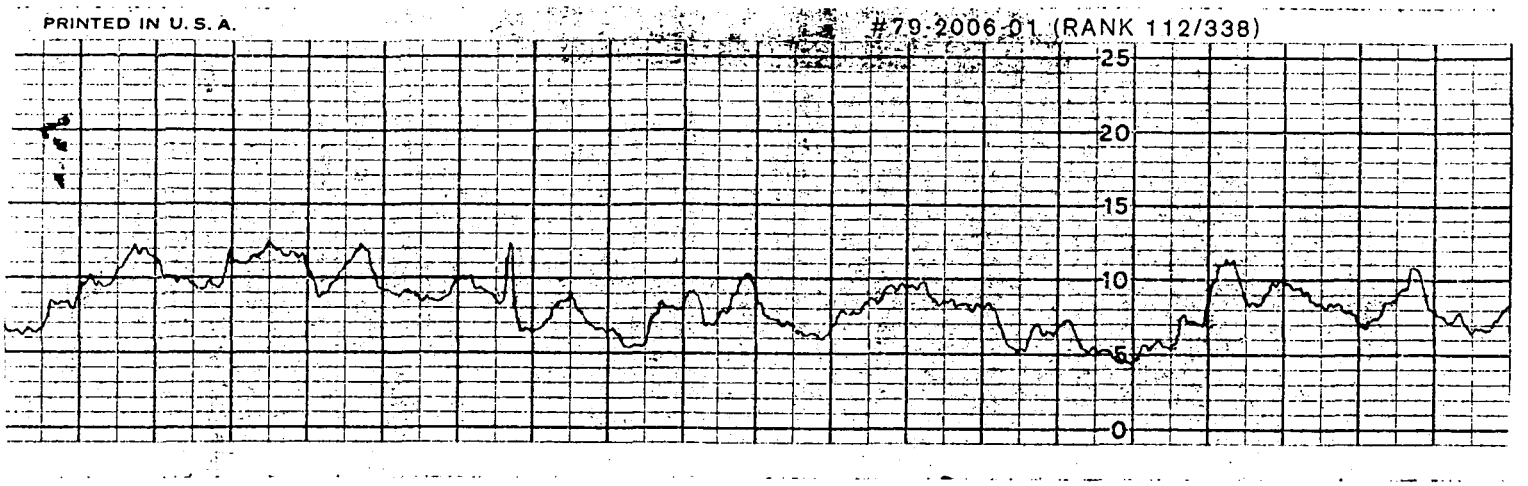

Figure 1. Surface Roughness of Al after Cutting with 1/16" Radius Carbon Tool Steel Blade. 1 Div. = 1μ.

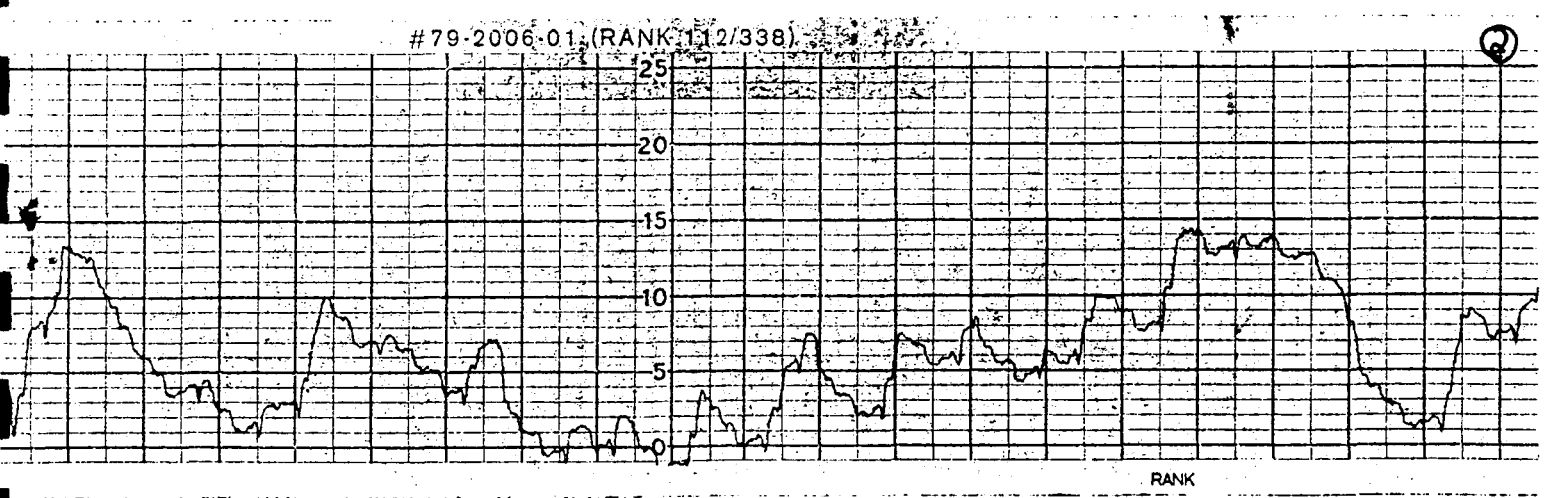

Figure 2. Surface Roughness of Al after Cutting with Single Point Carbon Tool Steel Blade. 1 Div. = 1μ.

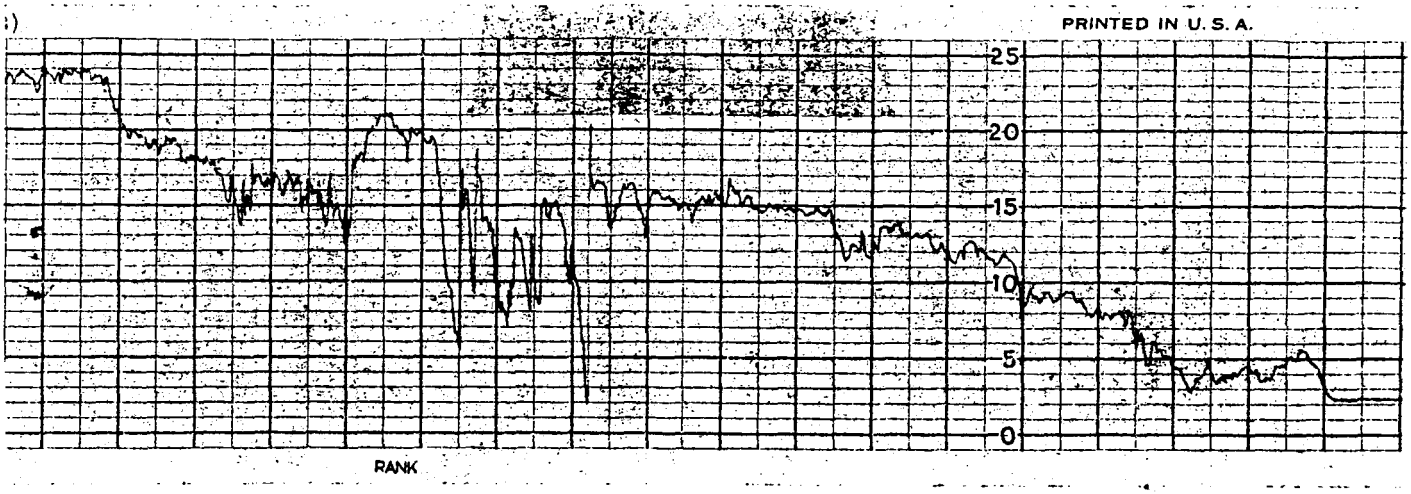

Figure 3. Surface Roughness of Al after Hand Shaving with Stainless Steel Razor Blade. 1 Div. = 1μ.

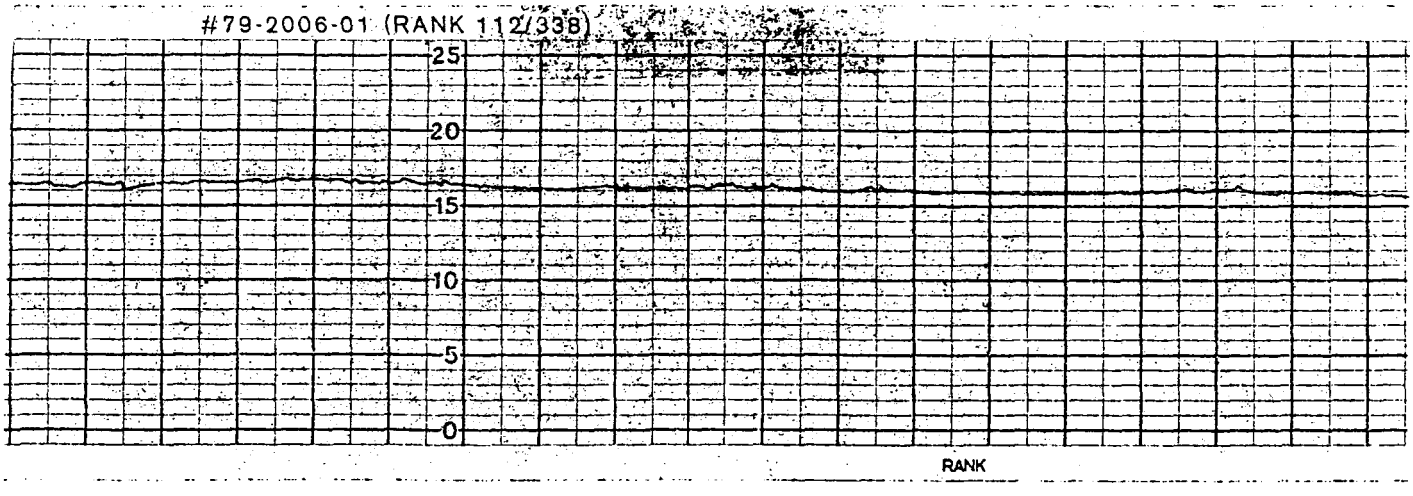

Figure 4. Surface Roughness of Al after .05 Micron Grit Polish. 1 Div. = 1μ.

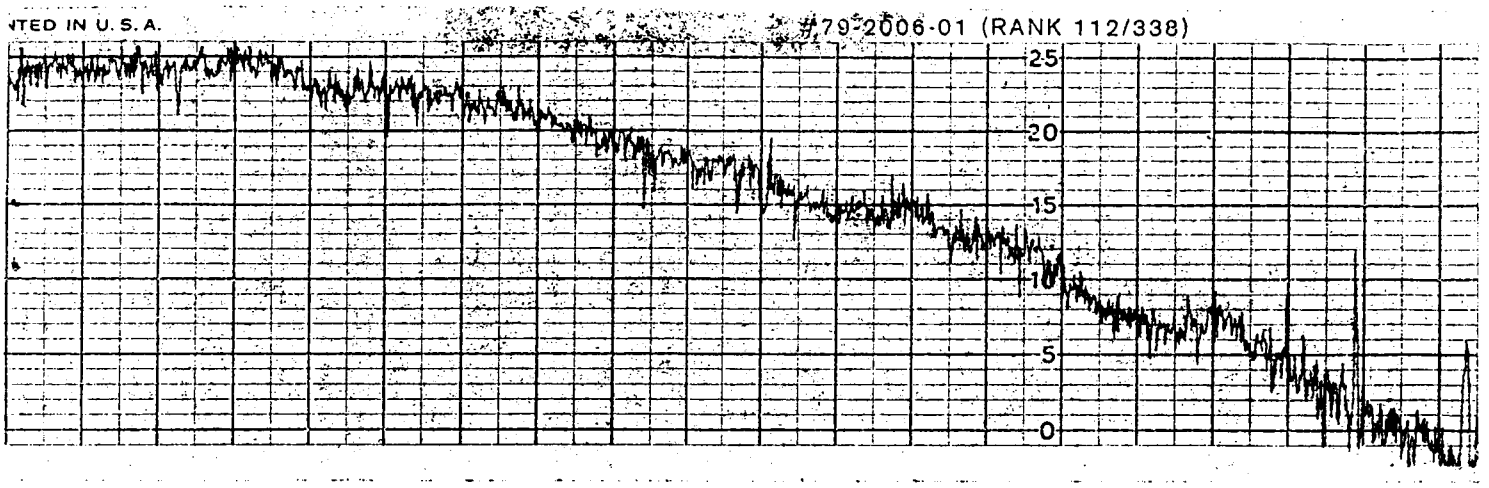

Figure 5. Surface Roughness of Al after 240 Grit Grinding. 1 Div. = 1μ.

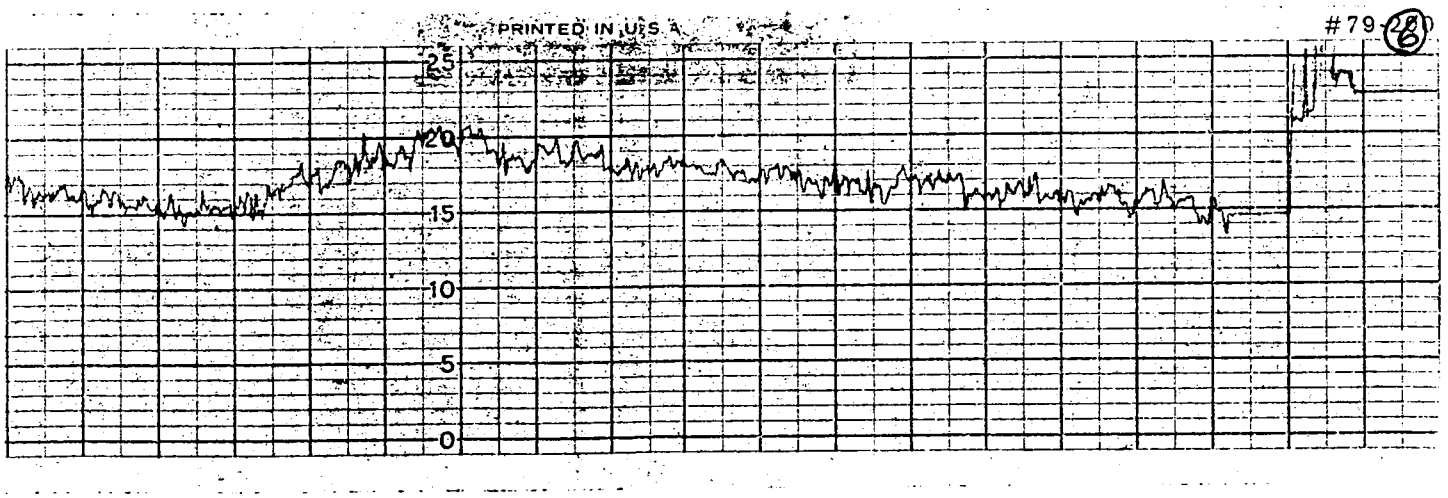

Figure 6. Surface Roughness of Al after 320 Grit Grinding. 1 Div. = 1μ.

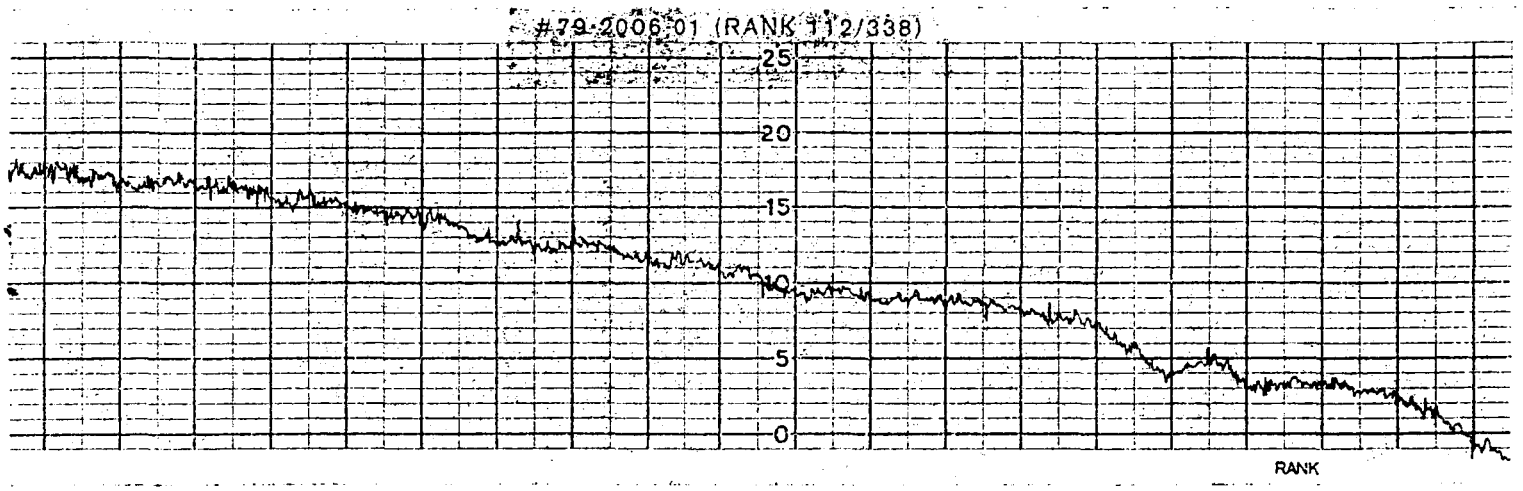

Figure 7. Surface Roughness of Al after 400 Grit Grinding. 1 Div. = 1μ.

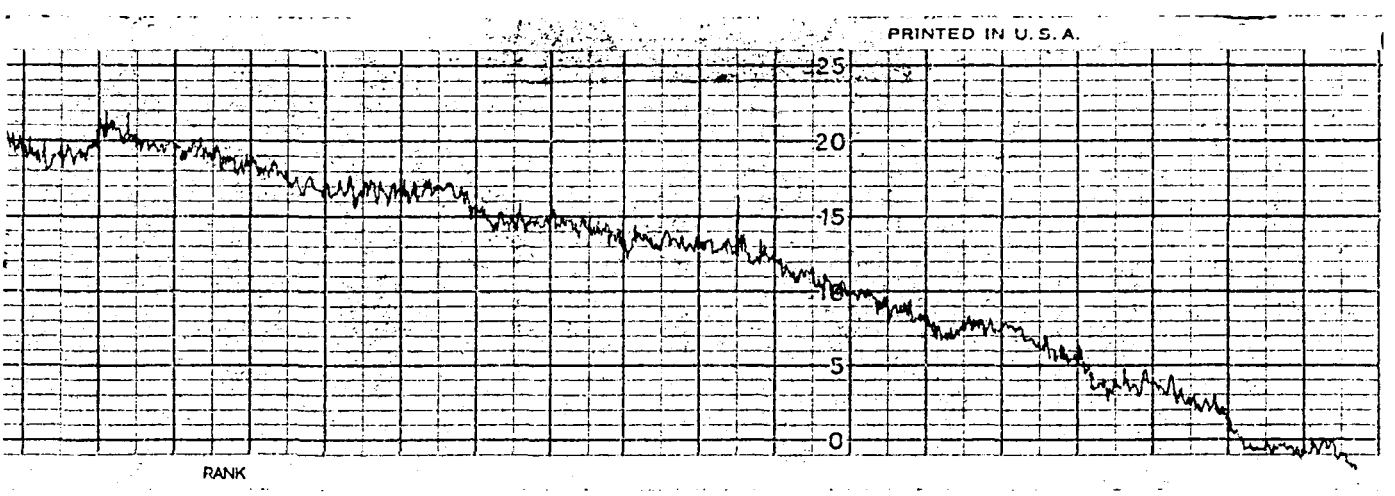

Figure 8. Surface Roughness of Al after 600 Grit Grinding. 1 Div. = 1μ.

Figure 9.
SEM Micrograph of Al
After 240 Grit
Grinding.

Figure 10.
SEM Micrograph of Al
After 320 Grit
Grinding.

Figure 11.
SEM Micrograph of Al
After 400 Grit
Grinding.

Figure 12.
SEM Micrograph of Al
After 600 Grit
Grinding.

FIGURE 13 METALLIC BONDING PROJECT TIMELINE

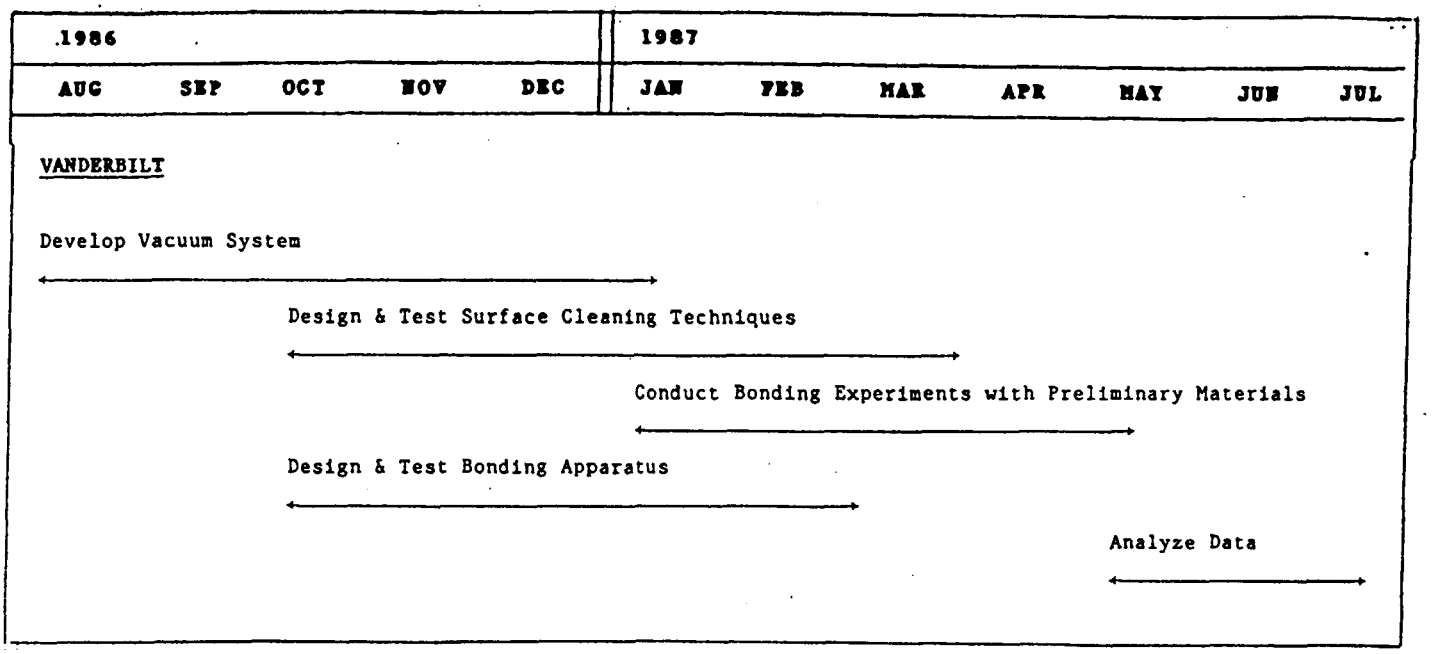

PROJECT TITLE: Development of Oxidation Resistant Niobium Alloys

COMPANY INVOLVED: Lockheed Missiles & Space Co., Inc.
Teledyne Wah Chang Albany

PROJECT LEADER: Robert J. Bayuzick, Vanderbilt University

PROJECT DESCRIPTION:

Nb alloys have potential for a variety of high temperature aerospace structural applications. In these applications, the combination of ductility, formability, strength, toughness, and oxidation resistance is of prime importance. In conventionally cast and wrought Nb alloys, there is a competition between ductility and oxidation resistance. Usually oxidation resistant alloys are brittle and ductile alloys are not oxidation resistant. There is some evidence that aluminum and silicon additions may have a beneficial effect in conventional cast and wrought oxidation resistant Nb alloys. Rapid solidification processing of new Nb alloys may result in a self-forming passivating surface barrier to oxidation.

On these bases, there is motivation for the development of bulk Nb alloys that are both ductile and oxidation resistant. One likely avenue to achieve self-passivating, ductile alloys in the bulk is rapid solidification through deep undercooling by containerless processing, and limited previous work indicates the Nb-Al, Nb-Si, and Nb-Ti alloy systems to be the most promising.

RESULTS TO DATE:

1. Project Planning and Organization

Considerable effort has gone towards project planning. This research is being conducted jointly by Vanderbilt University, Lockheed Missiles and Space Company, University of Florida, and Teledyne Wah Chang Albany researchers. The project has been structured to take maximum advantage of the capabilities of each participant.

The series of experiments to be carried out have been divided into the following categories:

A. Master Alloy Preparation

B. Arc Melting and Splat Cooling

C. EM Levitation and Supercooling

D. EM Levitation, Supercooling and Splat Cooling

E. Drop Tube and Supercooling

F. Drop Tube, Supercooling and Splat Cooling

G. "Special Powder Processing Technique" of Selective Compositions

H. Rapid Solidification Processing by Melt Spinning

The samples produced by each of the above mentioned processes will be analyzed via some or all of the following techniques:

A. Bulk compositional analysis, especially with respect to the interstitial impurities.

B. Microstructural analysis -- (i) optical microscopy and (ii) SEM.

C. Evaluation of oxidation properties -- (i) furnace oxidation and (ii) TGA.

D. Evaluation of mechanical properties -- (i) hot working capability, (ii) hot hardness testing, and (iii) high temperature mechanical testing.

E. Detailed microstructural and segregation analysis-- (i) Microprobe, (ii) STEM, and (iii) Auger.

F. High temperature studies -- (i) in-situ heated ESCA, (ii) DTA, and (iii) high temperature x-ray.

Based on the existing facilities, these tasks have been divided among the participants as shown in Table I.

2. Experimental Results

A summary of NbTi drops prepared to date in the 100 meter drop tube at the Marshall Space Flight Center is included in Table II. The major results of these NbTi experiments are summarized as follows:

1. Many NbTi drops exploded on recalescence, as indicated in Table II and Figures 1a and 1b. Perhaps this is caused by entrapped gas coming out of solution during solidification, due to the difference in solubility of oxygen or hydrogen in the material over the temperature range from melting to solidification. Another possibility is thermal stresses set up if the outside surface solidifies first and the volume of material inside contracts on cooling.

2. Progressively finer dendrites and less segregation is evident with larger degrees of undercooling in NbTi as seen in Figures 2 through 13.

3. Some contamination of specimens during processing has been noticed. Figure 14 shows carbides found in an undercooled sample of Nb-Ti alloy A. It is believed this contamination is being picked up from the levitation melting coil. Numerous samples will be destructively analyzed for the presence of impurities. Future experiments will be run using the electron beam furnace which is believed to be a cleaner technique.

Significant results are also being realized from NbSi drop tube experiments. Drop Tube experiments on two different Nb-Si alloys have been successful. Undercooling, of varying degrees, has been achieved in both compositions; the data is presently being analyzed to obtain quantitative results and analysis will be completed during the next quarter.

PLANS FOR THE COMING YEAR:

Drop tube experiments on NbTi alloys will continue using the E-beam furnace method of sample melting. Drop tube samples will be analyzed and characterized for material structure, dendrite size and shape, composition, porosity, and the presence of metastable phases.

Drop tube experiments of Nb-Si alloys will continue. These drops will also be analyzed and characterized. Drop tube experiments will also begin on Nb-Hf alloys.

ADDITIONAL PROJECT PERSONNEL:

G. J. Abbaschian, University of Florida
John C. Haygarth, Teledyne Wah Chang Albany
A. Joshi, Lockheed Missiles & Space Co., Inc.
Richard E. Lewis, Lockheed Missiles & Space Co., Inc.
Gail Whoriskey, Vanderbilt University

TABLE I

Tasks for Containerless Processing of Nb-Based Alloys

Tasks	Lockheed Missiles & Space Co.	Teledyne Wah Chang Albany	University of Florida	Vanderbilt University
Material Preparation				
A		X		
B	X			
C			X	
D			X	
E				X
F				X
G		X		
Material Analysis				
a		X		
b(i)	X	X	X	X
b(ii)	X	X	X	X
c(i)		X		
c(ii)		X	X	
d(i)	X	X		
d(ii)		X		
d(iii)				X
e(i)	X		X	
e(ii)			X	X
e(iii)	X			
f(i)	X			
f(ii)			X	
f(iii)			X	

TABLE II

UNDERCOOLING OF NbTi

Nb-Ti ALLOY	°K UNDERCOOLING	% UNDERCOOLING
A	*197	*9
	224	10
	323	15
B	57	3
	*236	*10
C	*45	*2
	152	6
D	90	4
E	333	13

* BROKE APART IN FLIGHT AT RECALESCENCE

Figure 1a. Macrograph of "Exploded" Drop

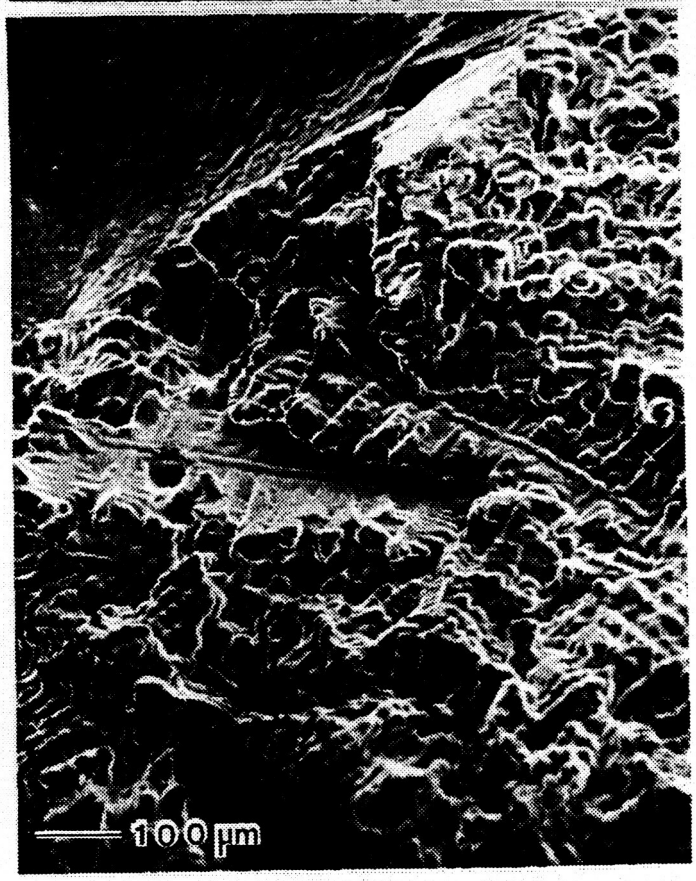

Figure 1b. Fracture Surface of "Exploded" Drop.

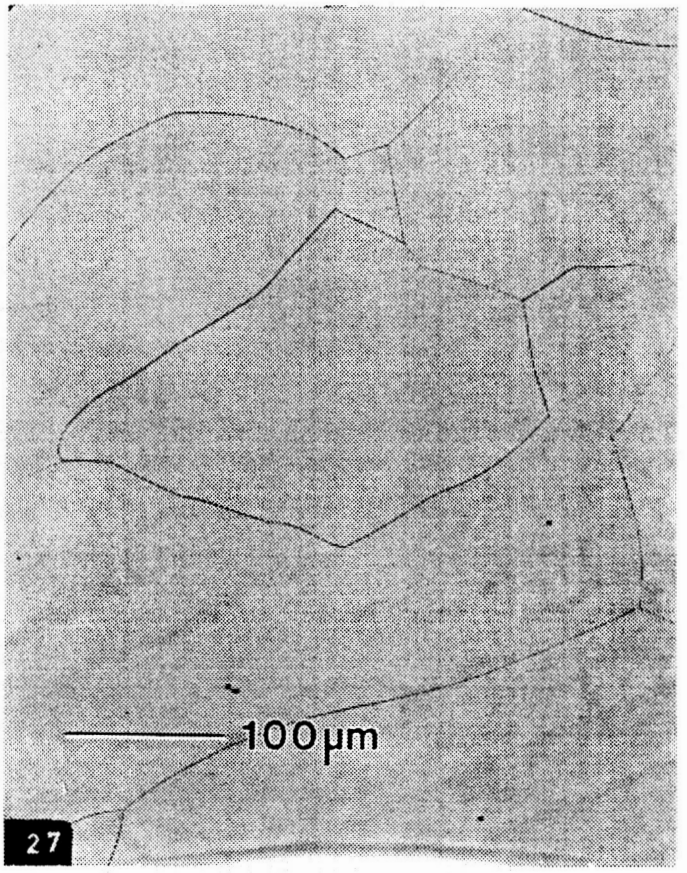

Figure 2. Alloy A.
As Received. Arc Melted
Button.

Figure 3. Alloy B.
Processed in Drop Tube.
No Undercooling.

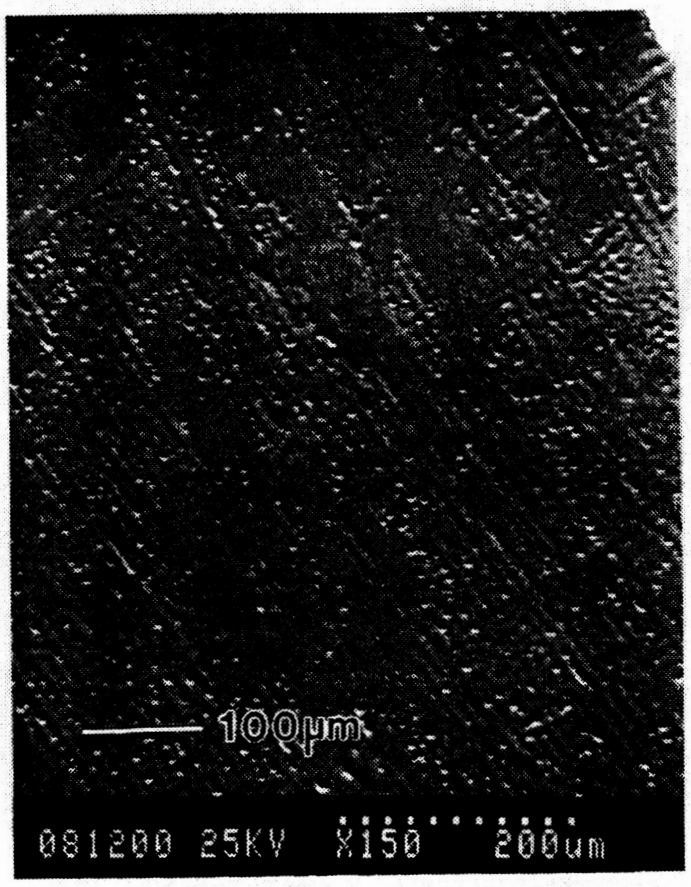

Figure 4. Alloy A.
Undercooled 323°C.

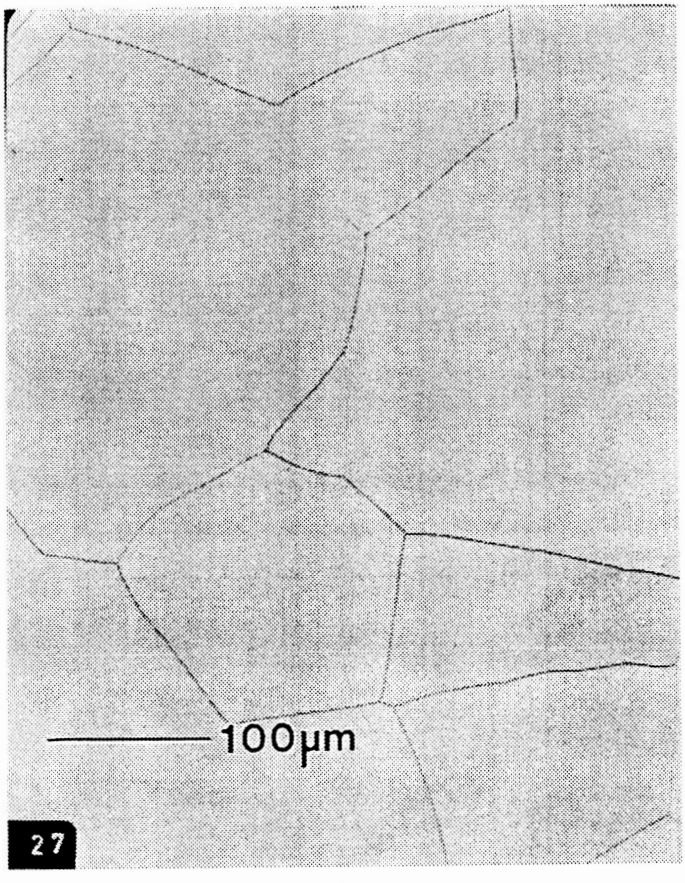

Figure 5. Alloy B.
As Received. Arc Melted
Button.

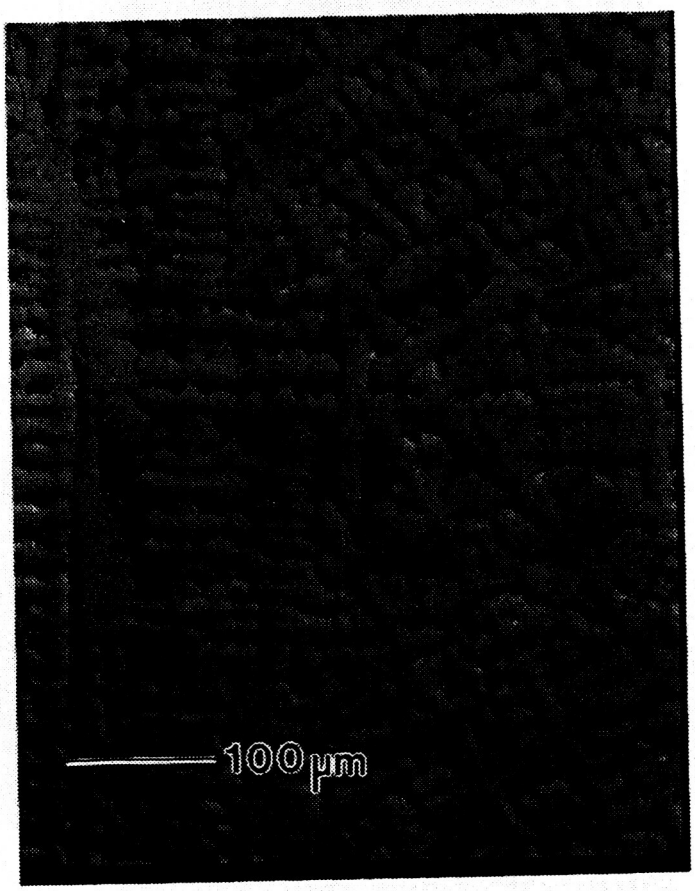

Figure 6. Alloy B.
Processed in Tube.
No Undercooling.

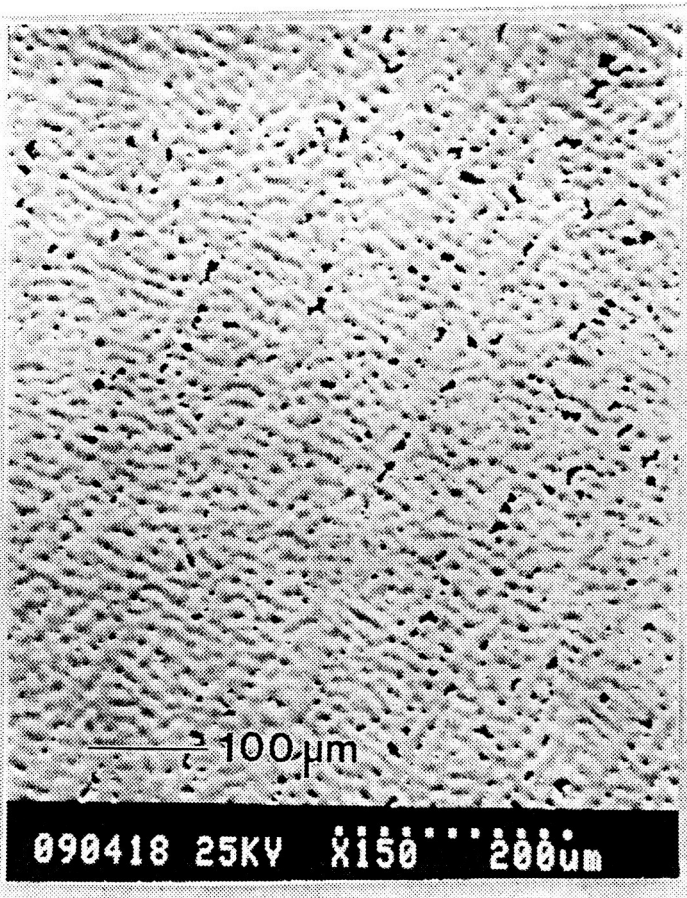

Figure 7. Alloy B.
Undercooled 57°C.

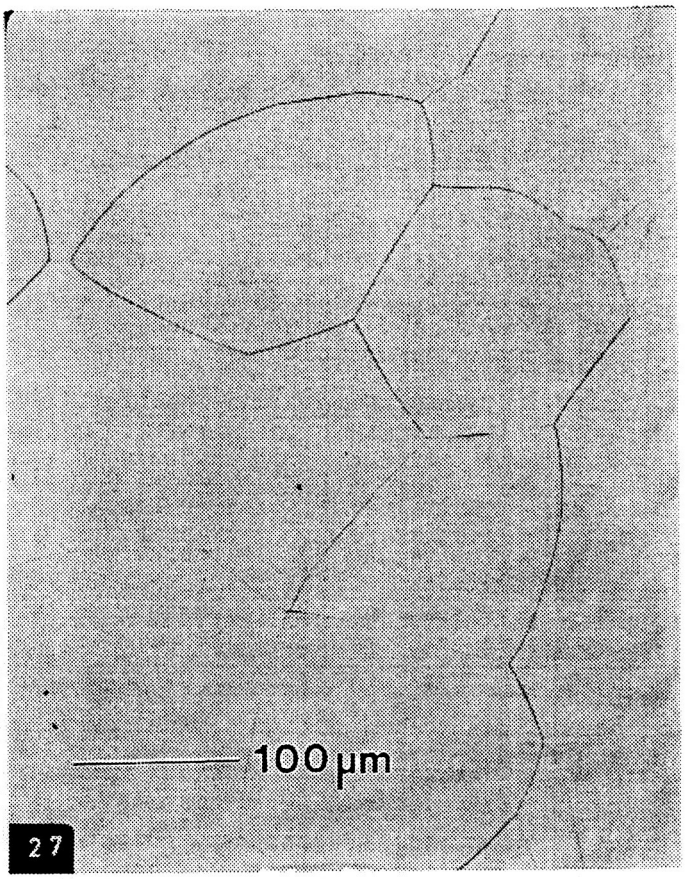

Figure 8. Alloy C.
As Received. Arc Melted
Button.

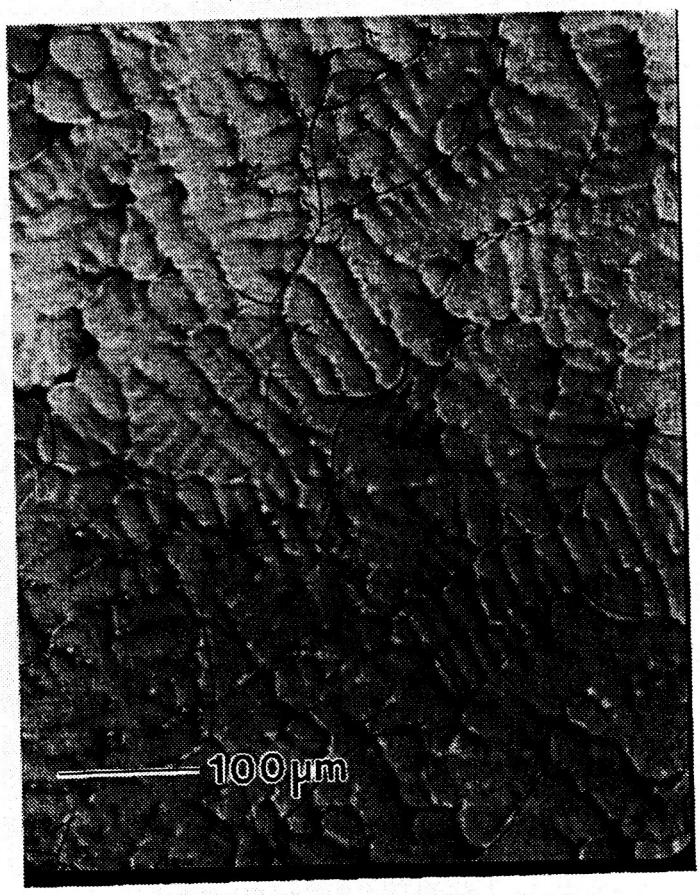

Figure 9. Alloy C.
Processed in Drop Tube.
No Undercooling.

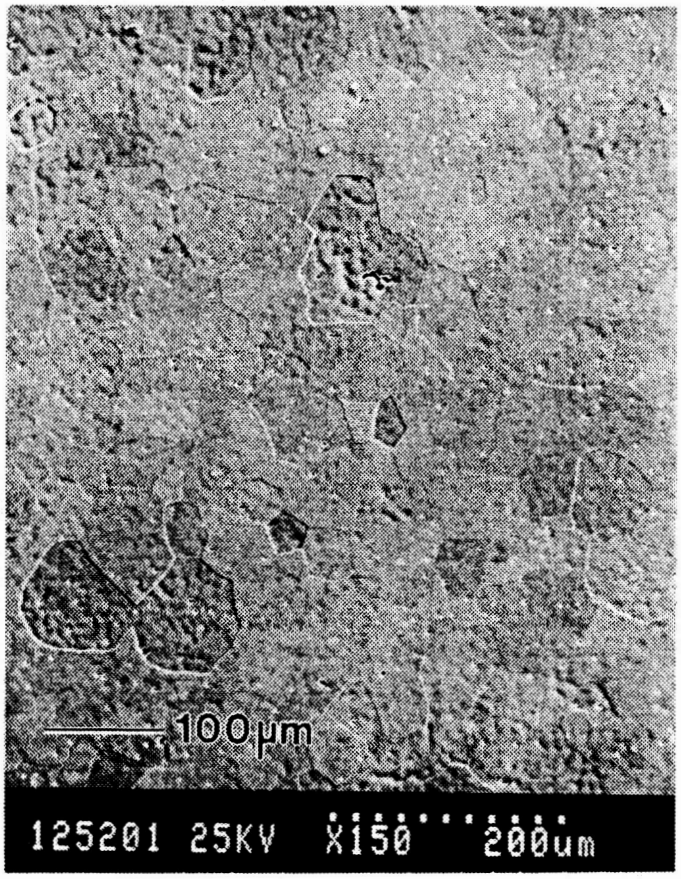

Figure 10. Alloy C.
Undercooled 152°C.

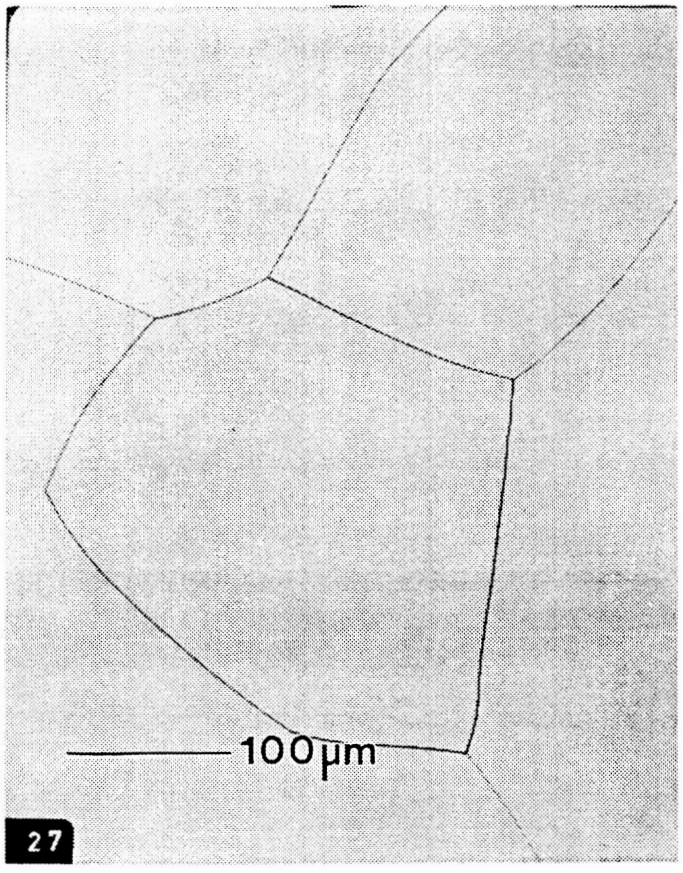

Figure 11. Alloy E.
As Received. Arc Melted
Button.

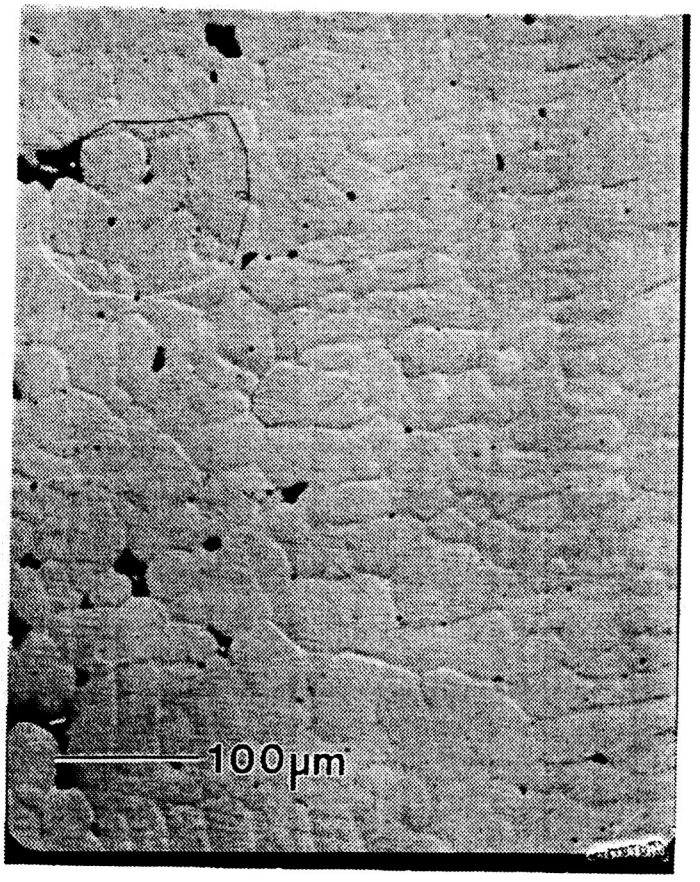

Figure 12. Alloy E.
Processed in Drop Tube.
No Undercooling.

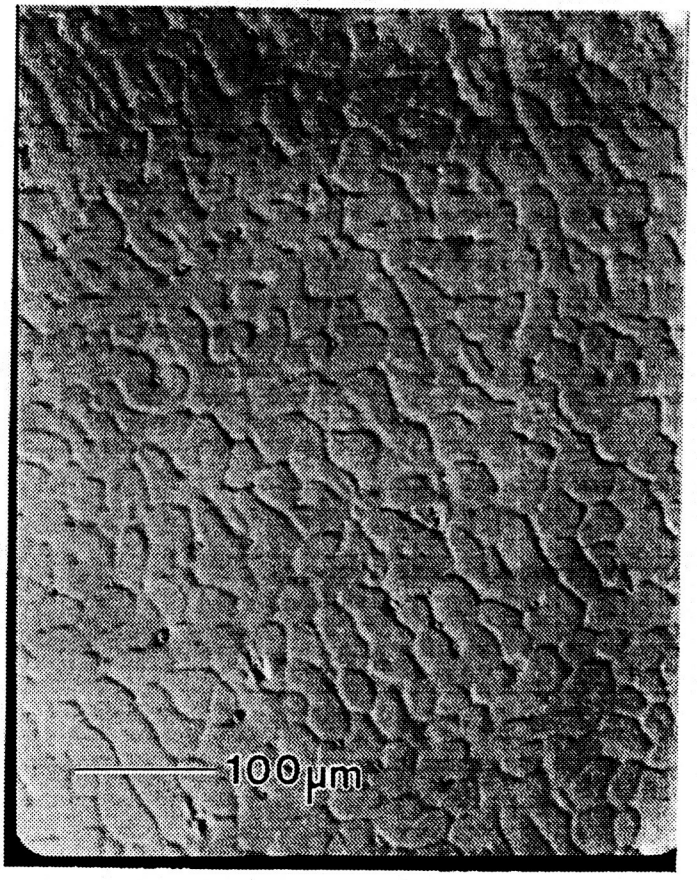

Figure 13. Alloy E.
Undercooled 333°C.

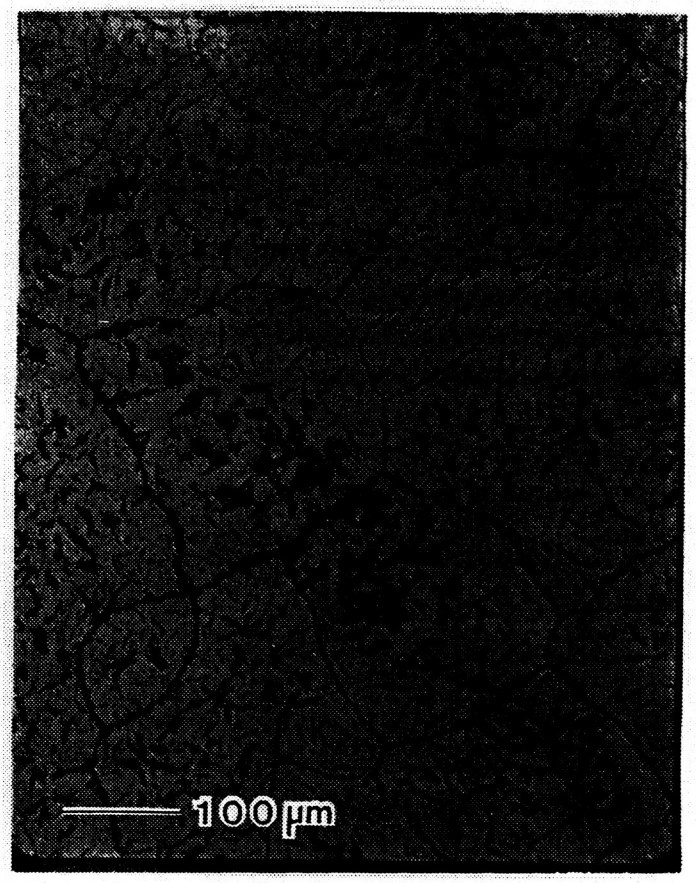

Figure 14. Alloy A.
With Carbides.

PROJECT TITLE: Oxide Strengthened High Temperature Alloys in the Nickel Chromium System

COMPANY INVOLVED: Special Metals

PROJECT LEADER: D. M. Stefanescu, University of Alabama

PROJECT DESCRIPTION:

The objective of this project is to investigate the behavior of oxide particles in nickel-chromium alloys during directional solidification in order to achieve:

* either homogeneous distribution of particles (particle entrapment) dispersion strengthened alloys
* or complete removal of particles (particle push) pure alloy.

Particle behavior ahead of the liquid-solid interface is a function of:

* interface energy (liquid-solid, liquid-particle, solid particle) which, in turn, is a function of metal matrix composition, oxide particle composition and oxide particle surface structure.
* oxide particles size and volume fraction
* rate of advance of interface (solidification rate)
* convection level

Since buoyancy driven convection can cause particle agglomeration in normal gravity conditions, the behavior of particles in front of an advancing interface is further complicated. Since in a low gravity environment both Stoke's forces and buoyancy-driven convection are not active anymore, the solidification rate becomes the main variable for a given system. Different researchers have shown that at a certain velocity of the solidifying front particles are no longer pushed, but are entrapped by the moving interface. The velocity has been designated as the critical velocity.

Uhlmann and his co-workers determined this velocity for many types of particles in several organic matrix systems. They observed that the critical velocity depends on the particle size and volume fraction for a given system. Chernov and his co-workers claimed that the critical velocity is a function of two characteristic lengths λ and 1:

$$\lambda = \left(\frac{\Omega\alpha}{\Delta SG}\right)^{1/2} \qquad \text{and } 1 = \left(\frac{B_3\Omega}{\Delta SG}\right)^{1/4}$$

where Ω = specific molecular volume of the melt

α = specific free energy of the crystal-melt interface

ΔS = entropy of melting

G = temperature gradient at growth front

B_3 = constant

For small particles, i.e., with $R<\lambda^2/1$,

$$V_C = \frac{0.14\ B_3}{\eta R}\left(\frac{\alpha}{B_3 R}\right)^{1/3}$$

while for large particles, i.e., with $R>\lambda^2 1$,

$$V_C = \frac{0.14\ B_3}{\eta R1}$$

where R = particle diameter

η = viscosity of the melt

This approach did not take Stoke's forces into account and all the particles were assumed spherical in shape.

This is not always the case, and the effect of particle shape on interface would appear to be unknown.

It is planned to use the variables which affect the behavior of the particles in front of an advancing interface, throughout the experimental work in order to determine the conditions for particle pushing and particle entrapment in the systems of interest.

RESEARCH WORK PERFORMED:

Oxide and Alloy Selection for Interfacial Energy Evaluation

The alloys which were selected for the interfacial energy measurements are, by weight percentage, Ni-20Cr, Ni-20Cr-1Al, and Ni-20Cr-4Al. Aluminum additions to the binary high temperature Ni-20Cr alloy were expected to change the interfacial energy between the liquid alloy and the oxide particle.

The oxides, which were selected for the surface energy tests, are Y_2O_3 and HfO_2. Y_2O_3 is significantly used as a dispersoid in oxide dispersion strengthened alloys. HfO_2 is significant as an inclusion in both cast and wrought superalloys. Another reason for selecting these oxides is that Y_2O_3 is less dense and HfO_2 is more dense than the Ni-20Cr base alloy. Since buoyant forces will change with the type of oxide, the other forces which control the dispersion of fine oxides during directional solidification would be easier to study experimentally.

Measurement of Interfacial Energies in Liquid Metal-Oxide Systems

As part of a study on particle behavior (entrapment/pushing) ahead of an advancing interface, sessile drop experiments were conducted to investigate wetting characteristics of Ni-Cr-Al alloys on different ceramic substrates and to calculate surface tension between liquid and vapor (σ_{LV}).

Because of its simplicity, the sessile drop technique is the most widely used technique to investigate the interfacial behavior between ceramic substrates and molten metal. The sessile drop technique consists of measuring the contact angle and sessile drop parameters, which, in turn, depend on interfacial and gravitational forces acting on the drop, and then calculating liquid vapor surface tension.

Under equilibrium conditions, the balance of interfacial tensions between the solid-vapor, solid-liquid, and liquid-vapor phases is given by Young's equation:

$$\cos \Theta = \frac{\sigma_{SV} - \sigma_{SL}}{\sigma_{LV}}$$

where: Θ = contact angle

σ_{SV} = solid-vapor surface tension

σ_{SL} = solid-liquid surface tension

σ_{LV} = liquid-vapor surface tension

Whether a liquid wets ($\Theta<90$) or does not wet ($\Theta>90$) a solid depends on the difference $\sigma_{SV} - \sigma_{SL}$. If σ_{SL} is greater than σ_{SV}, non-wetting conditions occur. Figure 1 shows the equilibrium forces on the periphery of a sessile drop.

The work of adhesion between liquid and solid phases can be expressed as:

$$W = \sigma_{SV} + \sigma_{LV} - \sigma_{SL}$$

or

$$W = \sigma_{LV} (1 + \cos \Theta)$$

It follows that the work of adhesion between liquid and solid phases can be calculated directly from sessile drop measurements.

Materials

The ceramic materials used in the experiments were Al_2O_3, Y_2O_3, and HfO_2.

These materials were the highest quality commercially available. They were hot pressed in one inch diameter and 1/4 inch thickness bars and sintered. The porosity was less than 5%. The metallic materials investigated were pure Ni, Ni-20Cr, Ni-20Cr-1Al, and Ni-20Cr-4Al. These alloys were vacuum induction melted and cold rolled. The oxygen content of these alloys was less than 20 ppm. All metallic specimens were cut in small cubes of about 1 gram and polished by mechanical methods.

Apparatus and Procedure

For these experiments the sessile drop furnace at Special Metals Company was used. The apparatus consists of a water-cooled electric resistance furnace, vacuum pumps, an automatic temperature controller, a telescope, and a camera. The telescope and the camera have fixed focus to avoid the magnification difference.

After firing the ceramic substrate at 1000°C for one hour, the ceramic substrate and the metallic specimen were placed on the specimen holder. The furnace tube was closed, and the furnace was evacuated to 10^{-6} torr. Then the temperature was gradually increased to 1500 $\pm$ 20°C. Immediately after melting of the metal, photographs of the sessile drop were taken at various time intervals over a 30 minute period to determine changes in surface tension and contact angle with time. The contact angle and drop shape parameters were measured from slides and the liquid-vapor surface tension was calculated by using the following equation:

$$\sigma_{LV} = \frac{\rho g x z^2}{6(x-z)}$$

where: σ_{LV} = liquid-vapor surface tension

x = horizontal radius of the sessile drop

z = vertical radius of the sessile drop

ρ = density of the molten metal

g = gravitational acceleration

Results

Figures 2 to 4 illustrate how the contact angle, θ, varies with time for Ni-20Cr, Ni-20Cr-1Al, Ni-20Cr-4Al alloys on different substrates. To check the experimental procedure, the liquid-vapor surface tension of pure Ni was calculated. The calculated value of 1725 ± 75 ergs/cm^2 was in the range of published data.

Ni-20Cr-1Al alloy was found to be non-wetting on all ceramic substrates that were studied. Ni-20Cr-4Al alloys showed wetting tendency on alumina and yttria but non-wetting tendency on hafnia.

Table 1 shows all the results obtained from the sessile drop tests.

Directional Solidification Processing

The directional solidification has been modified to allow for the inversion of the directional solidification furnace at the University of Alabama and one Ni-20Cr sample has already been directionally solidified. The experiment was successful and it has been verified that the directional solidification furnace has the capabilities for melting and directionally solidifying Ni-Cr alloys.

PLANS FOR NEXT YEAR:

Fabrication of Directional Solidification Samples

As a result of surface tension experiments, the following correlations were established between various oxides-metal matrix systems:

Alloy/Oxide	HfO_2	Y_2O_3	Al_2O_3
Ni-20Cr	Non-wetting	Wetting	Wetting
Ni-20Cr-1Al	Non-wetting	Non-wetting	Non-wetting
Ni-20Cr-4Al	Non-wetting	Wetting	Wetting

These alloy systems are in the process of preparation with powder metallurgy techniques (VIM Atomization Attritor HIP) at Special Metals Company, NY. After preparation of these alloy systems ground and flight samples will be machined and the samples will be sent to the University of Alabama.

Directional Solidification at the University of Alabama

Directional solidification experiments will be carried out to determine the critical velocities in Ni-Cr-Al-Y_2O_3 and Ni-Cr-Al-HfO_2 systems in high-g environment. The microstructures and particle behavior and distribution will be studied by using SEM, optical microscopy and image analysis systems. The validity of the critical velocity equations, which is given in the literature, will be studied for these systems. If needed, the required modification or new formulations will be designed.

KC-135 Solidification Processing

In a low-gravity environment, both Stoke's forces and buoyancy driven convection are not active. For a given system, the main variable becomes solidification rate. By using the same solidification rate with the ground samples, the change in critical velocities in low-g environments will be determined. Again, the micro-structures and particle behavior and distribution will be studied and the difference between low-g and high-g samples will be investigated.

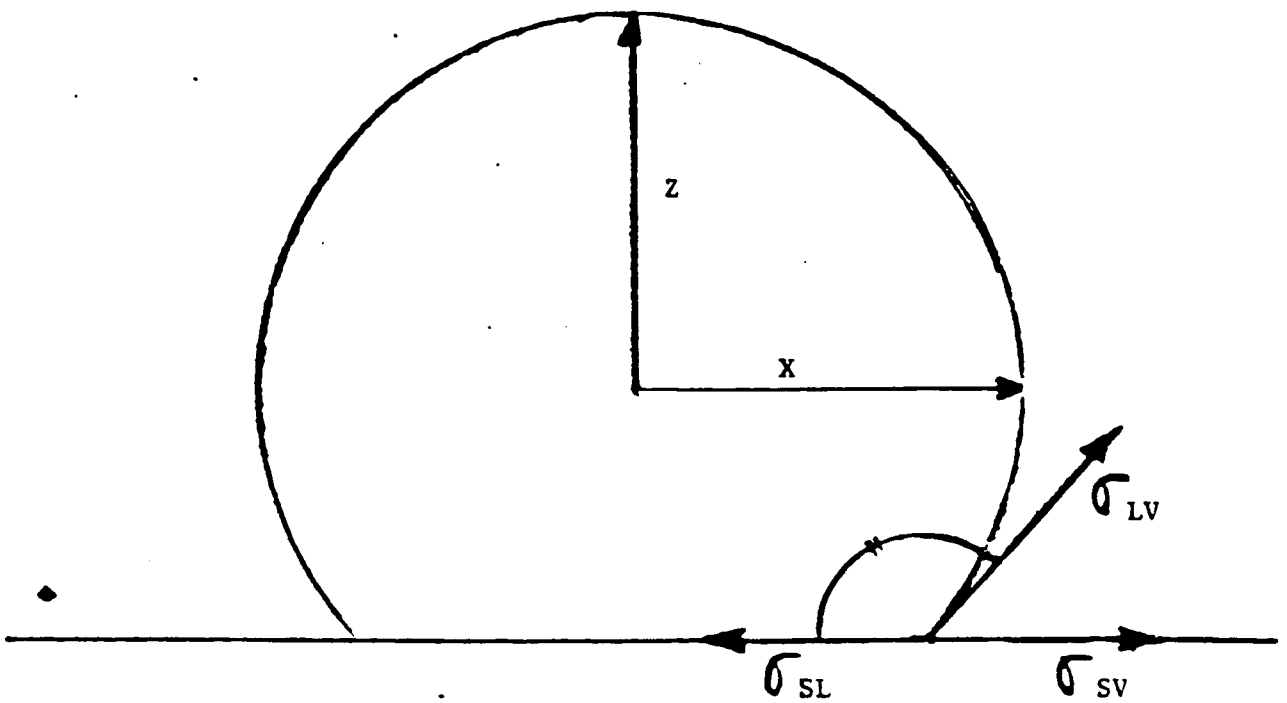

FIGURE 1: SCHEMATIC ILLUSTRATION OF A LIQUID DROP RESTING ON A CERAMIC SUBSTRATE

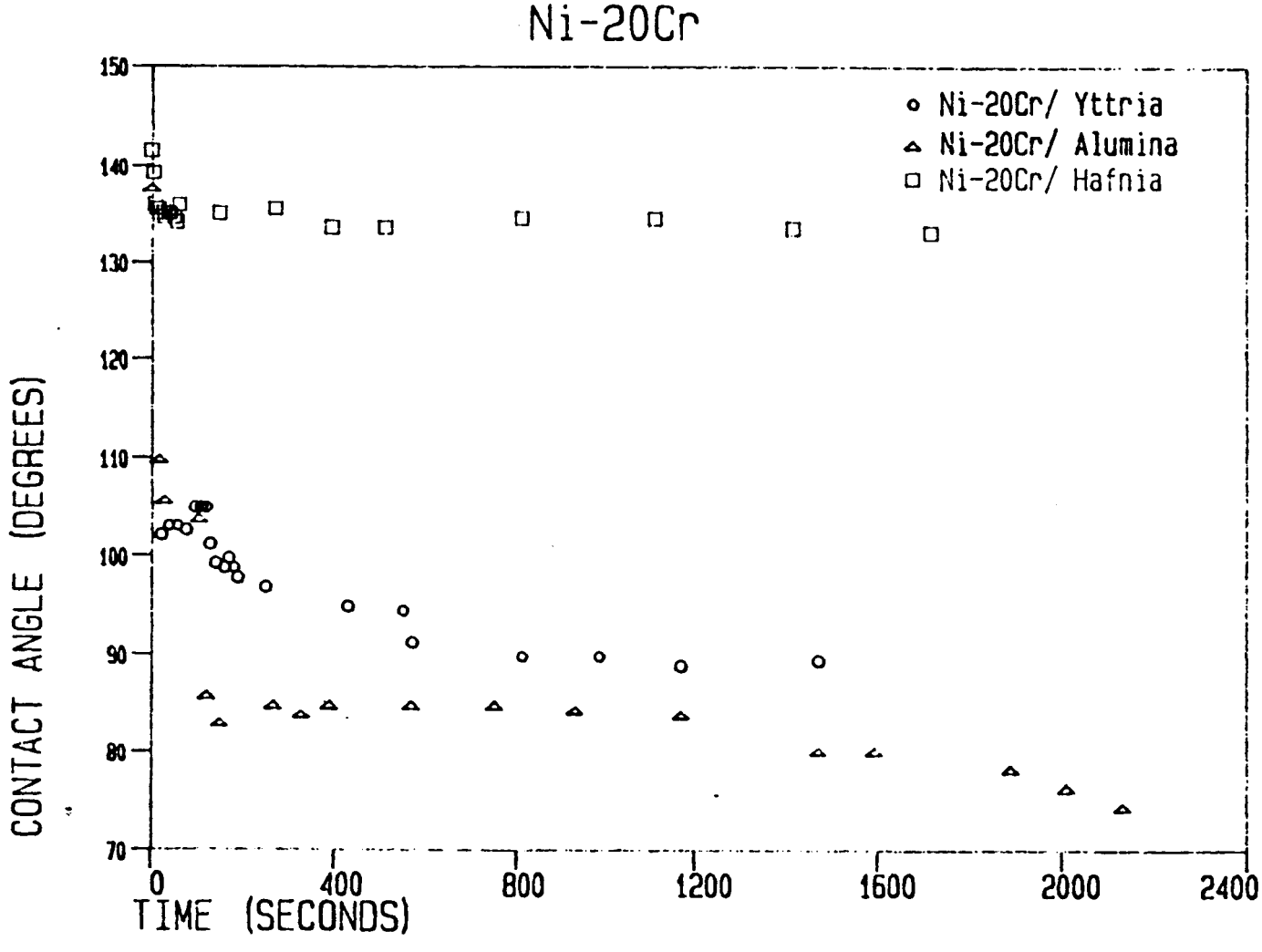

FIGURE 2: Contact Angle Versus Time for Ni-20Cr Alloy

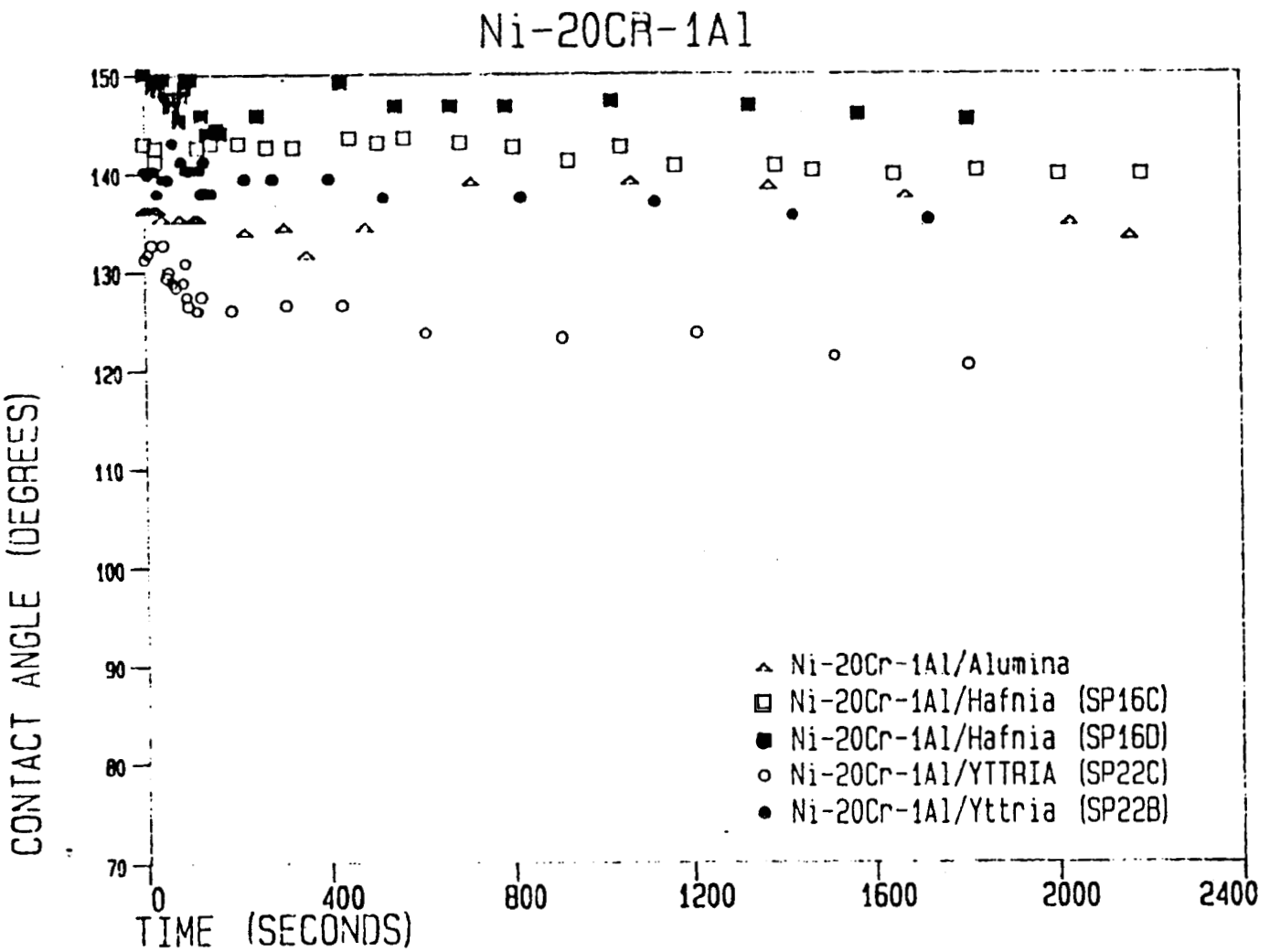

FIGURE 3: Contact Angle Versus Time for Ni-20Cr-1Al Alloy

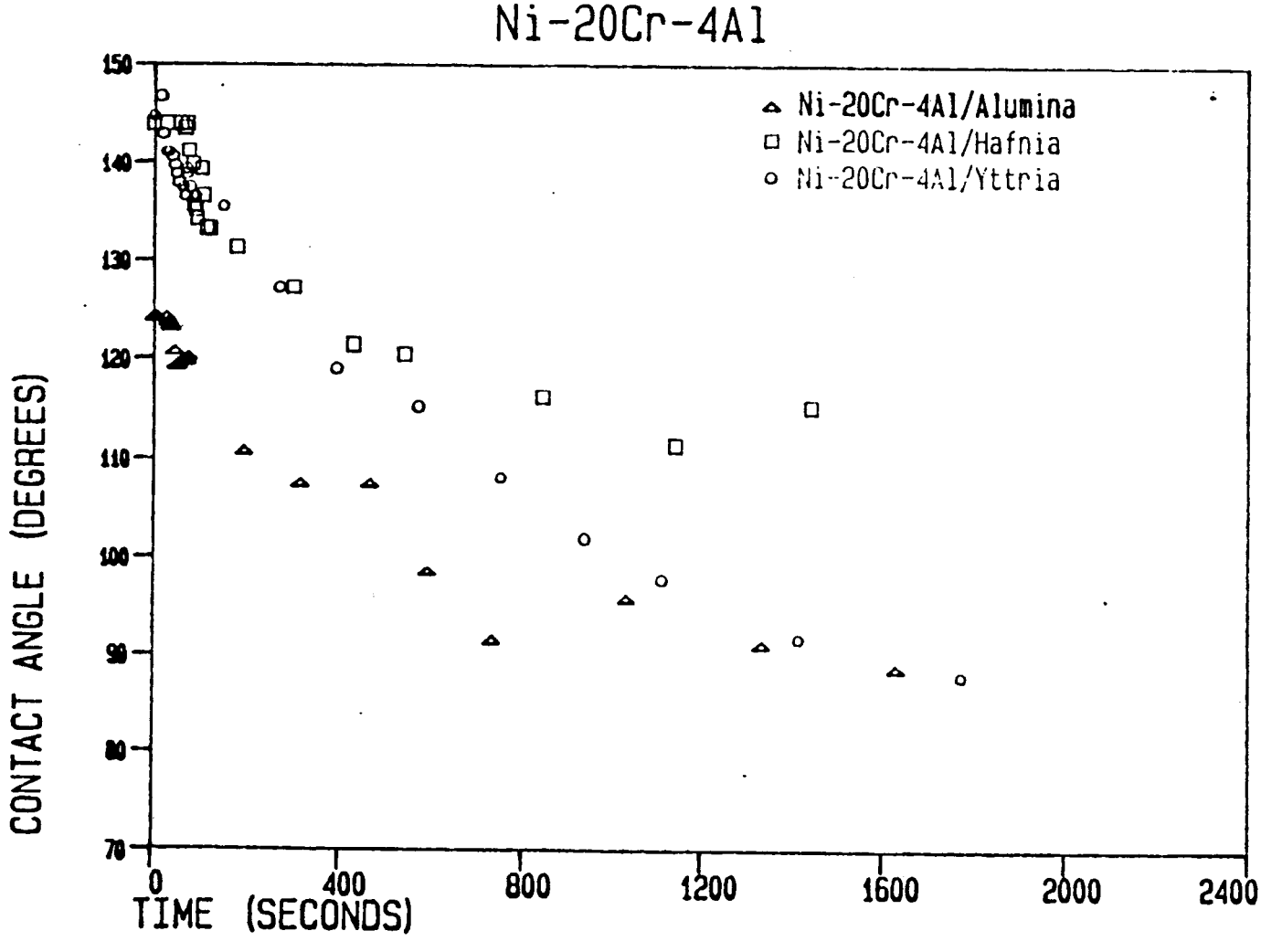

FIGURE 4: Contact Angle versus Time for Ni-20Cr-4Al Alloy

Table 1: Experimental Results

SPECIMEN	ALLOY	SUBSTRATE	CONTACT ANGLE 0 min	CONTACT ANGLE 30 min	SURFACE TENSION (ergs/cm^2)	WORK OF ADHESION 0 min (ergs/cm^2)
SP 10	Pure Ni	Al_2O_3	143	131.5	1715	347
SP 12	Ni-20Cr	Al_2O_3	138	74.5	2044	525
SP 15	Ni-20CR	HfO_2	141.5	133	1039	226
SP 15A	NI-20Cr	HfO_2	136	122	1340	376
SP 21C	Ni-20Cr	Y_2O_3	102	90	3187	2524
SP 13	Ni-20Cr-1Al	Al_2O_3	136.5	133.5	1143	314
SP 16C	Ni-20Cr-1Al	HfO_2	143	139.5	1079	217
SP 16D	Ni-20Cr-1Al	HfO_2	150	145.5	1082	145
SP 22B	Ni-20Cr-1Al	Y_2O_3	140	135	1276	299
SP 22C	Ni-20Cr-1Al	Y_2O_3	131	120.6	1369	470
SP 14	Ni-20Cr-4Al	Al_2O_3	124	89	1979	872
Sp 17A	Ni-20Cr-4Al	HfO_2	144	115	1374	262
SP 23B	Ni-20Cr-4Al	Y_2O_3	145	88	1227	222

PROJECT TITLE: Containerless Processing of Nb-Ti Alloys

COMPANY INVOLVED: Teledyne Wah Chang Albany

PROJECT LEADER: G. J. Abbaschian, University of Florida

PROJECT DESCRIPTION:

This is the first annual report on the containerless processing of Nb-based alloys. The report summarizes the research carried out at the Materials Science and Engineering Department of the University of Florida (UF), in collaboration with Teledyne Wah Chang Albany (TWCA), and Vanderbilt University (Vanderbilt).

The aim of this program is to produce Nb-Ti binary alloys with superior homogeneity. The program involves supercooling of the molten alloys under containerless processing conditions, followed by rapid heat extraction during recalescence and solidification. Electromagnetic levitation facilities at the University of Florida and drop tube facilities at the NASA Marshall Space Flight Center are being utilized to solidify samples under one g and low g conditions, respectively. The effects of supercooling, cooling rate, and gravity on the microsegregation profile and microstructure of the alloys are being investigated using SEM, Microprobe, and STEM. In addition, samples, processed under specified conditions, are supplied to TWCA for their in-house evaluation.

It should be noted that the University of Florida is involved in another project with TWCA, Lockheed, and Vanderbilt on development of high temperature oxidation resistant Nb-based alloys as reported elsewhere in this report. As such, some of the experiments and results between the two projects overlap.

RESULTS TO DATE:

The starting materials were supplied by TWCA in the form of rods (Nb-63 at.% Ti) or arc melted buttons (Nb-50 and 35 at.% Ti). Samples, each weighing between 1.5 to 2 grams were arc melted under an Ar atmosphere. A titanium getter was melted in the arc furnace prior to melting of the samples. The samples were then levitated using a levitation coil made up of two reverse wound Cu coils wound with insulating fiberglass tape. The lifting (or lower) coil is double wound and conical in shape.

The system is powered with a 10 KW generator operating at 450 kHz. A stepdown transformer is used between the coil and the generator to facilitate efficient coupling between the impedance of the coil, sample, and generator.

The temperature of the levitated sample was measured and continuously monitored using a two color pyrometer connected to a strip chart recorder. In order to improve the accuracy of the thermal data at higher temperatures, a single color pyrometer was added during the third quarter. The addition, as discussed later, has resulted in a considerable improvement in the results. A flow of high purity Ar and/or He was continuously maintained through a glass tube surrounding the sample to aid in the cooling and simultaneously prevent oxidation. The inert gases were purified by passing through a gas purifier which uses titanium at 800 °C as a getter. The oxygen concentration of the gases entering the levitation chamber was around 10^{-15} ppm.

The gas flow and the power to the unit were controlled to melt and subsequently supercool the samples. The levitated samples were then quenched from the supercooled state by cutting off the power to the coil. The quenching was done either in water or against a Cu substrate to observe the influence of varying cooling rates on microstructure.

Samples were also melted by the Vanderbilt University team using the electron beam melting apparatus at NASA Marshall and solidified in the drop tube. The various tasks performed by UF, Vanderbilt, and TWCA are summarized below:

*	Master alloy preparation	TWCA
*	Alloy processing by EM levitation	UF
*	Microstructural and compositional analysis of the processed alloys	UF
*	Supplying duplicates of the processed samples to TWCA	UF
*	Low-gravity processing using the NASA drop tube facility	Vanderbilt
*	In-house analysis	TWCA

Metallographic Sample Preparation Techniques

The metallographic sample preparation was improved by using semiautomatic grinding and polishing and separate etchants for alloys with different Ti contents. The preparation technique is based on the suggestions made by Paul Danielson of TWCA. This technique reduced the amount of metallographic artifacts such as embedded polishing compounds, surface relief, and surface deformation. Also, better delineation of the microstructures was obtained, resulting in improved image quality in both optical and electron microscopes.

The quenched samples were mounted using a phenolic resin powder. They were then ground on Alumina paper starting from coarse grit (grit #3) down to fine grit (grit #0), followed by a two stage polishing. First stage polishing was done on a silk cloth underneath which a metcloth was placed. A slurry made of 1 μm alumina, chromium trioxide, and water was used as the polishing compound. Second stage polishing was done on a microcloth using a slurry made of 0.05 μm alumina, water, concentrated nitric acid, and hydrofluoric acid. The etchants used for revealing the microstructure are as follows: 7 ml. lactic acid, 7 ml. hydrogen peroxide, 2 ml. nitric acid, and 2 ml. hydrofluoric acid for Nb-63 at.% Ti alloy, and 5 ml. hydrogen peroxide, 10 ml. nitric acid, and 2 ml. hydrofluoric acid for lower Ti concentrations. In each case, the samples were swab-etched for 15 seconds.

Electron Microprobe Analysis of As-Polished, Unetched Samples

Detailed microanalyses of the samples were carried out using a JEOL JXA 733 Superprobe and a JEOL JSM 35C Scanning Electron Microscope fitted with an ORTEC energy dispersive spectrometer. In the microprobe, two PET analyzing crystals together with a Tracor AUTOQUANT program were used. A Si(Li) high energy detector and an Ortec ZAF program were used for the energy dispersive spectrometer of the SEM.

In order to meet the specific requirements for compositional analysis of the processed samples, the following analysis scheme has been formulated: microhardness indentations are made on the as-polished samples in order to identify the area of interest. Backscattered electron (BSE) image analysis is carried out to identify the microstructural features and document the scan area.

The average composition of the area is determined using a large-beam (approximately 50 μm diameter) probe. This is followed by line scanning across only one cell or secondary dendrite arm to get the microsegregation profile in the sample. The line scans are made either continuously with 1 μm steps or discretely with approximately 1.5 μm steps.

Analysis of Etched Samples

Secondary Electron (SE) images of the scanned area at several magnifications were also made to identify and analyze the microstructural morphology. This analysis was especially important in highly supercooled alloys, which contain fine microstructural features not identifiable with the optical technique. Grain size and DAS measurements were made optically using the standard linear intercept method.

Improvements in Techniques

Compared to our second quarterly report, the maximum temperatures obtained in EM levitation have increased by 250 K, while the maximum supercooling obtained has been increased by 220 K, as summarized in Table 1. The higher temperature limit was increased through improved coil design while higher supercoolings were achieved by better control of gas flow rate and sample preparation techniques.

The quality of our thermal data has been improved through the use of a single color pyrometer (in contrast with the two color pyrometer used previously). The data acquired in this manner are less noisy, facilitating a more accurate analysis of the output. A comparison between the outputs of the two pyrometer is shown in Figure 1. The time-temperature data was obtained from pyrometers aimed simultaneously at the same area of the sample. In addition, we are currently in the process of computer-interfacing the single color pyrometer, which is expected to improve the quality of data analysis through the use of time-based derivatives.

Microstructural Analysis

During the first year of the project, Nb-63 at.% Ti, Nb-50 at.% Ti, and Nb-35 at.% Ti alloys were levitated and supercooled.

The maximum supercooling achieved in these alloys was 240, 320, and 200 K, respectively. Seventeen samples were produced as listed in Table 2. An additional thirty samples were also prepared with known supercoolings and sent to the companies involved; these samples are being tested as specified in our second quarterly report. The above mentioned samples were analyzed using optical microscopy, SEM, and Microprobe as discussed previously. A typical example of the results is given below.

Microstructures of samples with 63 at.% Ti, supercooled by 0, 40, 100, and 240 K are shown in Figures 2, 3, 4, and 5, respectively. In each case, the micrographs were obtained in the SEM at magnifications of 50, 200, and 500X in the SE imaging mode, and at 200X in the BSE imaging mode.

The micrographs taken in the BSE imaging mode (Figures 2d, 3d, 4d, and 5d) show a comparison between the topographical contrast in the SE imaging mode (Figures 2c, 3c, 4c, and 5c) and the compositional contrast of the BSE imaging mode.

The morphological features of these samples may be summarized as follows:

Supercooling, ΔT (K)	Microstructural Features
0	Well-defined columnar dendrites, distinct grain boundaries
40	"Spherical" elements (or cells), distinct grain boundaries
100	Well-defined equiaxed predominantly broken dendrites, no distinct grain boundaries
240	Fine, equiaxed spherical elements, no distinct grain boundaries

The particular type of morphology (spherical or dendritic) is known to depend on the existing fluid flow conditions which may or may not result in broken dendrites. However, in either type of morphology, the scale of the microstructure becomes finer with increasing supercooling.

In all the samples analyzed thus far, a predominantly spherical morphology is observed at high supercoolings ($\Delta T > 150$ K). This may be possibly due to a higher nucleation rate (the number of nuclei increases exponentially with decreasing temperature) at high supercoolings, or due to the dendrite fragmentation caused by fluid flow during recalescence.

Analysis of Microsegregation

A typical solute (Ti) microsegregation profile obtained from a line scan across a secondary dendrite arm is shown in Figure 6. The line scan was taken for a Nb-36 at.% Ti sample (nominally designated as Nb-35 at.% Ti) supercooled by 200 K. The profile was taken on a line between the end-points shown by triangles in Figure 6a. The partitionless solidification region at the center of the secondary arm is seen as a plateau with composition approximately equal to the average alloy composition; the composition decreases to 33.5 at.% Ti in the immediate vicinity, Figure 6b, beyond which it increases towards the edge of the arm. The difference between the maximum and minimum in composition across the secondary arm is approximately 3 at.% Ti. The dotted line in this figure shows the calculated compositional profile for a sample with no supercooling. The comparison between the two curves shows the drastic effect of the supercooling in reducing microsegregation in these alloys. The general trends observed in supercooled alloys may be summarized as:

* The amount of microsegregation decreases with increasing supercooling.

* The average dendrite arm spacing or cell size decreases with increasing supercooling.

* The average grain size decreases with increasing supercooling.

ADDITIONAL PROJECT PERSONNEL:

Robert J. Bayuzick, Vanderbilt University
Sunil George, University of Florida
A. Gokhale, University of Florida
John C. Haygarth, Teledyne Wah Chang Albany
Gautham Sarkar, University of Florida

Table 1: Improvements in High Temperature Capability and Maximum Supercooling

Quarter	Maximum Temperature Attained T, K	Maximum Supercooling Achieved ΔT, K
2nd	2190	100
3rd	2190	200
4th	2440	320

Table 2: List of Samples Processed by EM Levitation

Quarter	Composition at.% Ti	Supercooling ΔT, K	Replicates sent to Lockheed	Replicates sent to TWCA
2nd	63	0	X	X
	63	40*	-	-
	63	100	-	-
3rd	63	60	X	X
	63	120	-	-
	63	200	X	X
4th	63	80	X	X
	63	160	X	X
	63	240	X	X
	50	0	X	X
	50	60	X	X
	50	150	X	X
	50	160	X	X
	50	200	X	X
	50	320	X	X
	35	0	X	X
	35	200	X	X

Note: All samples processed by EM levitation were quenched against a copper substrate

* Water quenched

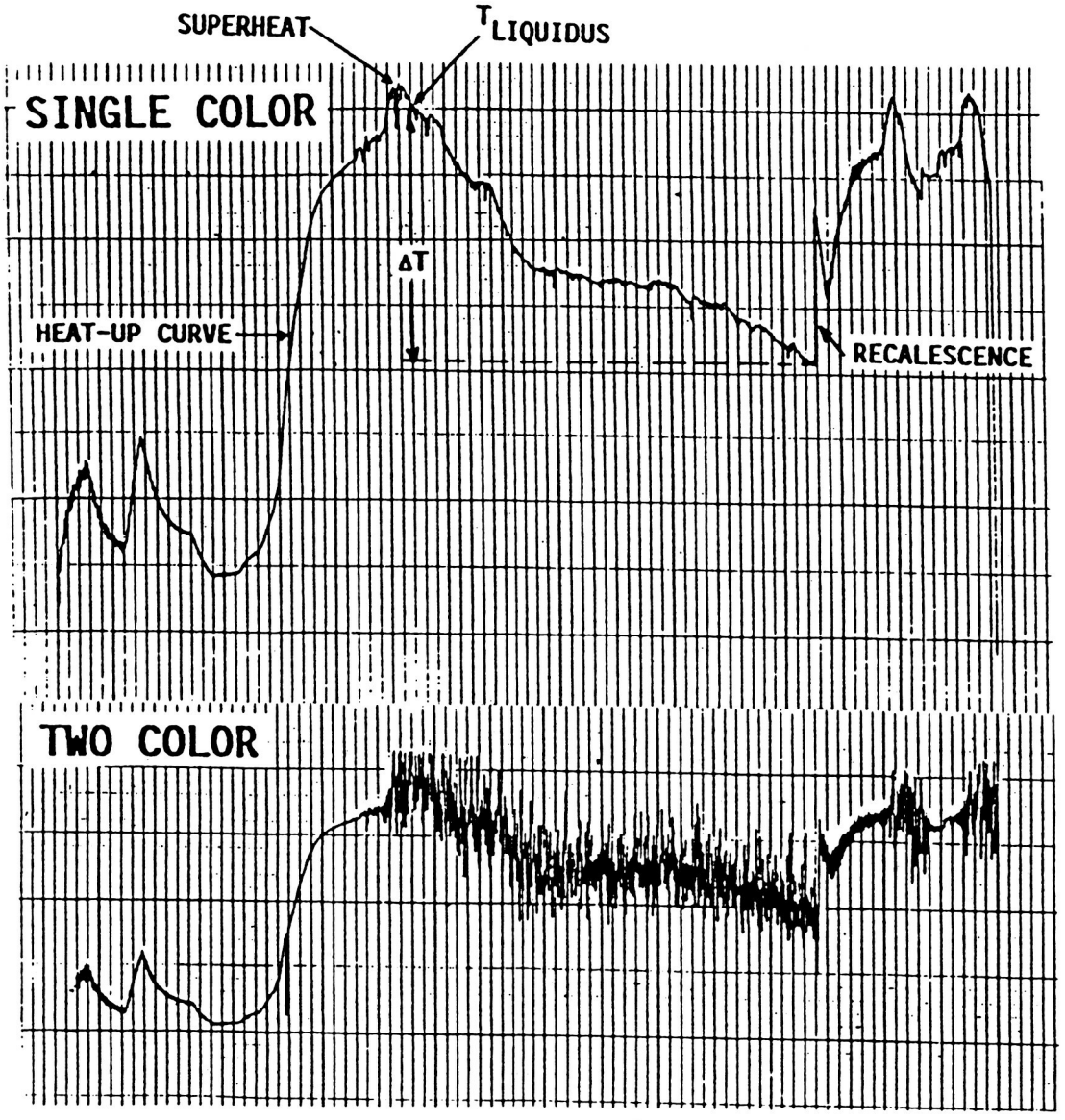

Figure 1 Comparison of temperature outputs from single color (top) and two color (bottom) pyrometers. The data were obtained from pyrometers aimed simultaneously at the same area of the sample. Various features of the thermal cycle are identified on the single color pyrometer output.

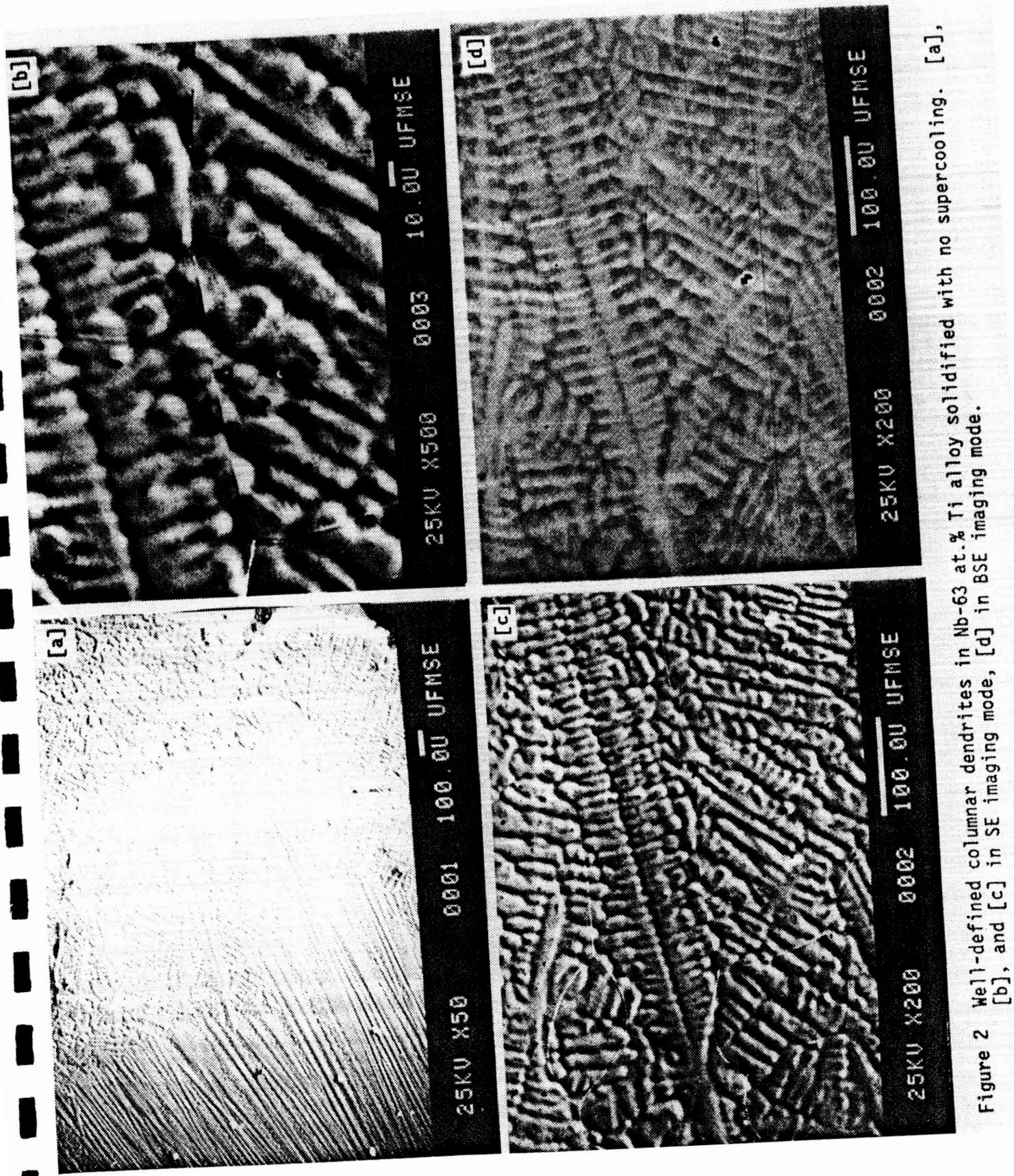

Figure 2 Well-defined columnar dendrites in Nb-63 at.% Ti alloy solidified with no supercooling. [a], [b], and [c] in SE imaging mode, [d] in BSE imaging mode.

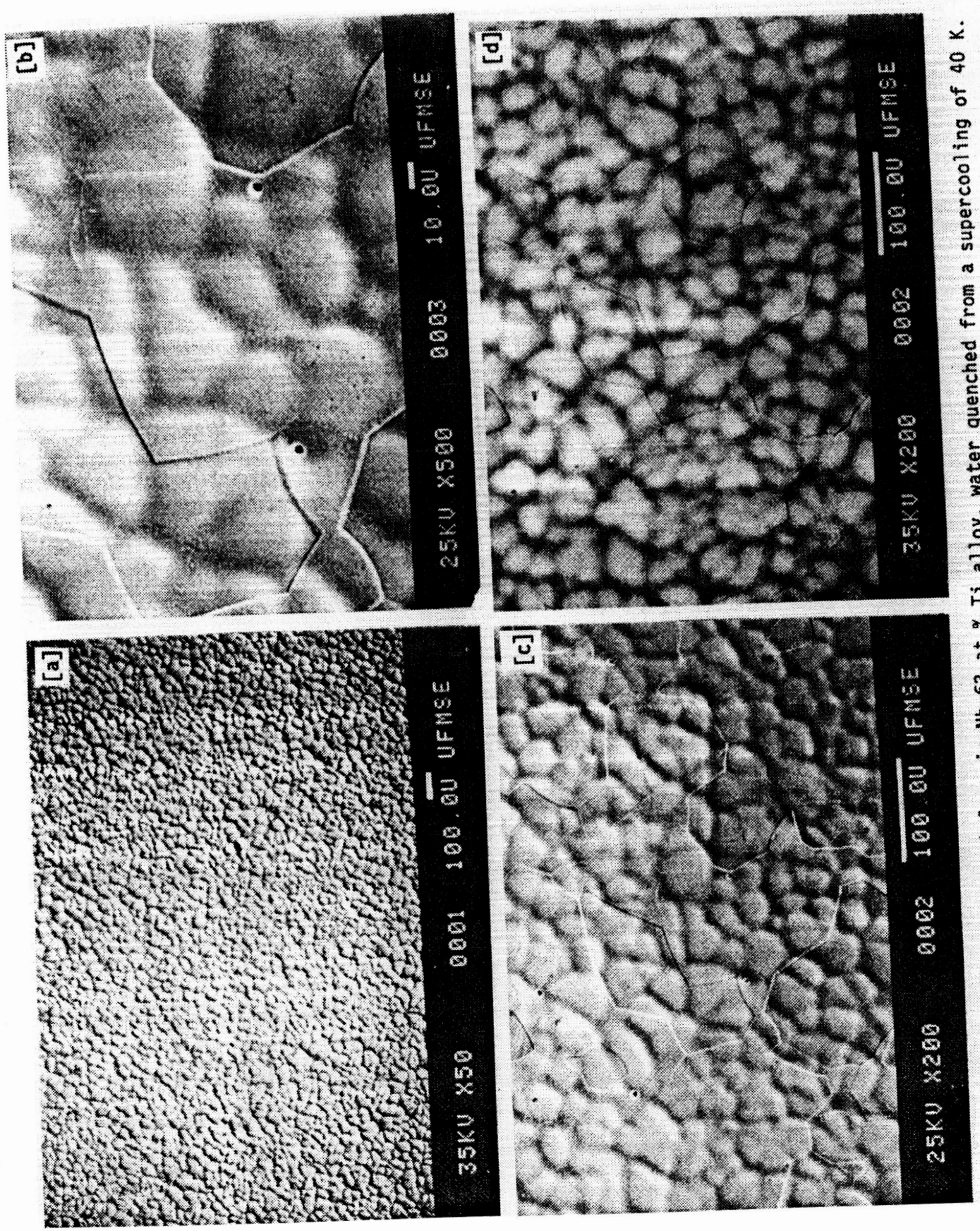

Figure 3 Spherical element morphology in Nb-63 at.% Ti alloy, water quenched from a supercooling of 40 K. [a], [b], and [c] in SE imaging mode, [d] in BSE imaging mode.

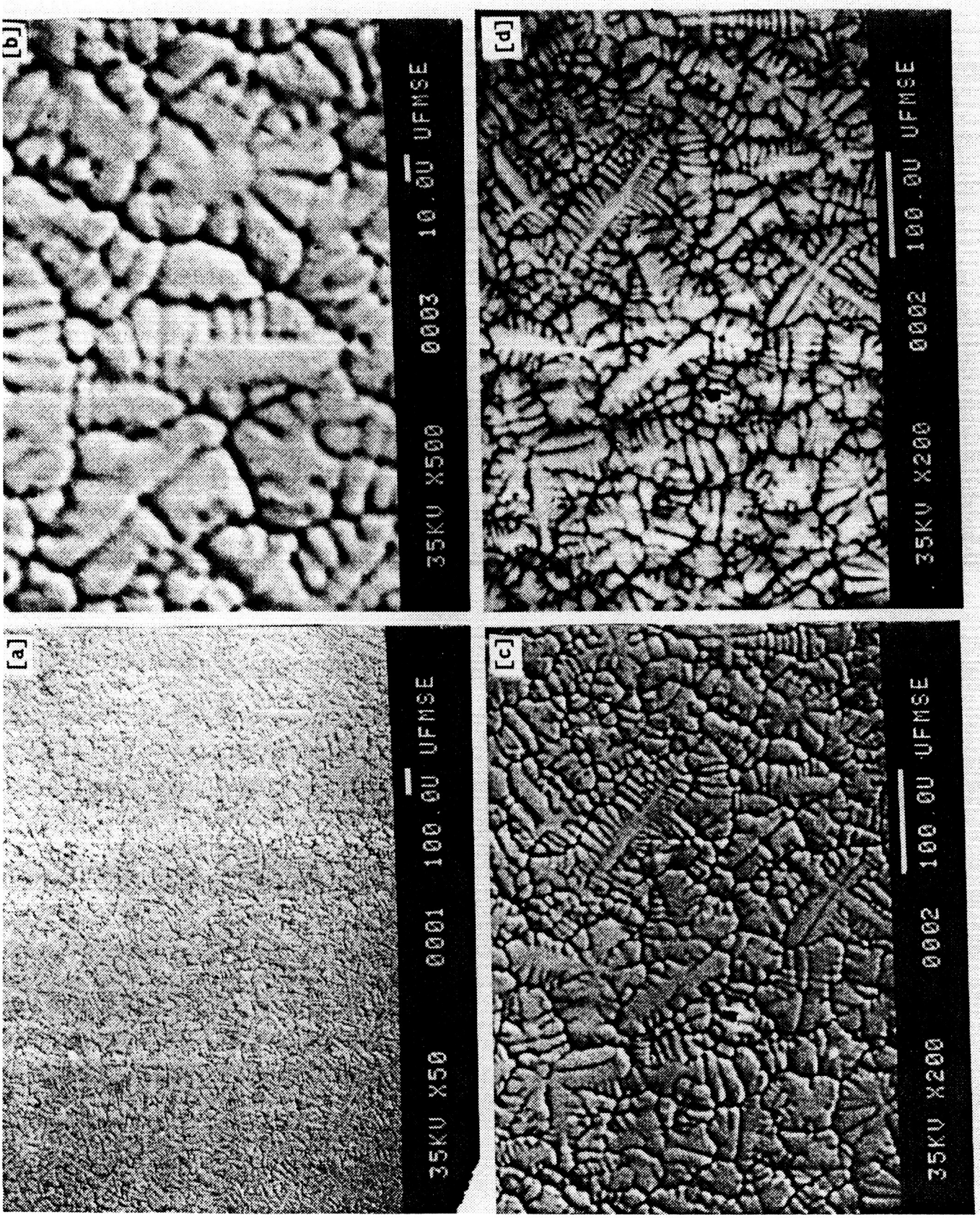

Figure 4 Well-defined, equiaxed, predominantly broken dendrites in Nb-63 at.% Ti alloy, quenched on a Cu substrate from a supercooling of 100 K. [a], [b], and [c] in SE imaging mode, [d] in BSE imaging mode.

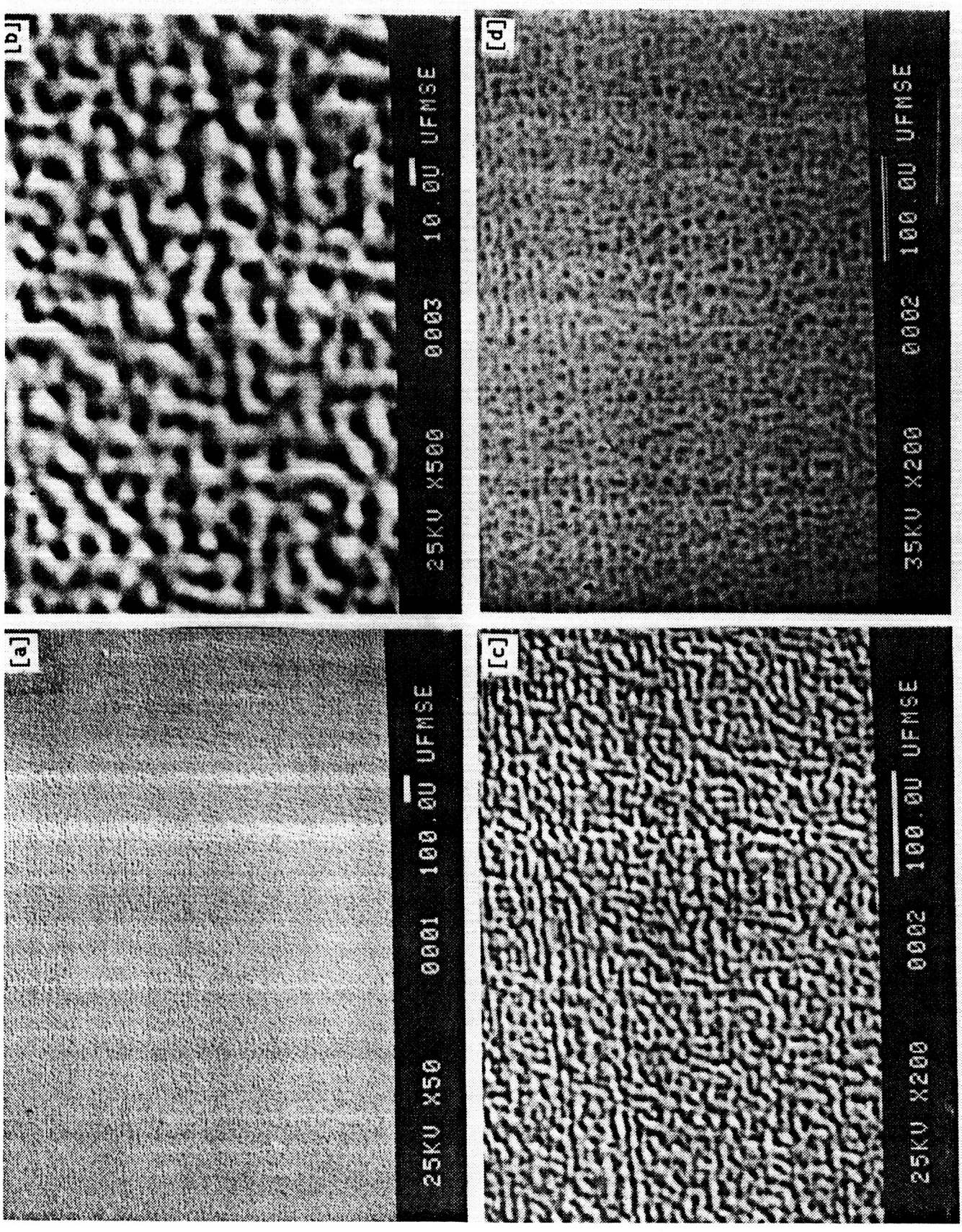

Figure 5 Fine, equiaxed, spherical element morphology in Nb-63 at.% Ti alloy, quenched on a Cu substrate from a supercooling of 240 K. [a], [b], and [c] in SE imaging mode, [d] in BSE imaging mode.

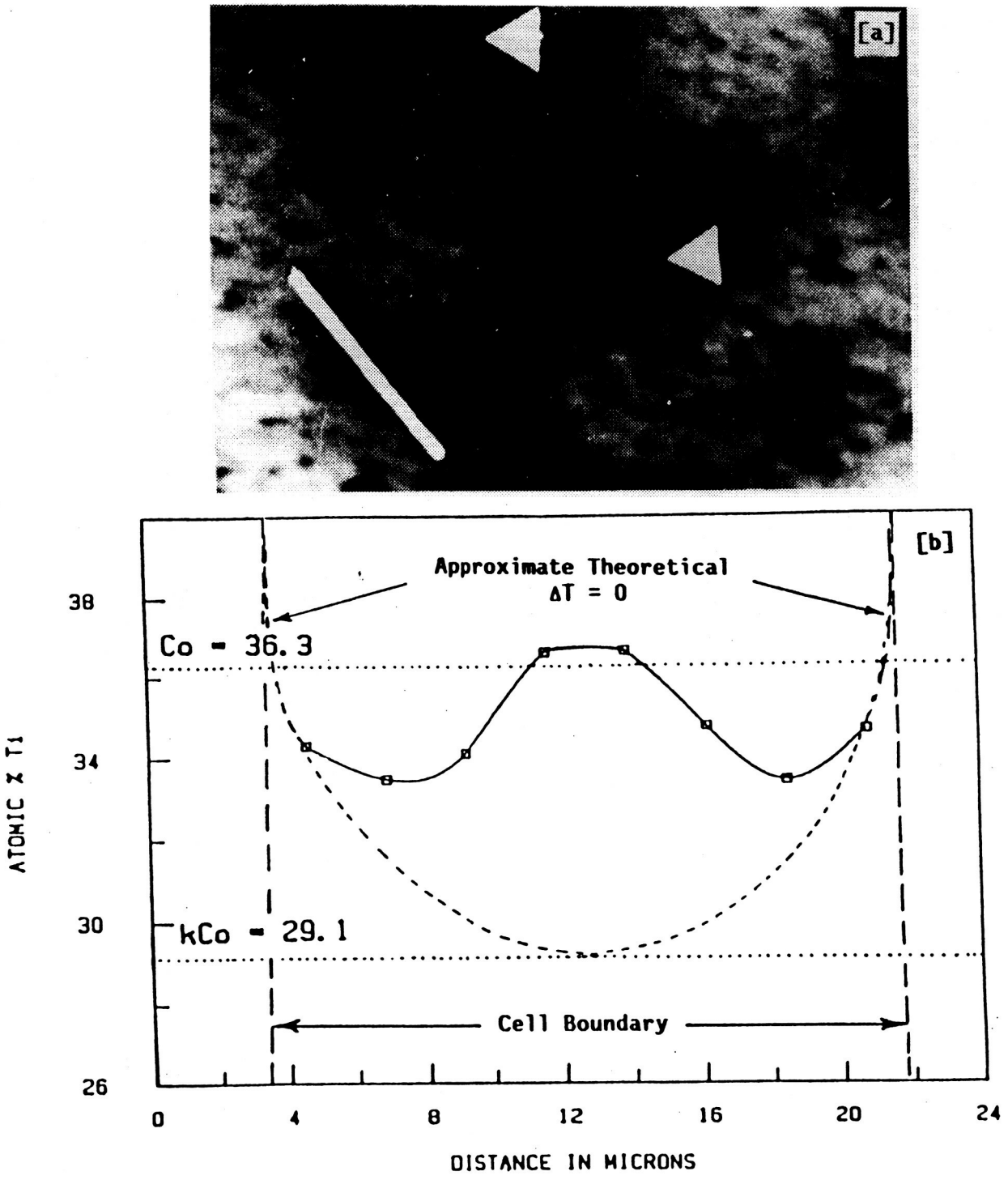

Figure 6 [a] Nb-35 at.% Ti, quenched on a Cu substrate from a supercooling of 200 K. Line scan taken between end points shown by triangles (BSE imaging mode). [b] Composition profile in atomic % Ti. Dotted line indicates profile expected at no supercooling.